EFFECTS OF TITANIUM AND BORON ADDITIONS ON THE MICROSTRUCTURE AND MECHANICAL PROPERTIES OF ALUMINUM CASTINGS

by

M. Bülent AKAGÜNDÜZ

B.S. in M.E., Boğaziçi University, 1983

Submitted to the Institute for Graduate Studies in Science and Engineering in partial fulfillment of the requirements for the degree of

Master of Science

in

Mechanical Engineering

Boğaziçi University

1986

EFFECTS OF TITANIUM AND BORON
ADDITIONS ON THE MICROSTRUCTURE AND
MECHANICAL PROPERTIES OF ALUMINUM CASTINGS

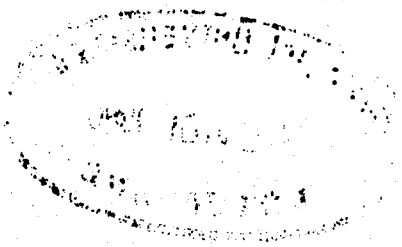

APPROVED BY

Doç. Dr. Sabri ALTINTAŞ S. Altıntaş
(Thesis Advisor)

Doç. Dr. Öktem VARDAR

Doç. Dr. Turan ÖZTURAN

DATE OF APPROVAL : 4/7/1986

ACKNOWLEDGEMENTS

I would like to express my most sincere appreciation to my thesis supervisor Doç. Dr. Sabri ALTINTAŞ for his most helpful advice and guidance throughout the coarse of this work.

I wish to thank ETİBANK for permission to carry out this research in Seydişehir Aluminum Company.

My grateful appreciation goes to Mr. Tamer GÜNEY, Head of the Research Department, for permission to carry out this study in Laboratories, to Mr. Kaya GÖKMENOĞLU for the metallography.

Finally, I wish to thank all technical staff of the Laboratory Department, Foundry Department and Energy Department for their assistance.

M. BÜLENT AKAGÜNDÜZ

EFFECTS OF TITANIUM AND BORON ADDITIONS ON THE MICROSTRUCTURE AND MECHANICAL PROPERTIES OF ALUMINUM CASTINGS

ABSTRACT

In this study, the production of various master alloys (Grain refiners) and their effects on the microstructure and mechanical properties of aluminum alloys such as Etial-7(1070), Etial-5(1050) and Etial-60 (6063) are investigated.

A brief review of the grain refinement processes and the theory of the master alloys are presented together with the effects of inoculation on the solidifying structures.

In the experimental work, AL-5Ti-1B master alloys, which are also called TIBOR, having block-like and flake-like structures are produced and added into various kinds of aluminum as grain refiners at different temperatures, holding times and impurity degrees. The mechanical properties are determined through tensile and hardness testing. The resulting microstructures are studied in detail to reveal the effects of produced master alloys on grain structure of aluminum castings.

Finally; the obtained grain size, ultimate tensile strengt yield strength data are correlated to the increasing casting temperature, holding time and the order of addition of the alloying elements.

ÖZET

Bu çalışmada, çeşitli ön alaşımların (tane incelticilerin) üretimi ve onların ETIAL-7(1070), ETIAL-5(1050), ETIAL-60 (6063) gibi aluminyum alaşımlarının mekanik özellikleri ile mikroyapısı üzerine etkileri incelenmiştir.

Tane inceltme yöntemlerinin kısa bir özeti ve ön alaşımların teorisi, katılaşan yapılarda aşılamanın etkileri ile beraber sunulmuştur.

Deneysel çalışmada, bloksal ve iğnesel mikroyapıya sahip TIBOR olarak da adlandırılan AL5TİlB ön alaşımları üretilerek aluminyumun çeşitli tiplerine tane inceltme amacıyla farklı sıcaklıklarda, tutma sürelerinde ve safsızlık derecelerinde katılmıştır. Mekanik özellikler çekme ve sertlik deneylerinden belirlenmiştir. Elde edilen mikroyapılar, üretilen ön alaşımların, aluminyum dökümlerinin tane yapıları üzerine etkilerini açıklamak için ayrıntılı bir şekilde incelenmiştir.

Sonuçta; tane boyu, çekme mukavemeti, akma mukavemeti ile artan döküm sıcaklığı, tutma zamanı ve alaşımlama elemanlarının ilave miktarları arasındaki ilişki sunulmuştur.

TABLE OF CONTENTS

LIST OF FIGURES

Page

LIST OF TABLES

LIST OF SYMBOLS

δ	: Disregistry
a, a_α, a_β, c	: Lattice parameters, $\overset{o}{A}$
D	: The spacing between dislocations, $\overset{o}{A}$
TIBOR,M.A	: Aluminum-Titanium-Boron Master alloy
X	: Supersaturation
ζ	: shear stress, N mm^{-2} or MPa
ζ_o	: The shear stress required to cause slip to occur in the absence of a grain boundary resistance, Nmm^{-2}
k_s	: A measure of the stress concentration which is generated at the tip of a slip band, N $mm^{-3/2}$
D_1	: Diameter of ball, mm
D_2	: Average grain diameter, mm
d	: Diameter of indentation, mm
d_1	: Diagonal length, mm
d_2	: Second diagonal length, mm
m	: Average orientation factor
σ	: Externally applied stress, N/mm^{-2} or MPa
P	: Applied load, N

I- INTRODUCTION

The idea of improving the quality of cast metal either by chemical or mechanical means is a very old one. Certain properties of materials depend directly upon the size and distribution of grains within the materials. Fine grain metals may be produced upon solidification from the melt in several basically different ways, i.e use of master alloys, mould coating or by electromagnetic stirring, oscillation, rotation and vibration |1-3|.

In the present work, first aluminum-titanium-boron master alloys are produced, then the effects of addition of master alloy into the casting are investigated and the improvements brought to the mechanical properties and microstructure of the alloys are stated.

It is well known that addition to a molten aluminium of an aluminum-titanium-boron master alloy which will promote grain-refinement on aluminum and aluminum alloy castings without introducing other noticable alloying effects will result in improved mechanical properties and surface finish in the aluminum and aluminum alloy castings. Further, the

use of suitable grain-refining master alloys can permit a radical increase in casting speeds. Grain-refining inoculants commonly used in the aluminum industry are master alloys containing titanium plus boron |4-8|. Grain refining additions are used mainly for two reasons : to obtain a fine , uniform grain structure and to reduce the formation of center cracks |9|.

The need to refine cast grain size of rolling blocks and extrusion billets has been universally acepted for over two decades. Early investigations established that the introduction of small amounts of titanium as a high purity aluminum-titanium master alloy effected grain refinements ; a practice which exists today. Further work discovered that titanium incombination with boron significantly enhanced the nucletion process at greatly reduced levels of addition |7|. This led to the development of a high purity aluminum based master alloy Tibor containing 5 % titanium, 1 % boron, a ratio found to be most effective as a refiner. Tibor, becasue of its superior grain refining performance, played an important part in achieving production of the larger sheet rolling ingot and extrusion billet now being demanded by the aluminum industry.

At present, there is really no theory for producing fine grains. In fact, the basis for all procedures can be stated very simply ; produce a number of grains sufficient to interact with each other before any appreciable growth of

these individual grains can occur |1|.

A ternary AL-Ti-B alloy in common use 5 pct Ti and 1 pct B, has two crystalline intermetallic compounds primarily discernible in the microstructure, namelly small crystallites of titanium diboride (TiB_2) and larger crytals of aluminides (AL_3Ti). The TiB_2 particles are typically sized about 0.5~2.0 μm in diameter, and located mainly at the cell boundaries. The size distribution and morphology of the boride particles are independent of the formation temperature |5|. The AL_3Ti particles are typically sized about 5~100μm in length. The size distribution and the morphology of the aluminide (AL_3Ti) particles are dependent on the formation temperature. AL_3Ti crytals can exhibit several different morphologies and show marked variation in size. Aluminide particles, in alloys where the titanium is added at high temperature ; have a needle like appearance, are called "flake-like", crytals. AL_3Ti crytals formed at a low temperature are more compact than the flake-like ones and are also smaller. This type of AL_3Ti particle is called as "blocky". Quenched alloys have small AL_3Ti crytals of a third morphology, namely the "petal-like" type.

There have been many papers written about the mechanism of grain refinement of aluminum by adding AL-Ti-B master alloy. It is currently accepted that Al_3Ti crytals are responsible for the nucleation at concentrations above 0.15 Wt % Ti (peritectic point) via a peritectic reaction

(Liq + $TiAl_3$ —— α_{Al}). For hypoperitectic compositions, where the Al_3Ti phase is not stable (Concentration of titanium is less than 0.15 Wt % Ti), there are two main theories advanced to explain this phenomenon :

1) The "boride-carbide theory".
2) The "peritectic reaction theory".

More information about these threories will be given in chapter IV.

Grain refining efficiency of the master alloy can be explained briefly as follows ; surviving aluminide (Al_3Ti) particles nucleate the aluminum grains via a peritectic reaction. The peritectically nucleated grains generally remain very tiny. After nucleation, these new grains surrounded by liquid of aluminum can act as heferogeneous sites on which the primary phase (α_{Al}) will nucleate when the temperature gradient becomes sufficiently small.

As the microstructure and mechanical properties of the studied inoculated aluminum alloys with tibor were invesgitated, it was found that the inoculated ingot castings cast with different temperatures, holding times and addition rates presented an improved tensile strength, yield strength and elongation data for Etial-60 (6063) aluminum alloy. Also, decreasing grain sizes were obtained by using tibor as inoculation reagent for all of the types of aluminum

alloys (ETIAL-7 (1070), ETIAL-5 (1050), ETIAL-60 (6063)).

In the following chapters, in chapter II and III a brief review of the grain refinement and ternary Al-Ti-B master alloys will be given. Next, the mechanism of grain refinement of aluminum castings inoculated with Al-Ti-B master alloys and the results obtained in previous studies will be presented. In chapter V experimental work of the present study will be given.

II GRAIN REFINEMENT

Certain properties of materials depend directly upon the size and distribution of grains within the materials. Fine grain metals may be produced upon solidification from the melt in several basically different ways |1| ;

- The rate of grain nucleation can be increased by varying the thermal conditions of freezing,

- The nature and morphology of the solid-liquid interface can be manipulated, thereby altering the kind and distribution of growing crystallites,

- Nucleation can be promoted by special concentration variations and inoculant.

There is really no theory for producing fine grains. In fact, the basis for all procedures can be stated very

simply ; produce a number of grains sufficient to interact with each other before any appreciable growth of these individual grains can occur |1|. The many attempts to accomplish this goal are shortly discussed below.

2.1 Variations in the thermal Environment :

The production of fine grained material by an interaction of heat and fluid flows with both nucleation and growth mechanism will be discussed in this section. There are two basically different ways of proceeding.

1- If the rate of heat flow is suddenly made very high by surronding the molten metal with a sink of infinite heat capacity, the liquid is very quickly undercooled. The number of nucleation centers increases while the size of these centers decreases (the number of atoms in a center typically being less than 200) |1,3|, and nucleation takes place-almost catastrophically-everywhere in the Liquid. Techniques such as splat cooling, slab and die casting, and the application of chills utilize this approach (with varying efficiency according to melt size) in order to change the nucleation rate.

2- The other approach to increasing the number of grains is based on dentrite morphology during growth rather than on any aspect of the processes in nucleation. The latent heat production during extremely fast growth velocities is

large and may remain sufficiently localized to remelt and detach the neck by which secondaries and higher order dentrite branches are attached to each other. These detached dentrites then either melt or reattach themselves to the growing solid. In the latter instance, they will be misoriented in the process and a spectrum of grain orientations will result.

2.2 Interaction with External Fields :

The advantages of field induced grain refinement are easy application and the low segragation in relation to solute-induced grain refinement. |1|

It is easier to obtain grain multiplication from existing sources than to increase nucleation rates, since existing solids can be easily fragmented by an external field applied to the solidifying system. New solid must arise primarily through the detachment of dentrites from a solid-liquid interface. When portions of solid are detached they will remelt if the temperature is too high, and thus a close control over the thermal environment is necessary to create extensive sources of new grains. Also if the growth rate is rapid, detached detrite bits will not have sufficient time to grow to a macroscopic size and they will be incorporated or occluded by the growing s/L interface.

Dentrite detachment can occur naturally in any system

under the action of natural convection which is generally present and by the separation of fragments, from the top surface and elsewhere, due to density differences between solid and Liquid. When these natural sources are prevented from operating, ingot structures are usually composed of long columnar grains. To increase the natural forces, some method of providing forced fluid motion is needed, and this can be accomplished by mechanical vibration |1,2|, alternating magnetic fields, electric magnetic field interactions, oscillation methods, and ultrasonic fields. In general, while detachment is obtained with all of these external fields, maximum grain refinement is obtained when the detached dentrites are removed from their position near the s/l interface to be redistributed throughout a liquid near its melting point.

2.3 Variations in Concentration :

The chemistry of nucleation can be considered in two different ways. |1|

1- The nucleation of grains may take place in a natural manner in alloy systems, where it is necessary to examine how the kind and quality of alloying elements affect solidifying structures.

2- The nucleation of grains can also be promoted by chemical additives not necessary as alloying elements.

One important feature is that when no purposefully added nucleants are present in a liquid, grain structure is an inherent property of the heat flow and the alloy ; when purposeful nucleants are present, grain structure becomes a function of the heterogeneously added nucleating materials.The term purposeful is used since it is evident that nucleation in alloy melts occurs heterogeneously and when no inoculants are purposefully added, nucleation must take place on some impurity or substrate of which we have little knowledge. However, when purposeful nucleants of inoculants are externally added, their properties can at least be semi-quantitatively described. That is,even though there are no exact theories to predict the efficacy of a given inoculents, certain prescriptions can be catologued. By the way, the efficacy of the titanium- boron on the aluminum castings will be discussed in the next chapters.

It was noted earlier and must now be emphasized, just how important it is to prevent the growth of grains in the general heat flow direction. This can only be accomplished by inhibiting and blocking columnar growth with grains which have either been seperately preserved or freshly nucleated ahead of the solid-liquid interface.

When molten metal is cast into an ingot mold, grains may nucleate ahead of the solid-liquid interface when the temperature gradient reaches a critical value depending upon the solute concentration. We may thus expect a portion of an

ingot, to be finer grained and equiaxed and a proportion of which is columnar, the ratio of the two being a function of the thermal conditions as well as the alloy concentration. No complete theory for the natural formation of equiaxed grains has been developed. However, several descriptions and hypotheses have been out-lined and any or all of dentrite detachment, constitutional supercooling and heferogeneous nucleation at cruible walls may be important depending on the thermal and constitutional nature of the system.

The addition of inoculants has been one of the oldest method to obtain fine grain metallic structures through solidification, and commercial grain refiners are now available for most alloy systems. Epitaxy, low disregistry and high s/l interfacial energy between substrate and solid are necessary attributes for a good inoculant |1|. In addition, density differences between the substrate and liquid should be minimized in order to prevent settling of the inoculants, which must be solid at the solidification temperature of the liquid. A typical example can be afforded by the addition of Titanium and Boron to aluminum which they must be added into the liquid aluminum as master alloy of Al-Ti-B in order to obtain more effective grain refinement.

A term called the disregistry, δ, may be defined as $\delta = \frac{a_\alpha - a_\beta}{a_\alpha}$, $a_\alpha > a_\beta$ where, a_α and a_β are lattice paratemers.

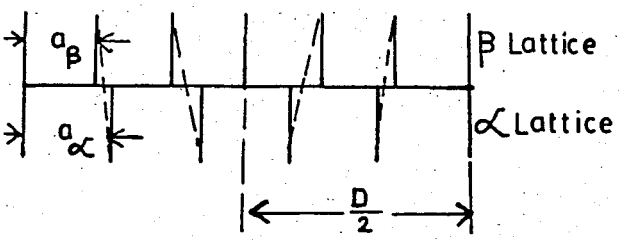

The spacing between the dislocations, D, is related to the disregistry as $D = \frac{a_\beta}{\delta}$ when D becomes sufficiently small one obtains complete disregistry across the boundary and hence an incoherent boundary.

Modifiers are another important type of inoculant extensively studied, as in the Al-Si system. Additions to the melt are required to inhibit the growth of long Si needles and S and P are typically employed for this effect. These elements adsorb on the growing interface affecting the s/l interfaicial energy balance of the Si in the eutectic, which must then repeatedly nucleate (giving in effect a very fine grain size), forming a globular network rather than the needle growth form |1|. As with the choice of an effective inoculant, the suitability of a given modifier can only be determined by painstaking experimental verification.

An important feature of inoculations is that there is a thermal environmental critical for maximum efficiency because nucleation is a process competitive with the growth from an advancing s/l interface. When the size and number of grains are sufficiently high, extension of any columnar growth will be inhibited, and an ingot will be composed of

fine equiaxial grains. However, if the complexes in the melt do not have sufficient time to act, any interface front will merely incorparate the small grains.

Finally, it is important to note the best ways in which inoculants may be added to a melt. Active elements may be introduced in combination with a dispersing agent which becomes gaseous on contact with the melt, because undispersed solid may have insufficient time to dissolve before freezing commences. (in many cases, however, the active elements are so reactive, that vaporization occurs, and the effect of the inoculant fades.) Active ingradients are often added as a wash or coating to the crucible in which freezing to take place so that the turbulance of pouring can remove portions of coating to react with the matrix alloy.

III- TERNARY AL-TI-B MASTER ALLOYS

The grain refinement of aluminum by the addition of Titanium and Boron has attracted so much interest over the years. We have dealt with the practical aspects of grain refinement, and tried to explain theoretically the mechanism by which grain refinement is accomplished by the elements that are added. Today the most common way to grain refine aluminum is by adding special master alloys, but with the exception of some descriptions in the patent literature practically nothing has been written about the production of such master alloys for proprietory reasons. The theoretical or the practical problems in grain refinement can be studied fruitfully with the whole sequence of events during the production and processing of master alloys, their subsequent dilution and contact time, and the nucleation and growth phenomena occuring in the aluminum alloy melt are all seen in one context.

3.1 Al-5Ti-1B MASTER ALLOY (TIBOR)

Titanium in combination with Boron significantly enhances the nucleation process at greatly reduced levels

of addition. This led to the development of master alloy Tibor based on commercially pure (99.7 %) aluminum. Tibor contains 5 % Titanium, 1 % Boron and excess aluminium. This ratio (Ti : B = 5) is found to be most effective as refiner |4-7|. Tibor, because of its superior grain refining performance plays an important part in achieving production of the larger sheet rolling ingot and extrusion billet, now is demanded by the aluminum industry.

A ternary Al-Ti-B alloy in common use contains 5 pct Ti and 1 pct B, and has two crytalline intermetallic compounds primarily discernible in the microstructure,namelly small crystallites of titanium diboride (TiB_2) and larger crystals of aluminides (Al_3Ti). The TiB_2 particles are typically sized about 0.5~2.0 microns in diameter, and located mainly at the cell boundaries. The size distribution and the morpholog of the boride particles are independent of the formation temperature |5|.

While the size and morhology of the boride particles seem to vary very little, this is not the case with the Al_3Ti crytals. Al_3Ti crytals can exhibit several different morphologies and show a marked variation in size. The Al_3Ti particles are typically sized about 5~100 microns in length.

Aluminide particles, in alloys where the titanium was added at a high temperature, have a needle-like appearence, but are really plates, as can be seen in the lower left-hand

corner of Figure 1. These particles are called "flake-like" cystals |5|. The flake-like aluminide crystals are typically sized about 50~100 microns in length.

Figure 1- Typical Microstructure in master alloy where Ti was added at high temperature |5|.

Al_3Ti crytals formed at a low temperature are more compact than the flake-like ones and are also smaller. This type of Al_3Ti particle (figure 2) is called as "block-like" crystal |5|. The block like aluminide crytals are typically sized about 5~30 microns in length. The blocky form of aluminides is dominant in the binary Al-Ti alloy and rod type of ternary Al-Ti-B master alloy. Ingot type ternary Al-Ti-B master alloy contains almost completely flake-like crystals.

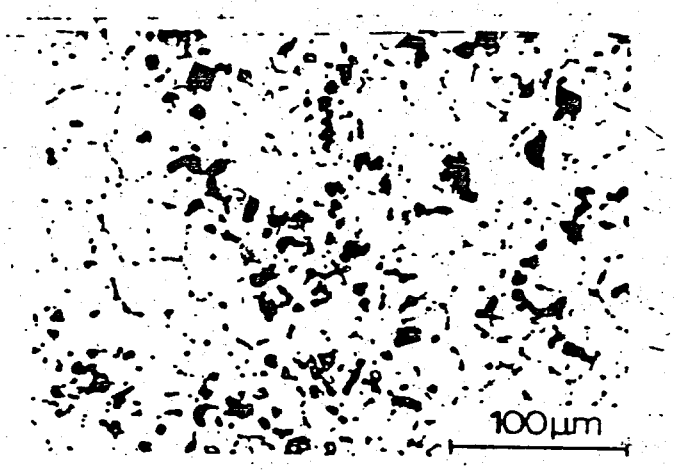

Figure 2- Typical microstructure in master alloy where Ti was added at low temperature |5|.

Quenched alloys have small Al_3Ti crytals of a third morphology, namely the "petal-like" type |5|. Figure 3 shows the typical microstructure of the petal-like crystal.

Figure 3- Typical microstructure in quenched master alloy |5|.

Al_3Ti crytals found in the master alloys can exhibit quite different morphologies, depending on the conditions under which they have formed, and that three main types of crytals can be distinquished : those with "block-like", "flake-like", and "petal-like" aluminide particles. Since it is demonstrated that the morphology of the aluminide crytals seems to influence the optimum grain refinement via the optimum contact time ; it is important to know the conditions causing the shapes of these three types of aluminide particles in the master alloy. Table I reported by L.Backerud et.al. |5|.shows the composition, origin, and aluminide morphology of the different types of the master alloys. Although, an important data is given in Table I about the production of master alloys but there is not any information about the conditions of the commercial master alloys containing 5 pct Ti, 1 pct B and excess aluminum due to proprietory reasons.

Table I. Composition, origin, and aluminide morphology of the Master alloys |5|.

Designation	Concentration Wt%		Temparature at Ti addition ^{o}C	Cooling Rate Ks^{-1}	Aluminide (Al_3Ti) Morphology
	B	Ti			
G	0.4	2	900	0.5	Flake-like
H	0.4	2	750	0.5	Blocky
Q	0.4	2	1000	Quenched	Petal-like
J [x](ingot)	1	5	.....	.....	Flake-like
I [x](Rod)	1	5	.....	.....	Blocky

[x] Commercial Master Alloys.

In the present study, Al-5Ti-1B master alloy containing flake-like aluminide crytals is obtained by the simultaneous adddition of the salts (K_2TiF_6 and KBF_4) into the liquid aluminum (99.7 %) at 900°C with ≈0.6 Ks^{-1} cooling rate. Al-5Ti-1B master alloy containing block-like aluminide crytals is obtained by the simultaneous addition of the salts (K_2TiF_6 and KBF_u) into the liquid aluminum (99.7 %) at 800°C with ~0.6 Ks^{-1} cooling rate.

From the Table I, following results are claimed ;

a) Flake-like aluminide (Al_3Ti) crytals are obtained at high temperature and moderate cooling rate | At low supersaturation or at liquid temperature|.

b) Petal-like aluminide (Al_3Ti) crytals are obtained at high temperature and high cooling rate.

c) Block-like aluminide (Al_3Ti) crytals are obtained at low temperature and moderate cooling rate |At high supersaturation |.

3.2 GROWTH BEHAVIOUR OF THE ALUMINIDE CRYTALS

Aluminide crytals exhibit quite different growth behaviour, depending on the conditions under which they have formed. The following can be said about the growth behaviour of aluminide crytals.

3.2.1 GROWTH BEHAVIOUR OF THE FLAKE-LIKE ALUMINIDE CRYTALS

When all the titanium is in liquid solution before cooling and the cooling rate is moderate, the growth is controlled by long-range diffusion and is dentritic (Figure 4a). The dentrite arms grow in <110> directions. Growth is restricted in the |001| directions, so the crytals are almost two-dimensional, but occasionally a new layer can nucleate on the (001) plane. This second layer has the same growth behaviour as the first one |5| .

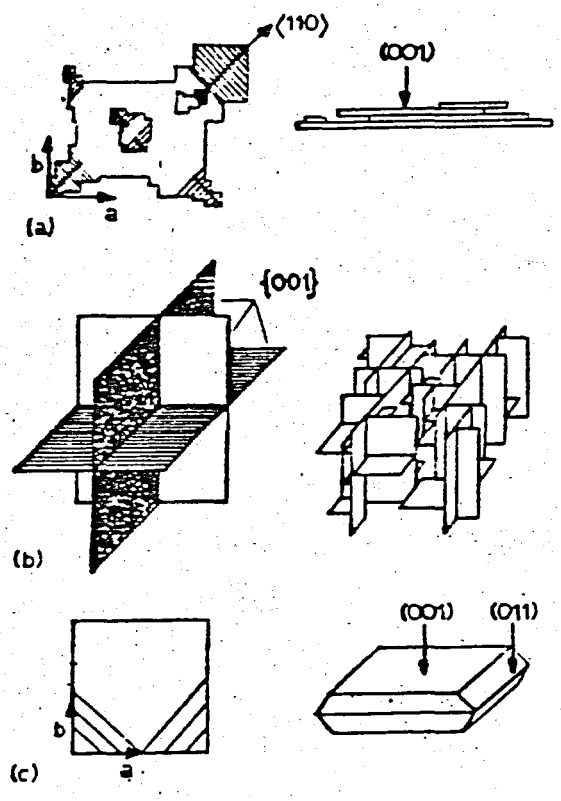

Figure4- Schematic drawings of Al_3Ti crytals with different Morphologies, showing boundary planes |5|.

(a) flake-like ; (b) petal-like ; (c) block-like

3.2.2 GROWTH BEHAVIOUR OF THE PETAL-LIKE ALUMINIDE CRYTALS

If the cooling rate is high or the titanium concentration low, another growth mechanism starts to operate. Under these conditions the titanium concentration at the edges of a growing plate will soon be very low and growth will be retarded. The temperature will drop and, at some undercooling, twinning of the crytal will occur with the c-axis of the new crytal prependicular to the c-axis of the old one. The new crystal can grow until titanium is again depleted at the edges, and thus growth will proceed by repeated twinning. This growth mechanism results in the petal-like crytals shown in Figure 4b |5|.

3.2.3 GROWTH BEHAVIOUR OF THE BLOCK-LIKE ALUMINIDE CRYTALS

If supersaturation is very high, frequent nucletion of new layers on the {001} planes can occur. Once nucleated, a layer will spread by lateral advance of the step bounding the layer. The crytals are faceted and show well developed {001} and {011} surfaces, as shown in Figure 4c |5|.

Finally, master alloys containing mostly block-like aluminides are associated with short optimum contact times, while master alloys with mainly flake-like or petal-like

crytals need a longer contact time to develop maximum grain refinement |5,6|.

IV- THE MECHANISM OF GRAIN REFINEMENT OF ALUMINUM CASTINGS INOCULATED WITH AL-TI-B MASTER ALLOYS

It is well known that addition of Ti produces grain refinement in aluminum alloys. It is also well estaslished that additions of Boron of Titanium-bearing alloys enhance the grain refinement |7|.

There have been papers written about the mechanism of grain refinement of aluminum by adding Al-Ti-B and Al-Ti-B master alloys. It is currently accepted that Al_3Ti crytals are responsible for the nucleation at concentrations above 0.15 Wt % Ti (Peritectic point) via a peritectic reaction (Liquid Al + $TiAl_3$ — α_{Al}) (See Figure 5). For hypoperitectic compositions, where the Al_3Ti phase is not stable, (concentration of Titanium is less than 0.15 Wt % Ti) there are two main theories advanced to explain this phenomenon :

1) The "Boride-carbide theory"
2) The "Peritectic reaction theory"

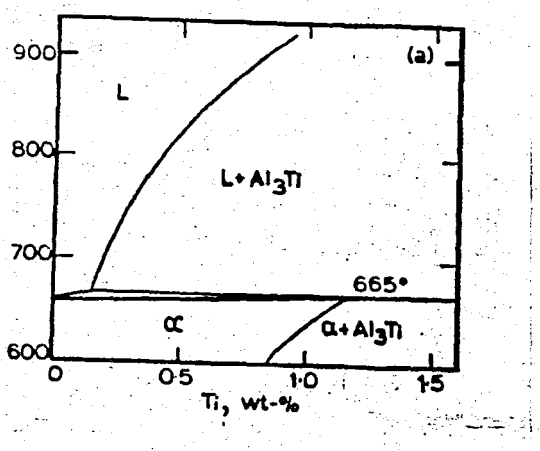

Figure 5- Al-rich section of phase diagram for Al-Ti system |10|.

4.1 THE "BORIDE-CARBIDE THEORY"

Cibula |11| has shown that when carbides of Ti and borides of aluminum and Titanium are present in aluminum alloys, pronounced grain refinement is produced through nucleation. The main arguments for the nucleation being due to the carbides or borides are :

1) The carbides and borides are very stable (have very high melting points) (see Table II). The TiB_2 particles are insoluble and are distributed evenly throughout the melt. The $TiAl_3$ phase, however, is soluble and quickly dissolves in the melt. The combination of TiB_2 particles and the excess dissolved Ti from the $TiAl_3$, is essential for a good

grain refining effect.

2) The atomic spacing in the close packed planes of the borides are only a few percent different from the corresponding spacing in aluminum.

Table II. Properties of boride and aluminide particles

	Melting Point (^{o}C)	Density (g/cm^3)	Crystal Structure	Lattice parameters α (A^{o})	C (A^{o})
Al	660	2.7	fcc	4.050	-
TiB_2	2850	4.38	Hexagonal	3.0311	3.2291
AlB_2	975	3.16	Hexagonal	3.009	3.252
$TiAl_3$	1340	3.36	Body Centered Tetragonal	3.86	8.68

4.2 THE "PERITECTIC REACTION THEORY"

The peritectic reaction theory is supported by Mondolfo |7| and Backerud |4,5|. The boride theory suggests that TiB_2 nucleates aluminum, and that the Al_3Ti particles in the master alloy used disolve rapidly to-create constitutionally favourable growth conditions for the aluminum grains. However, the peritectic theory assumes that surviving Al_3Ti particles nucleate the aluminum grains via a peritectic reaction. The role of the boride crytals would then be to nucleate the aluminide crytals or to stabilize them by various

mechanisms. The following series of events proposed by Backerud eplains the grain refining mechanism when TiB_2 particles are added to an aluminum melt|4| :

1) TiB_2 + Al ——(Ti,Al) B_2 + Ti

2) Ti + 3Al —— Al_3Ti

3) Al_3Ti + Liq.—— α_{Al} |Peritectic Reaction|

4.3 SOURCE OF GRAIN REFINEMENT ACTION

4.3.1 EFFECTS OF TITANIUM

Experience has shown that, of all the solute elements added to commercial or pure aluminum singly, the most effective in grain refinement action on casting is Titanium, though there is little accord about the mechanism involved. The influence of Titanium on the nucleation of aluminum crytals has been argued to be due to either to

1) a form of constitutional supercooling,or

2) its presence in effective heterogeneous nuclei.

1) Solute Titanium :

Moriceau |12| claimed that the grain-refining effeciency of solute Titanium was due to its power to restrict the growth of previously nucleated crytallites of aluminum, and (from the relevant part of the binary phase-diagram Al-Ti) he cited as index of this power the product (Solute distribution ratio x Slope of Liquidus). This index is useful

in quantifying effects due to constitutional supercooling, and in aluminum is highest for solute Titanium. However, in dilute solution, this kind of index has much more relevance for eutectic systems (e.g Al-Cu) than for peritectic systems (e.g. Al-Ti) because the maximum extent of the constitutional supercooling feasible, being roughly related to the difference in composition between the alloy used and that at the lower end of the relavant liquidus is large (for eutectic systems) and very small (for peritectic systems).

To take a quantitative example : after allowing for insoluble Ti it may be accepted that in commercial grain-refining practice a typical concentration of disolvèd Titanium may be 0.002 pct by mass. By reference to the binary system Al-Ti, from which the quantitative reference points 0.0 pct Ti, 660^{o}C (Melting point of pure aluminum) and 0.15 pct Ti; 665^{o}C (peritectic point) are taken and from Henry's law,the maximum elevation of the liquids relative to the freezing point of pure aluminum, which is all that is available for constitutional supercooling, is seen to be only about $|(665-660)/0.15|x0.002$ ^{o}K, equal to about 0.07 ^{o}K.

This presumably ineffective level is to be compared with the sometimes tens of Kelvins of constitutional supercooling which can occur in uncontrolled coring of dilute alloys of eutectic character. Of course, normal supercooling can still occur.

It therefore seems likely that, at these very low levels of Titanium addition, even allowing for some excess of Titanium over that required for stoichiometry with boron, the effect of constitutional supercooling by solute Titanium will add only a negligible amount of grain refinement by restriction of grain growth. In any case, all such supercooling effects can operate only as a secondary process which is wholly dependent on prior succesful nucleation |6|.

2) Hetergeneous Particles containing Titanium :

The argument supporting the theory of hetergeneous nucleation is more popular than the constitutional supercooling effect of solute titanium. But there is no consensus even as to the identity of the effective nucleant, or about why a particular nucleant should be effective. The two main schools of thought about the mechanism of nucleation are, 1) the Peritectic theory and 2) the boride theory which are described above.

4.3.2 Effects of Boron

The better grain refinement produced by addition of boron to aluminum-titanium alloys is not due to nucleation of aluminum by borides. Boron produces two effects |7| :

1) It expands the field of primary crytallization of $TiAl_3$ to lower Titanium contents by reducing the solubility of Titanium in Liquid aluminum. This results in grain

refinement at lower Titanium contents.

2) Boron also steepens the slope of the liquidus. In the liquid there are many solid particles which can nucleate $TiAl_3$ at different undercoolings. If the liquidus line is relatively flat as shown in Figure 6a, a slight undercooling (ΔT_A) produces a pronounced supersaturation(x), which leads to nucleate on the available heterogeneous centers. If the liquidus is very steep, as in Figure 6b, the same supersaturation requires a much larger undercooling (ΔT_B) that permits nucleation not only on the same centers, but also on many other centers that act at higher undercooling. In addition, the time to cool from the temperature at which $TiAl_3$ is nucleated to that at which aluminide (Al_3Ti) nucleates aluminum is longer in case(a) and much coagulation and growth of Al_3Ti particles takes place, further reducing the number of nuclei. This explains the more pronounced grain refinement, as shown in Figure 7 d, that is obtained by boron additions |7|

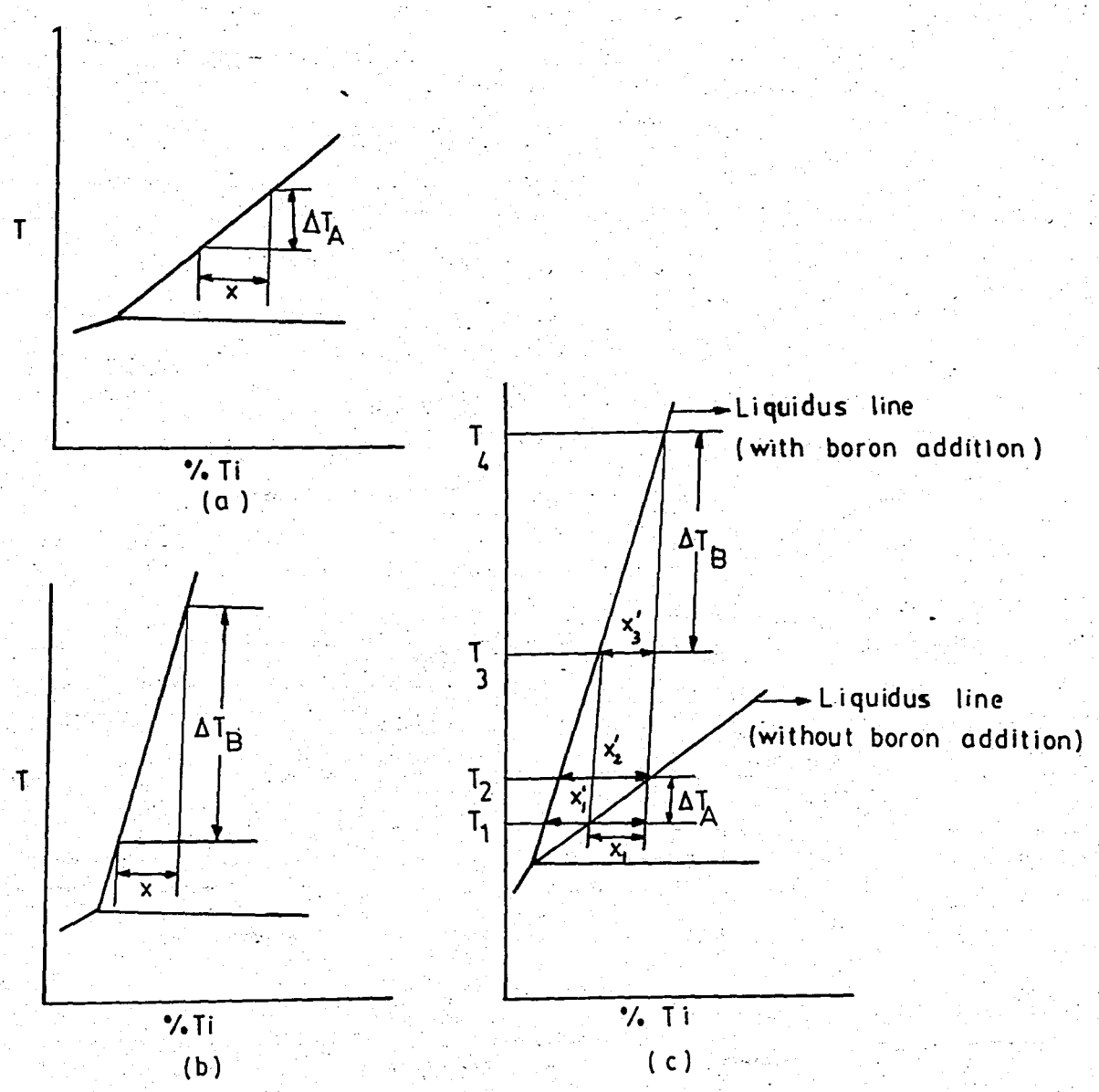

Figure6- Effect of Liquidus slope on undercooling for nucleation (a) Supersaturation x is reached with ΔT_A ; (b) The same supersaturation is reached with much larger ΔT_B ; (c) Effect of Boron addition on the liquidus slope.

From the Figure 6c, The following results are obtained ;

1) At temperature T_1 ; a) with Boron (supersaturation X_1')
b) without Boron (supersaturation X_1)

Since supersaturation (X_1') is greater than X_1 due to boron addition the nucleation rate of Al_3Ti particles is greater in castings with boron addition than castings without boron addition.

2) At temperature T_2 ; a) with B (supersaturation X_2')
b) without B (There is no supersaturation, all of the alloy is in saturated liquid state)

3) At temperature T_3 ; a) with B (Supersaturation X_3')
b) without B (There is no supersaturation, alloy is in Liquid State)

The supersaturation (X_3') of the alloy with Boron at temperature T_3 is equal to the supersaturation (X_1) of the alloy without Boron at temperature T_1, but undercooling ΔT_B of the alloy with Boron is greater than undercooling ΔT_A of the alloy without Boron.

4) At temperature T_4 ; a) with B (There is no supersaturation, alloy is saturated Liquid state)
b) without B (There is no supersaturation, alloy is in Liquid state)

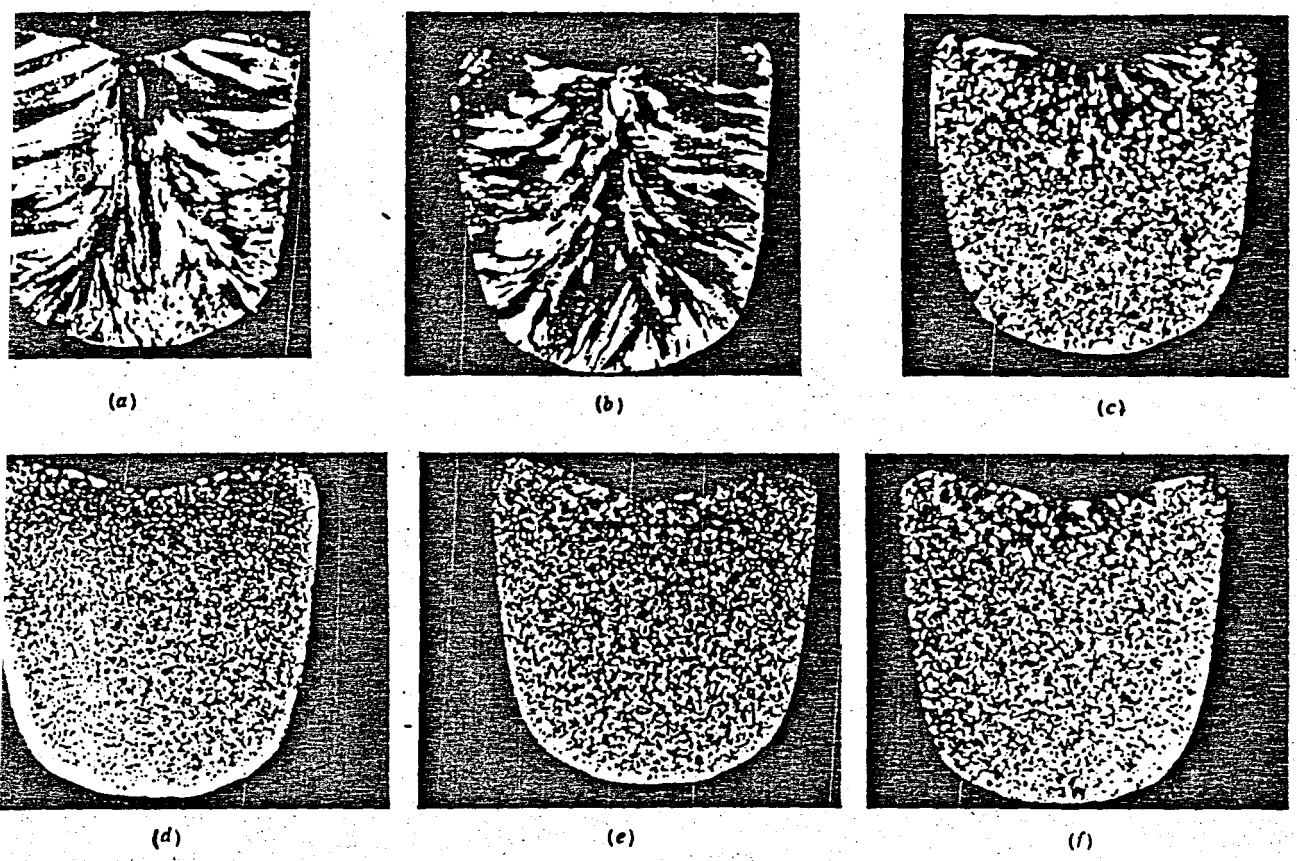

Figure7- Effect of Ti-B ratio on grain size. All samples natural size. (a) Coarse(C), 0.00 pct. Ti, 0.06 pct B ; (b) Coarse (C), 0.04 pct Ti,0.04 pct B ; (c) Medium fine (MF), 0.10 pct Ti, 0.025 pct B ; (d) Very fine (VF), 0.12 pct Ti, 0.022 pct B ; (e) Very fine (VF), 0.15 pct Ti, 0.001 pct B ; (f) Fine (F), 0.20 pct Ti, 0.00 pct B |7|

4.4 Grain Refining Effects of Boride and Aluminide Particles

In order to throw more light on the mechanism of grain refinement of aluminum by adding Al-Ti-B master alloy, the effects of each particle (TiB_2, $TiAl_3$) will be explained below.

4.4.1 Grain Refining Effect of Boride Particles

AlB_2 and TiB_2 are isomorphous with lattice parameters a = 3.009 ^{o}A, c = 3.252 ^{o}A, and a = 3.011 ^{o}A, c = 3.2291 ^{o}A, respectively. A ternary $(Al,Ti)B_2$ phase where aluminum atoms have replaced Titanium atoms randomly in the TiB_2 lattice would show cell parameters somewhere between the values for pure AlB_2 and pure TiB_2.

Holding the diluted master alloy samples for prolonged times does not change the lattice parameters of the TiB_2 phase. However, a careful examination of the diffractograms shows that the samples taken immediately after dilution(short holding time ~3 min) all contain small amounts of the AlB_2 phase and that the diffraction peaks obtained from the TiB_2 phase are broadened towards the AlB_2 side, indicating that some $(Al,Ti)B_2$ phase is also present. After a holding time of 3 h, all traces of the AlB_2 diffraction lines have disappeared and the TiB_2 lines have become sharp in all cases. These therefore indicate that no stable $(Al,Ti)B_2$ phase, where Titanium and aluminum atoms are randomly interchangeable, exists|5|. The occurence of $(Al,Ti)B_2$ and AlB_2 phases in Al-Ti-B master alloys is a result of the order and the way in which the alloying elements are added, and the time allowed for the reaction to be completed. After some holding time all boride particles seem to convert into TiB_2 phase.

The great majority of the particles in all master alloys investigated consisted of hexagonal crytals, some single and some twinned (see Figure 8 and 9). The size of these crytals varied between 0.05 an 3 μm [5].

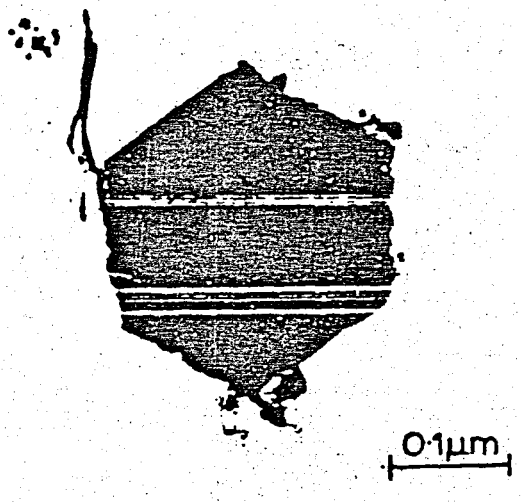

Figure8- TiB_2 crytals of hexagonal morhology[5].

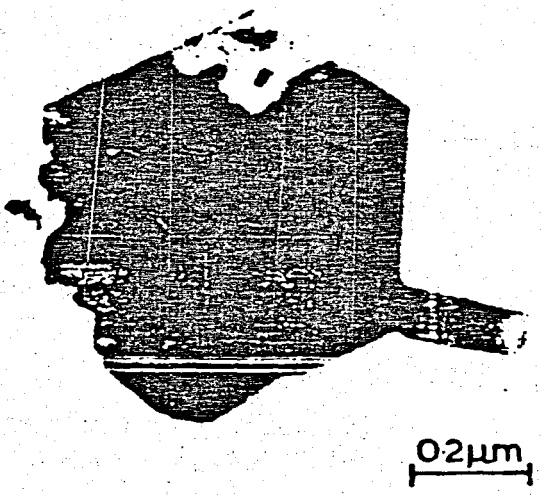

Figure9- Twinned TiB_2 crytals [5].

The electron-diffraction patterns and x-ray spectra from extracted particles showed that these were mainly TiB_2. All boride crytals exposed the same boundary faces,namely {100} and {001}. The twinning of TiB_2 crytals gives rise to re-entrant grooves of 60^o,90^o and 120^o. According to the classical theory of heterogeneous nucleation, these grooves should be preferred sites for nucleation, if nucleation does

start on boride particles. The other important effect of TiB_2 particles can be explained as the following way ;

An aluminide (Al_3Ti) phase slowly develops around boride particles ; titanium atoms in the TiB_2 phase are substituted by aluminum atoms.

$$|TiB_2 + Al \longrightarrow (Al,Ti)B_2 + Ti|$$

The titanium atoms rejected from the TiB_2 phase would create a layer around the boride particles with a higher titanium concentration than in the surrounding melt, so that the Al_3Ti phase could form or survive at least for a limited time at the surface on the TiB_2 phase, even in hypoperitectic alloys (<0.15 wt % Ti).

$$|Ti + 3Al \longrightarrow Al_3Ti|$$

Such aluminide (Al_3Ti) particles were observed to develop during a holding time in the melt of a few hours |5|.

After long holding time, as used by Morimune et al. |5|, the ternary boride phase $(Al_{0.06}Ti_{0.94})B_2$ must be completely developed and no transport of titanium atoms from the inside of the boride particles can occur. Under these conditions the aluminide phase must dissolve again as it is not thermodynamically stable at the low concentration level employed. The final result of this process would be boride particles with an ordered, aluminum-containing structure.

4.4.2 Grain Refining Effect of Aluminide Particles

Aluminide crytals have body-centered-tetragonal (bct) cell structure and lattice parameters a = 3.86 and c = 8.68 $\mathring{A}$ (Ti atoms at 0,0,0 etc. ; Al atoms at 0,0,1/2, etc., and at 0,1/2,1/4 etc.) |5|. (See Figure 10).

The existence of a preferred orientation relationship between

Al_3Ti and Al suggests that the aluminide crytals (Al_3Ti) have been active as substrates for the nucleation of aluminum in the alloys produced by using tibor (Al5Ti1B) master alloy addition. The orientation relationship found in the two structures of $TiAl_3$ (bct) and Al(fcc) can, within experimental error, be expressed as $(011)_{Al_3Ti} \; || (012)_{Al}$; $[010]_{Al_3Ti} \; || [010]_{Al}$ or $(001)_{Al_3Ti} \; || (010)_{Al}$; $[010]_{Al_3Ti} \; || [010]_{Al}$.

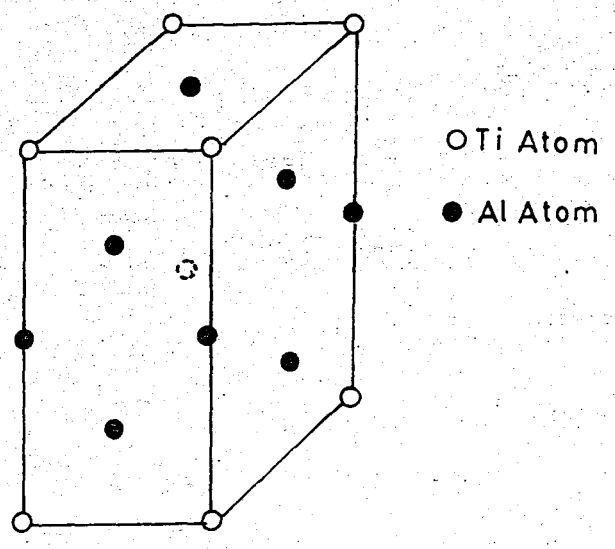

Figure10- Body-centered-tetragonal Al_3Ti lattice structure.

The atomic distributions in the $(011)_{Al_3Ti}$ and $(012)_{Al}$ lattice planes are similar (See Figure 12 a and 14 a). A comporison of the atomic distributions in the $(001)_{Al_3Ti}$ and $(010)_{Al}$ planes also shows a good crytallographic match between these planes (see Figure 12 b and 14 c).

The linear disregistries shown below imply that the surface energy between $(011)_{Al_3Ti}$ and $(012)_{Al}$ on the one hand, and $(001)_{Al_3Ti}$ and $(010)_{Al}$ on the other, are low. It should be noted, however, that the $(001)_{Al_3Ti}$ plane is occupied by both Al and Ti atoms, while the $(011)_{Al_3Ti}$ surface is occupied by three successive layers of Al atoms which can be regarded as somewhat distorted $(012)_{Al}$ lattice planes, see Figure 11. Nucleation of aluminum on the $(011)_{Al_3Ti}$ surface then merely requires the continuing growth of this existing distorted aluminum lattice. Thus, from a crytallographic point of view, the block-like Al_3Ti crytals which exhibit {011} planes should be very suitable, and probably more efficient than flake-or petal-like crytals, as substrates for heterogeneous nucleation of aluminum.

The basic difference between the nucleation by the two types of crytals (Aluminides and Borides) is that, whereas $TiAl_3$ can nucleate aluminum solid solution without undercooling and in most cases (through the peritectic reaction), at temperatures above the freezing point of aluminum ($660^{o}C$), Borides (AlB_2,TiB_2 and $(Al,Ti)B_2$)

require some undercooling below the freezing point of aluminum to nucleate it. Normal impurities tend to nucleate aluminum with very limited undercooling, thus the borides have little or no chance to be effective nucleants |7|.The peritectic reaction facilitates grain refinement by insuring nucleation of aluminum by $TiAl_3$ before the normal impurities can act.

$$Al_3Ti + Al_{liq} \longrightarrow \alpha_{Al} \quad \text{(Peritectic Reaction)}$$

The following result is claimed from the above discussion ; Surviving aluminides (Al_3Ti) particles nucleate the aluminum grains via a peritectic reaction. The peritectically nucleated grains generally remain very tiny. After nucleation, these new grains surrounded by liquid of aluminum can act as heterogeneous sites on which the primary phase (α_{Al}) will nucleate when the temperature gradient becomes sufficiently small. An important feature of peritectic nucleation is that the nucleated grains are formed inside the melt, and an otherwise uncontaminated or clean interface is exposed for nucleating the matrix phase (α_{Al}) and thus to the equiaxed zone. The occurence of equiaxed zone in the solidified structure causes the grain refinement of aluminum castings.

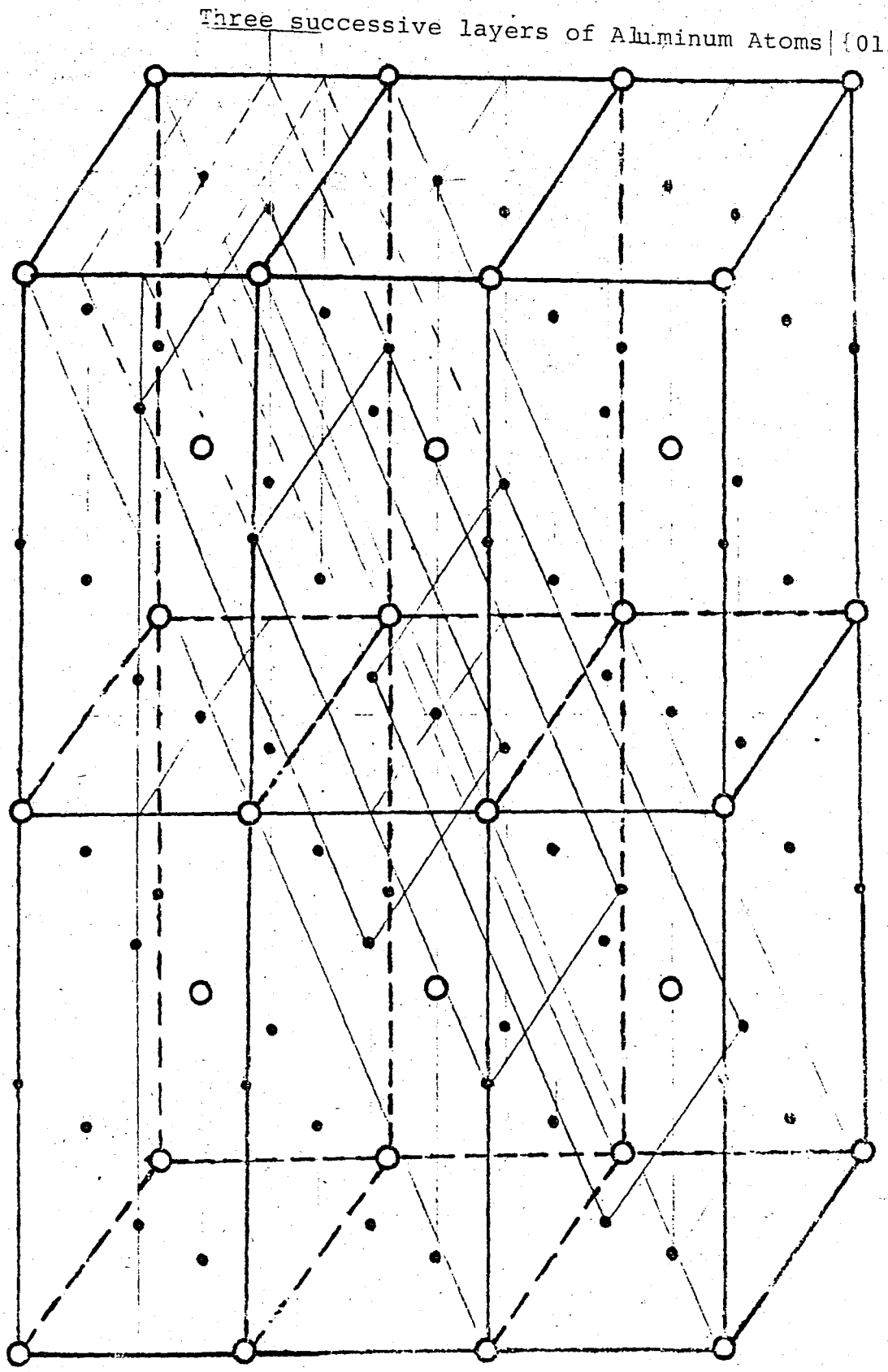

Figure 11 Aluminide (Al_3Ti) structure, showing some of the {011} lattice planes (O Ti atom ; ● Al atom).

Titanium Atoms : 8 x (1/8) = 1 at the corners

1 x 1 = 1 at the lattice center

There are two Ti atoms in an aluminide (Al_3Ti) lattice

Aluminum Atoms : 4 x (1/4) = 1 at the lattice edges

10 x (1/2) = 5 at the lattice surfaces

There are six aluminum atoms in an aluminide (Al_3Ti) lattice

Ti/Al = 2/6 = 1/3 $\Longrightarrow$ Al_3Ti

This lattice structure corresponds Al_3Ti molecular structure.

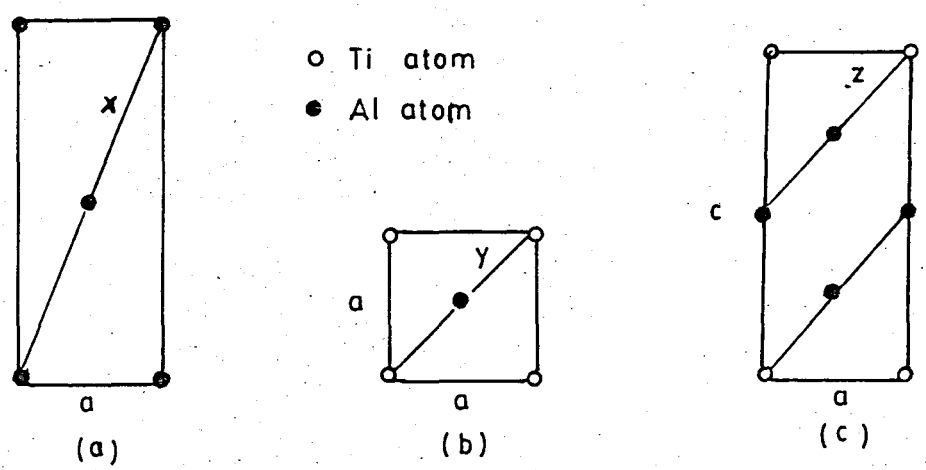

Figure 12— Different planes in Al_3Ti lattice.

(a) (011) plane ; (b) (001) plane (c) (010) plane

For Bct Al_3Ti Lattice ; a = 3.86 $\overset{0}{A}$; c = 8.68 $\overset{0}{A}$

From Figure 11 and 12 (a) ;

Distance between atoms on the diagonal of {011} planes of Al_3Ti Lattice is 5.1269 $\overset{0}{A}$ in length (x).

From Figure 12(b) ;

Distance between atoms on the diagonal of(001) plane of Al_3Ti

Lattice is 2.7294 $\overset{0}{A}$ in length (y).

From Figure 12(c) ;

Distance between atoms on the diagonal of (010) plane of Al_3Ti lattice is 2.9041 $\overset{0}{A}$ in length (z).

Aluminum Lattice Structure (Fcc)

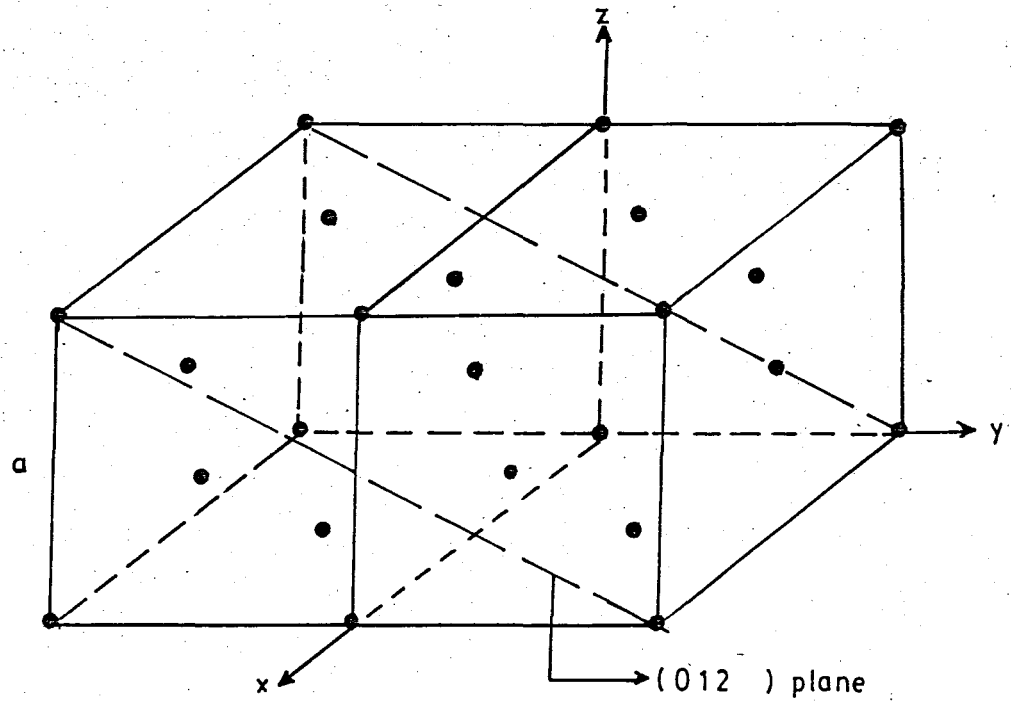

Figure 13 - Face-centered-Cubic Aluminum lattice structure.

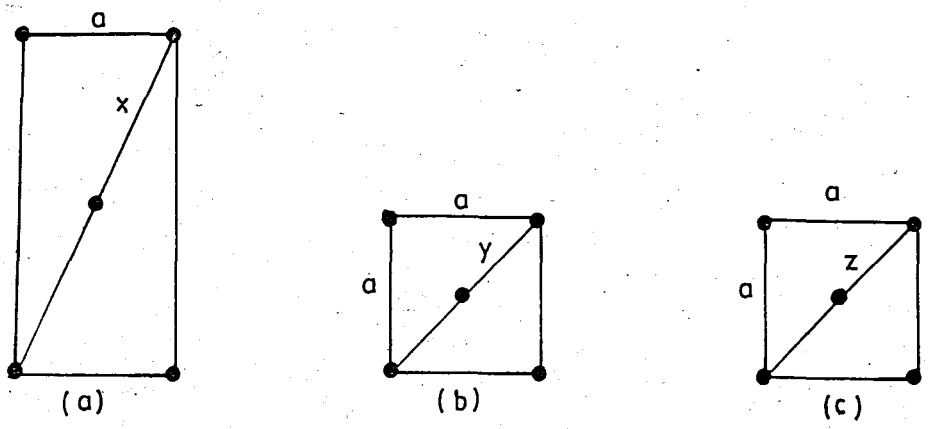

Figure 14 - Different planes in Aluminum lattice.

(a) (012) plane ; (b) (001) plane (c) (010) plane

For Fcc Aluminum lattice ; a = 4.050 $\overset{0}{A}$

From Figure 13 and 14(a)

Distance between atoms on the diagonal of (012) plane of Al Lattice is 4.9602 $\overset{0}{A}$ in length (x).

From Figures 14(a) and 14(b)

(010) aluminum plane is the same as (001) aluminum plane.

Distance between atoms on the diagonals of (001) and (010) planes of aluminum lattices are 2.8638 $\overset{0}{A}$ in lengths (y and z).

The Linear disregistries between aluminum and aluminide (Al_3Ti) lattices are given below :

a) Between the atoms on diogonals of (012) aluminum planes and {011} aluminide planes ;

   100 x (5.1269-4.9602)/ 5.1269 = 3.25

b) Between the atoms on short sides of (012) aluminum planes and {011}aluminide planes ;

   100 x (3.86-4.050)/3.86 = -4.9223

c) Between the atoms on sides of (001) aluminum planes and (001) aluminide planes ;

   100 x (3.86-4.050)/ 3.86 = - 4.9223

d) Between the atoms on diagonals of (001) aluminum planes and (001) aluminide planes ;

   100 x (2.7294-2.8638)/2.7294 = -4.9242

e) Between the atoms on sides of (010) aluminum planes and short sides of (010) aluminide planes ;

100 x (3.86-4.050)/3.86 = -4.9223

f) Between the atoms on sides of (010) aluminum planes and long sides of (010) aluminide planes ;

100 x (4.34-4.050)/4.34 = 6.6820

g) Between the atoms on diagonals of (010) aluminum planes and (010) aluminide planes ;

100 x (2.9041-2.8638)/2.9041 = 1.3877

4.5 Results Obtained By The Previous Workers

Detailed studies related to the grain refinement of aluminum and production of Al-Ti-B master alloys were performedby L.Backerud, L Arnberg, H.Klang |5| and by G.P Jones, J.Pearson|6|, and by J.A.Marcantonio, L.F.Mondolfo |7 .

L. Backerud |4,5| studied a great number of Al-Ti and Al-Ti-B master alloys varying parameters such as the order of addition of the alloying elements, the relative and absolute amounts of titanium and boron, the temperature of addition, the holding time before cooling, and the cooling rate. Table III shows preparation of binary Al-Ti and ternary Al-Ti-B master alloys by addition of salts (K_2TiF_6 and KBF_4) at different temperatures. Samples A-C were made by simultaneous addition of the salts at different temperatures and in amounts that gave titanium and boron concentrations of 0.88

and 0.40 wt %, respectively. The concentration ratio Ti/B corresponds to the stoichiometric ratio in the compound TiB_2 and these alloys are called as stoichiometric alloys. Some binary Al-Ti (D and E) and ternary Al-Ti-B (F-H) alloys were also made by adding salts to liquid aluminum at different temperatures. Samples Q_1 and Q_2 were prepared by adding KBF_4 at 750°C, raising the temperature to 1100°C or 900°C, and then adding the titanium. After the addition of the salts, samples Q_1 and Q_2 were quenched on a cold copper plate. Two commercial master alloys given in Table III are designated I and J and are of the rod and ingot type, respectively. The addition temperatures of the salts are not given in Table III for these two commercial master alloys.

TableIII- Prepartion of binary Al-Ti and Ternary Al-Ti-B master alloys by addition of salts at different temperatures.[5]

Alloy designation	Ti addition temperature, °C	B addition temperature, °C	Concentration, wt %	
			Ti	B
A	750	750	0.88	0.40
B	900	900	0.88	0.40
C	1100	1100	0.88	0.40
D	750		2.0	
E	1100		2.0	
F	1100	1100	2.0	0.4
G	900	900	2.0	0.4
H	750	750	2.0	0.4
I (rod)[x]	-	-	5	1
J (ingot)[x]	-	-	5	1
Q_1 quenched	1100	750	2.0	0.4
Q_2 quenched	900	750	2.0	0.4

[x]Commercial Master Alloys.

L.Backerud tested the efficiencies of all the master alloys as grain refiners of aluminum and the time characteristics, i.e. the change in grain-refining potency with contact time, were determined. Table IV shows the results of grain-refinement test for samples grain refined with different master alloys and solidified after different contact

times. Each master alloy was tested as a grain refiner by adding master alloy to ~60 g. of molten aluminum (99.7 %) in a graphite crucible at 750°C. The melt was stirred with a graphite rod for 2 min immediately after addition and allowed to stand and cool at a rate of ~0.5 Ks^{-1}.

The concentrations of Ti and B were 0.03 and 0.006 wt. %, respectively. In same cases a stoichiometric alloy was added to aluminum at 750°C, in an amount corresponding to the same boron concentration of 0.006 wt. % (0.0132 Wt Ti), and held at this temperature for 5,30,60,or 120 min before a binary Al-Ti alloy was added to give a total titanium concentration of 0.03 Wt %. In other samples the stoichiometric and the Al-Ti alloys were added simultaneously.

TableIV Results of grain-refinement test for samples grain refined with different master alloys and solidified after different contact times |5|

Sample Number	Master alloy added	Al_3Ti Morphology	Contact time, min TiB_2	Contact time, min Al_3Ti	Grain refinement (See Fig.15)
1	A	...	5	...	1
2	A	...	60	...	1
3	B	...	5	...	1
4	B	...	60	...	1
5	C	...	5	...	1
6	C	...	60	...	1
7	A†D	Blocky	10	5	4
8	A†D	Blocky	35	5	4
9	A†D	Blocky	65	5	4
10	A†D	Blocky	125	5	4
11	C†D	Blocky	10	5	4
12	C†D	Blocky	35	5	4
13	C†D	Blocky	65	5	4
14	A†D	Blocky	125	5	4
15	A†E	Flaky	10	5	2
16	A†E	Flaky	35	5	2
17	A†E	Flaky	65	5	2
18	A†E	Flaky	125	5	2
19	D	Blocky	...	5	4
20	D	Blocky	...	60	1
21	E	Flaky	...	5	2
22	E	Flaky	..	60	1
23	A†E	Flaky	5	5	3
24	A†E	Flaky	60	60	3
25	A†E	Flaky	120	120	2
26	A†D	Blocky	5	5	5
27	A†D	Blocky	60	60	2

Sample Number	Master alloy added	Al_3Ti Morphology	Contact time, min TiB_2	Contact time, min Al_3Ti	Grain refinement See Fig 15
28	A†D	Blocky	120	120	1
29	F	Flaky	5	5	2
30	F	Flaky	30	30	3
31	F	Flaky	60	60	4
32	F	Flaky	120	120	4
33	G	Flaky	5	5	2
34	G	Flaky	30	30	3
35	G	Flaky	60	60	5
36	G	Flaky	120	120	5
37	H	Blocky	5	5	6
38	H	Blocky	30	30	4
39	H	Blocky	60	60	3
40	H	Blocky	120	120	2
41	I	Blocky	5	5	6
42	I	Blocky	30	30	5
43	I	Blocky	60	60	4
44	I	Blocky	120	120	3
45	J	Flaky	5	5	3
46	J	Flaky	30	30	4
47	J	Flaky	60	60	6
48	J	Flaky	120	120	6
49	Q_1	Petal	5	5	3
50	Q_1	Petal	60	60	5
51	Q_2	Petal	5	5	3
52	Q_2	Petal	60	60	5

Summarizing the grain refinement results from Table IV, the followings emerge ;

a) grain refinement can not be achieved by using a stoichiometric alloy (sample 1-6)

b) the grain refinement is independent of the temperature at which the boride particles formed (samples 7-14)

c) the grain refinement is also independent of the contact time allowed for the the TiB_2 crytals (this statement is verified by samples 7-18)

d) the grain refining efficiency decreases with contact time for the addition of binary Al-Ti master alloys, as well as for the simultaneous addition of a stoichiometric and an Al-Ti master alloy, irrespective of the morphology of the Al_3Ti crytals (samples 19-28)

e) the grain refinement improves with contact time when ternary Al-Ti-B master alloys containing flake or petal-like aluminide particles are used whereas it is reduced when Al-Ti-B master alloys with blocky Al_3Ti crytals are added (Samples 29-52).

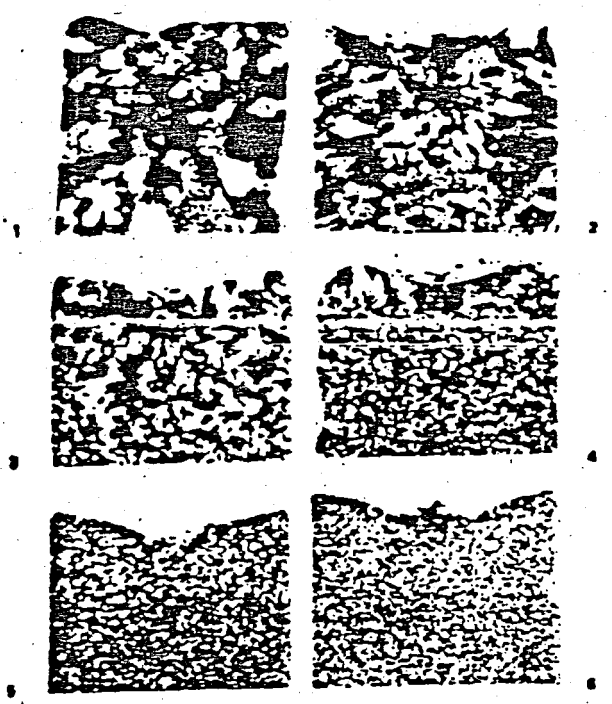

Figure 15 - Grain refinement scala, natural size|5|.

G.P Jones and J. Pearson |6| studied the development of grain-refining techniques for the casting of aluminum and the results achieved using additions of ternary Al-Ti-B master alloys were described. They obtained grain refining curves and investigated master alloy characteristics. A typical grain refining curve is seen in Fig 16. A typical grain refining curve has two distinct sections : after addition of the grain refiner, the grain-size initially decreases with time (the line AO), reaching a minimum-the "ultimate grain-size"-at 0. The time to reach this point is generally referred to as the "contact-time" of the grain-refiner. After this, further holding gives only increasing grain-size, the upward line OB indicating the phenomenon known as "fade".

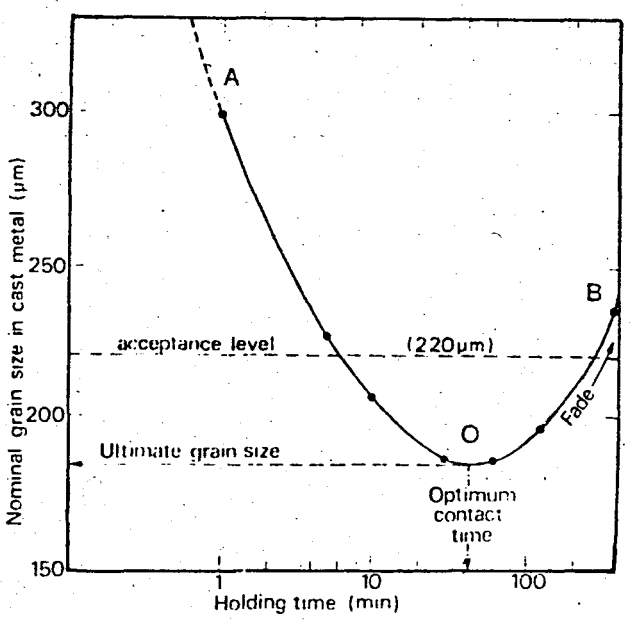

Figure 16- Typical form of grain-refining curve |6|.

Figure-17 shows the results using three different types of grain-refining additive, all used rates which produce the same increase in the titanium content of the bulk melt, namely 0.005 pct. The additives are the salt mixture of K_2TiF_6 and KBF_4 in tablet form, an Al-6 pct Ti binary master-alloy, and the ternary master alloy Al-5pct Ti-1pct B. From the Figure-17, relative positions of the curves show not only that the ternary alloy is superior to the binary alloy, revealing that boron has a very significant effect on grain-refining performance, but also that the ternary alloy is superior to the salt mixture,even though the mixture introduces both titanium and boron into the melt. The ternary Al-5 % Ti-1 % B master-alloy is usually about 4 or 5 times more efficient than a binary Al-6 pct Ti master alloy, or salt tablets. They presume that the nucleant particles formed from the salts might either be not active as those introduced by the master-alloy, or are perhaps much larger and consequently present in fewer numbers |6|.

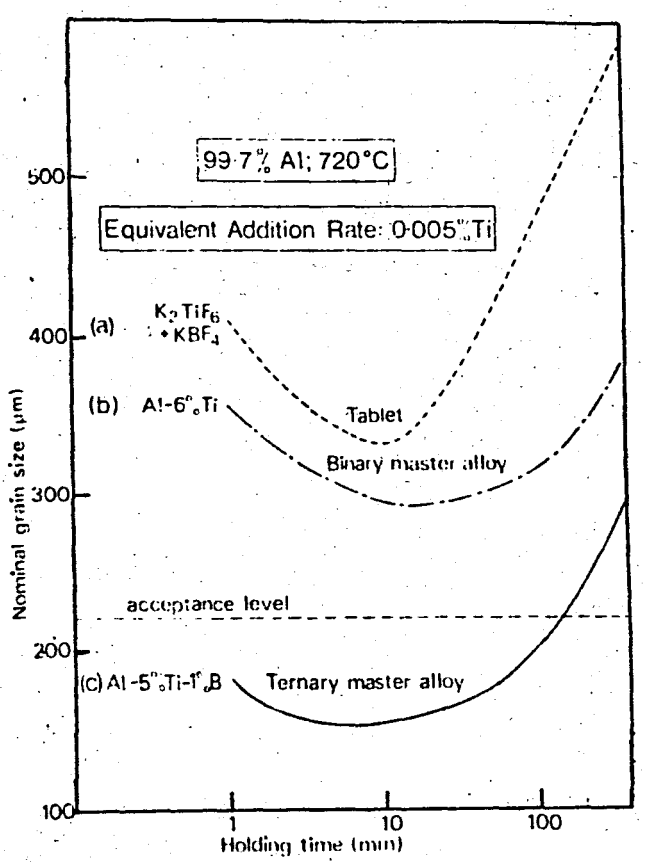

Figure 17 - Comparison between different grain-refining agents at equivalent addition rates |6|.

J.A. Marcontonio and L.F. Mondolfo|7| investigated the effect of boron on the grain refining performance of master alloys (Figure 7). They showed that, the addition of boron to aluminum-titanium alloys expands the field of primary crystallization of $TiAl_2$ toward lower titanium contents and steepens the liquidus and in equilibrium conditions, pronounced grain refinement is found only in alloys in which $TiAl_3$ is primary and nucleates the aluminum solid solution before other impurity can act.

Many Workers have dealt with the practical aspects of

grain refinement, some of them have tried to explain theoretically the mechanisms by which grain refinement is accomplished by the elements that are added. For proprietory reasons, practically nothing has been written about the production of commercial master alloys with the exception of some descriptions in the patent literature.

In this study, the production of commercial master alloys (Al5TilB) is performed and their grain refining effects are observed on different types of aluminum castings. In the next chapter, experimental studies will be given in detail.

V. EXPERIMENTAL WORK AND RESULTS

5.1 Apparatus

Experimental studies were performed in the laboratories of ETIBANK Seydişehir Aluminum Factory. For melting process electrical resistance furnace was used (Figure 18). In order to keep the temperature constant during the production of master alloy and addition of the master alloy into the casting, some changes were made onto the lid of the furnace as shown in Figure 19. As container graphite crucibles and for stirring graphite rod were used. The temperature at the center of the sample was measured with a chromel/alumel thermocuple and the cooling curve was recorded graphically (See Appendix).

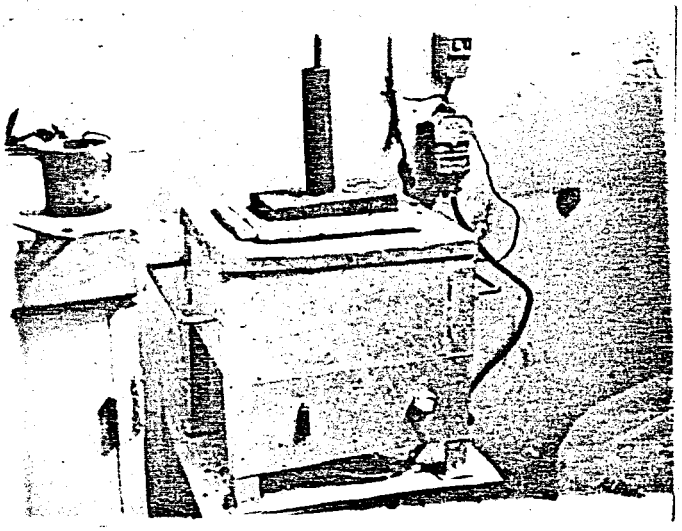

FIGURE 18. Electrical Resistance Furnace.

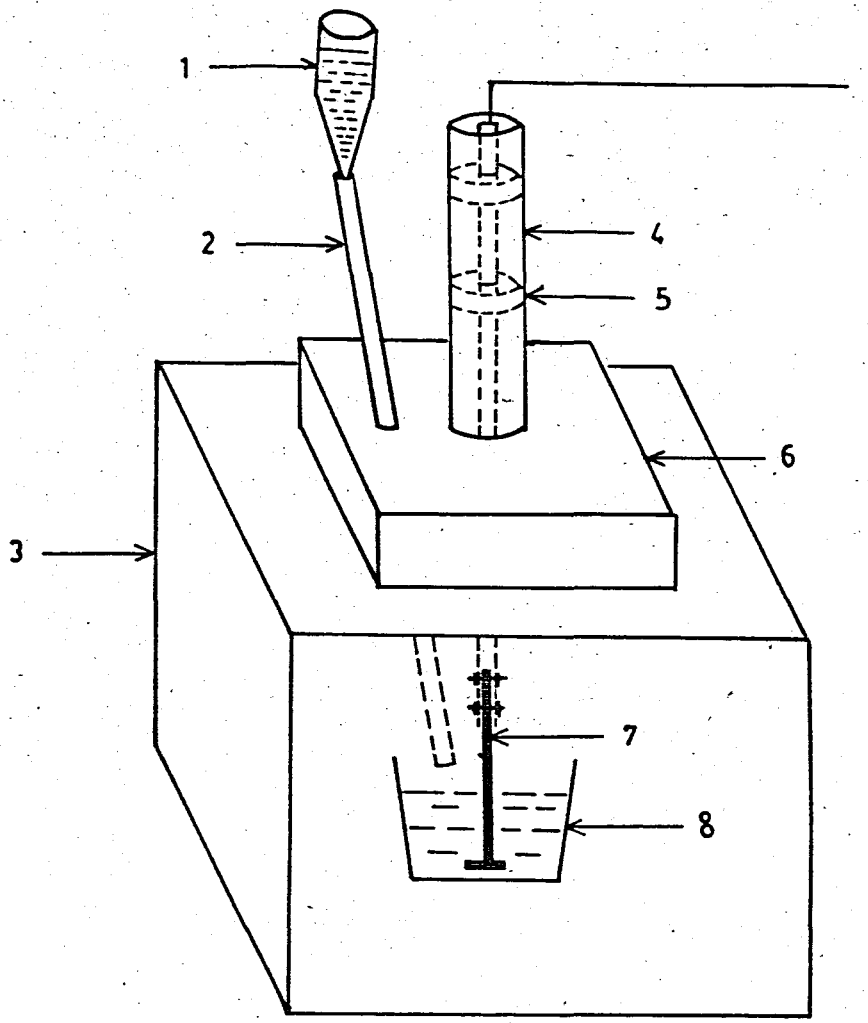

FIGURE 19. Schematic drawings of the resistance furnace and equipments used in melting process.

1 - Salts $|K_2TiF_6 + KBF_4|$

2 - Salt feeder (Cr-Ni Tube)

3 - Resistance Furnace

4 - Stirring Tube

5 - Bearing

6 - Firebrick Lid

7 - Graphite Rod

8 - Graphite Crucible and Liquid Alloy

Chemical analyises were performed with spectral Quantometer (see Figure 20). For grinding process of the specimens KNUTH-ROTOR instrument was used. Electrolytic polishing and etching were carried out by Lectropol instrument (See Figure 21)

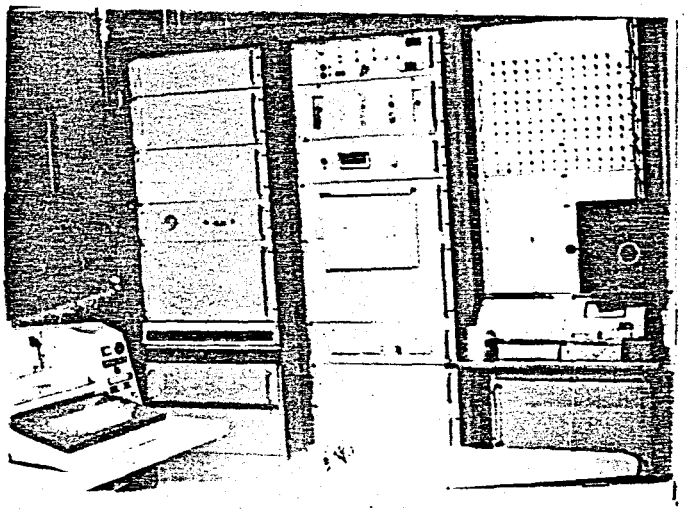

FIGURE 20. Spectral Quantometer.

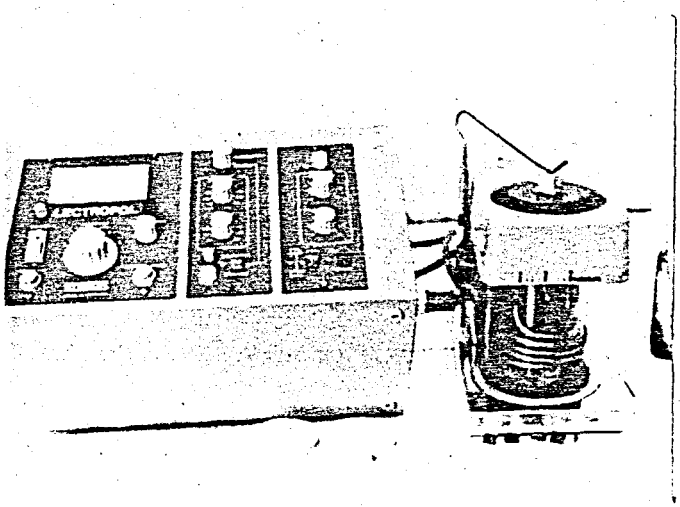

FIGURE 21 - Lectropol (Electrolytic polishing and etching machine).

Brinell hardness numbers of the specimens were measured with Karl Frank GMBH instrument (See Figure 22). Vickers hardness numbers were measured with Wolpert hardness instrument in İ.T.Ü. Laboratories. For tension tests,"Prüf und Mess MFL systeme" instrument was used in İ.T.Ü.

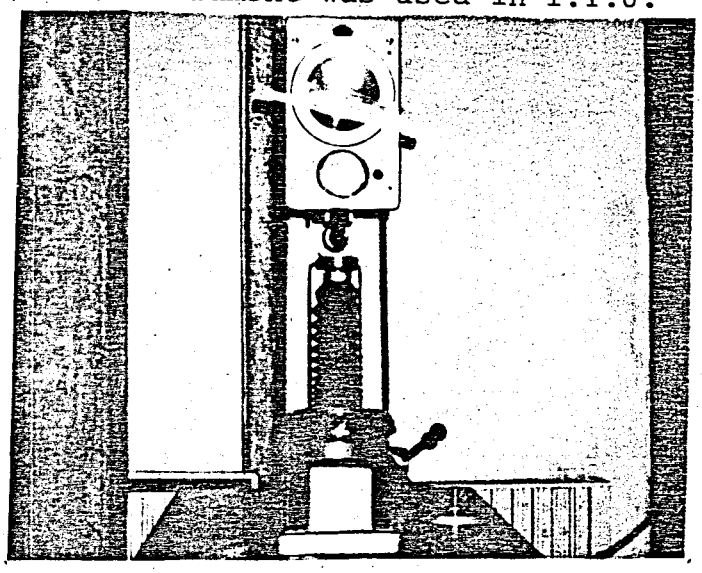

FIGURE 22-Karl Frank GMBH Hardness instrument.

The microscopic examination of the specimens and taking microphotographs were carried out by using optical microscope (see Figure 23).

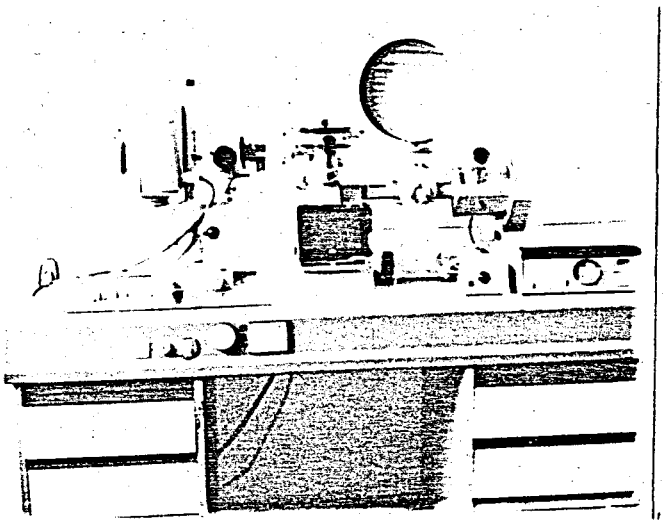

FIGURE 23-Optical microscope.

5.2 EXPERIMENTAL TECHNIQUE

5.2.1 Master Alloy (Tıbor) Preparation

The master alloy AL-5Ti-1B is prepared by using a commercial grade 99.7% purity aluminum (ETIAL7), chemical analysis of which is given in Table V, supplied from seydişehir Aluminum Foundary and the salts of potassium hexafluorititanate (K_2TiF_6) and potassimborofluoride (KBF_4), with purities of 97%, imported from Fluka Company in Switzerland.

TABLE V. Chemical Analysis of the used aluminum alloys

Element	Chemical Analysis (wt %)		
	ETIAL-7*	ETIAL-5*	ETIAL-60*
Fe	0.133	0.267	0.235
Si	0.045	0.067	0.421
Ti	0.006	0.007	0.006
Mn	0.000	0.007	0.034
Zn	0.012	0.020	0.007
Cu	0.000	0.008	0.114
mg	0.002	0.003	0.521
Ni	-	0.000	0.005
Pb	0.001	0.016	0.006
Sn	0.000	0.007	0.003
Cr	0.000	0.007	0.003
V	0.009	-	0.005
B	0.000	0.001	0.001

*

ETIBANK ETINORM	TSE TS-412	U.S.A A.A
ETIAL-7	AL99.7	1070
ETIAL-5	AL99.5	1050
ETIAL-60	ALMgSi	6063

The information on the Al-Ti-B equilibrium diagram is scanty. The binary diagrams for aluminum-titanium and aluminum boron are reasonably well established. In order to make the problem easy the attention was focused onto the binary aluminum-titanium phase diagrams (Figure 24).

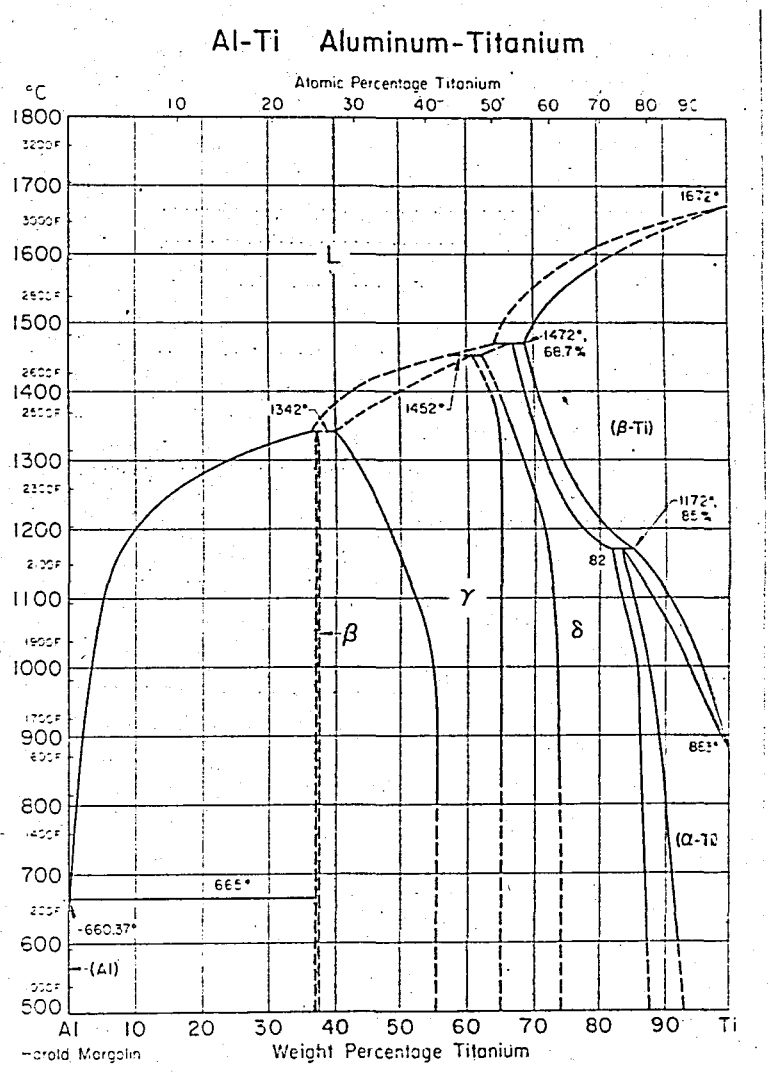

FIGURE 24-Al-Ti phase diagram |13|.

The generally accepted phase diagram for aluminum rich Al-Ti alloy is shown in Figure 25 |14|. At 665°C ΔT is equal to 4.9°C and peritectic point is at 0.15 wt % Ti. Titanium solubility in the solid is 1.15 pct Ti. The hyperperitectic solubility of $TiAl_3$ in the liquid is given by the relationship:

$$\log_{10} \text{pct Ti} = -3996/T + 3.435$$

where T is the absolute temperature.

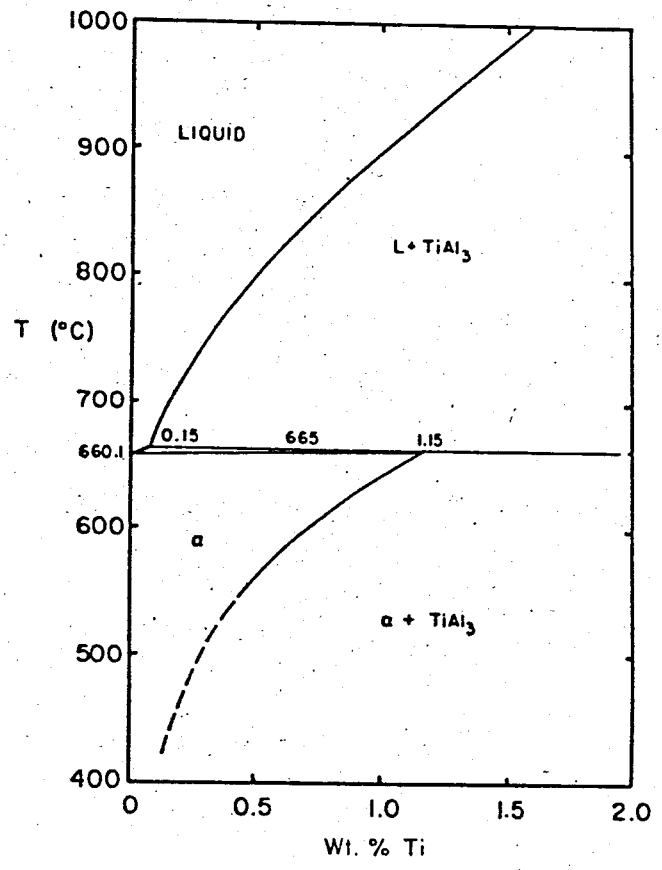

FIGURE 25-The aluminum-rich side of the Al-Ti phase diagram |14|.

Figure 26 |14| shows the Al-B binary phase diagram on the aluminum-rich side. It shows the eutectic composition of 0.022 wt pct at 659.7°C (Liquid → solid + AlB_2). The hypereutectic solubility of AlB_2 in weight percent can be represented by the equation

$$\log_{10}\text{pct B} = -5255/T + 3.975$$

where T is the absolute temperature (°K)

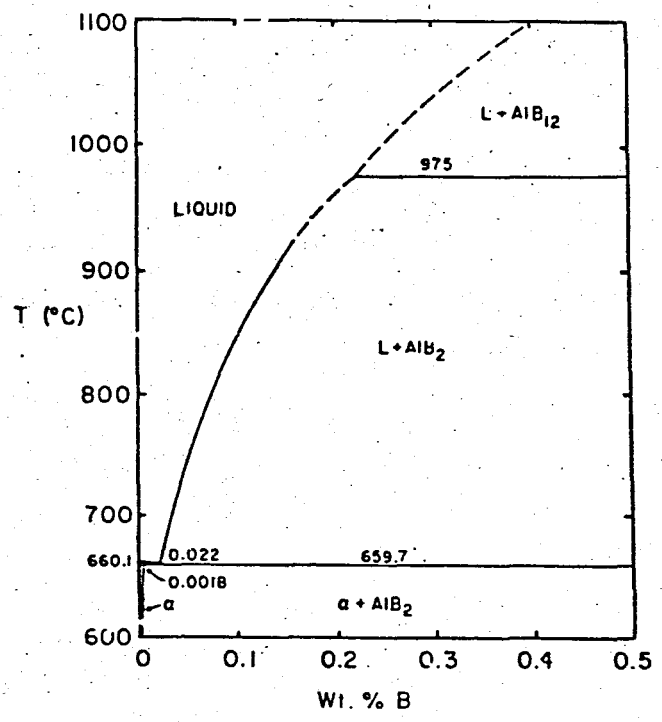

FIGURE 26–The aluminum-rich side of the Al-B phase diagram |14|.

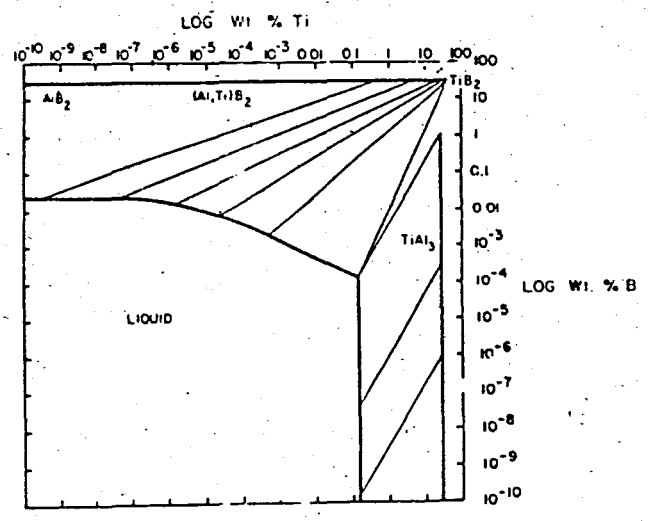

FIGURE 27–The Al-Ti-B system at 666°C (ΔT = + 5.9 °C) |14|.

Figure 27|14| shows the ternary Al-Ti-B system at 666°C (ΔT = + 5.9°C). Heavy lines show compositions of the equilibrium phases. Thin Lines are tie lines between phase fields. Liquid aluminum dominates the lower left-hand corner. In the absence of boron, titanium may be added to 0.15 pct Al_3Ti crystals appear. This corresponds to moving from left to right along the bottom of the figure. At this titanium content,boron may be added up to 1.32 ppm, where TiB_2 will form. This composition is monovariant: a liquid metal solution containing 0.15 pct Ti and 1.32 ppm boron, solid TiB_2 and solid $TiAl_3$ may coexist with one another at this temperature. Continuing to increase boron, the liquid composition moves toward the upper left. Finally, (Al, Ti) B_2 begins to form and the liquid composition line first curves, and then flattens out as the (Al,Ti)B_2 composition becomes close to the binary AlB_2 phase.

As one goes to temperatures below the peritectic, solid aluminum starts to appear as shown in Figure 28|14| . As the temperature decreases, the solid phase field grows at the expense of the liquid, until it moves off the scale of the plot (Figure 29|14|).

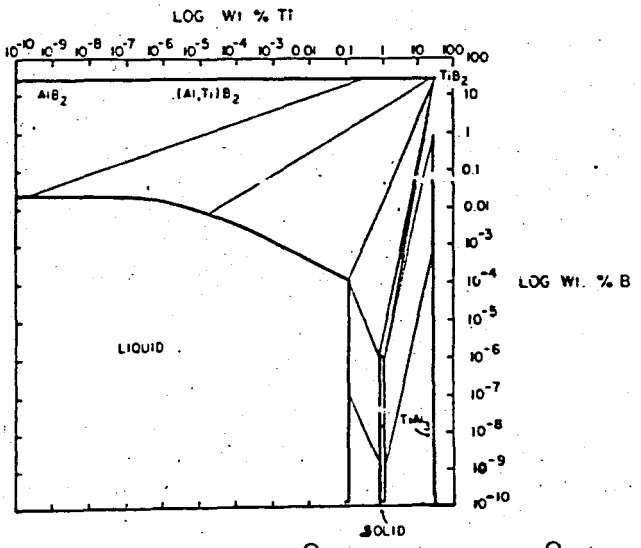

FIGURE 28 – Al-Ti-B system at 664°C (ΔT = 3.9 °C)|14|.

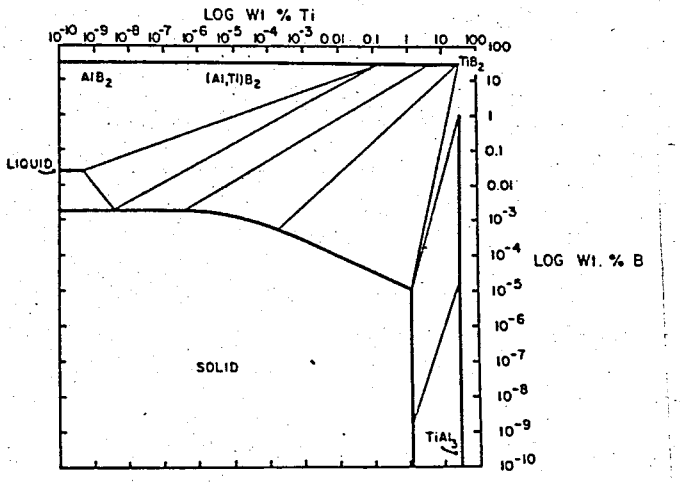

FIGURE 29-Al-Ti-B system of 659·708^{o}C
($\Delta t = -0.392^{o}C$) |14|.

5.2.2 The Production of Master Alloys

The master alloys were prepared on a laboratory scale (150-300 g. samples) using resistance furnace and graphite crucibles. The starting materials were aluminum (99.7%) and the salts of K_2TiF_6 and KBF_4 (purity>97%).

Carefully weighed amounts of aluminum were melted in graphite crucibles by the use of an electric resistance furnace and then the needed amounts of K_2TiF_6 and KBF_4 salts were added simultaneously into the molten aluminum and stirred for different holding times with a graphite rod.

Each sample was then carefully removed from the furnace, placed in a hole (just adequate for the mould) in a firebrick and allowed to cool at a rate of $\sim 0.5^{o}Ks^{-1}$. In this way a

reproducible cooling rate of approximately 0.5 $^{o}Ks^{-1}$ was obtained. In some cases, after the samples were removed from the furnace, they were solidified into the steel mold or in graphite crucibles in air with high cooling rate.

General procedure to prepare the master alloys :

a. Melting of the aluminum (99.7%) at different temperatures
b. Simultaneous addition of the salts (K_2TiF_6 and KBF_4) into molten metal.
c. Stirring of the mixture of Liquid aliminum and salts for different holding times.
d. Carefully removing from the furnace and placing in a hole in a firebrick.
e. Solidifying of the master alloy at different cooling rates.

Experience has shown that optimum grain refining properties are obtained using master alloys with a titanium: boron raito of about approximately 5:1. Because of this reason, the master alloys with ∿5% Ti, ∿1 %B were prepared, varying parameters such as the order of addition of the alloying elements, the temperature at addition, the stirring time before cooling and cooling rate (Table VI).

TABLE VI. The preparation of ternary Al-Ti-B master alloys

Sample Number	Casting Temp. (°C)	Stiring Time (min)	Ingredients (gr)			Chemical Analysis		Solidification	Aluminide (Al_3) Morphology
			Al	K_2TiF_6	KBF_4	Ti%	B%		
1	900	7	150.73	40.66	18.3	5.38	0.4	in firebrick	Flake-Like
2	900	5	150.73	40.66	18.63	5.01	0.75	in firebrick	Blocky
3	900	10	150.73	40.66	18.63	3.38	0.5	in firebrick	Flake-Like
4	900	10	150.73	40.66	18.63	5.38	0.7	in steel Mold in air	Flake-Like
5	900	5	188.42	50.83	23.29	4.97	0.9	in graphite	Flake-Like
6	900	4	150.73	40.66	18.63	5.09	0.6	in firebrick	Flake-Like
7	900	5	150.73	40.66	18.63	5.21	0.4	in graphite Grucible in air	Flake-like, Blocky
8	900	5	150.73	40.66	26.09	4.97	>1	In frebrick	Flake-Like

Sample Number	Casting Temp. (^{o}C)	Stirring Time (min)	Ingredients (gr) Al	K_2TiF_6	KBF_4	Chemical Analysis Ti %	B %	Solidification	Aluminide (Al_3Ti) Morphology
9	800	5	150.73	40.66	18.63	5.40	0.3	In firebrick	Blocky
10	800	7	150.73	40.66	18.63	5.21	0.5	" "	Blocky
11	800	10	150.73	40.66	18.63	5.45	0.6	" "	Blocky
12	800	9	150.73	40.66	18.63	5.15	0.9	" "	Blocky
13	800	4	150.73	40.66	18.63	5.67	0.9	" "	Blocky
14	900	5	150.73	40.66	22.36	5.38	0.6	" "	Flake-like, Blocky
15	800	7	150.73	40.66	22.36	5.47	0.3	" "	Blocky
16	850	5	150.73	40.66	22.36	5.38	0.7	" "	Flake-like, Blocky
17	800	9	301.46	81.97	40.98	5.25	0.82	"asbestos	Blocky
18	900	10	301.46	81.97	52.16	5.07	0.80	" "	Flake-like

5.2.3 Master Alloy Addition Into The Castings

In order to be able to discriminate between moderately efficient and highly-efficient additives, the prepared master alloys are required a reliable grain-refining test, not only for routine quality control, but also for research into the production of more efficient grain refining master alloys.

Grain refiners (master alloys) are generally tested at different rates of addition, at various titanium and boron contents, at different temperatures for different contact times(See Table VII). The test level is calculated to increase the titanium and boron content of the bulk alloy by approximately 0.01 wt % and 0.002 Wt % respectivelly.

In the testing of master alloys about 500 g. of commercially pure aluminum ingots (99.7 pct Al) are melted in the graphite crucibles by using an electrical resistance furnace which is held at different temperatures. Master alloys are also added into ETIAL-5 and ETIAL-60 aluminum alloys.

The smallish part of the master alloy (~1g). to be tested is placed on the surface of the aluminum melt, immediately plunged under the surface and stirred with a thin graphite rod for 2 min. After the stirring, melt is allowed to stand for various contact times in the furnace, and then removed from the furnace, poured into the steel mold from the graphite crucible, solidified in cold water in a quench tank. After the

test samples were chilled, metallographic examination, hardness tests and tension tests were performed.

General procedure of the master alloy addition into the castings:

a- Melting of the aluminum (ETIAL 7, ETIAL 5 or ETIAL 60) at different temperatures.

b- Addition of the master alloy into the molten aluminum.

c- Stirring of the mixture of master alloy and molten aluminum with graphite rod for 2 min.

d- Allowing to stand the melt for various contact times (1,5,10,30,60,120 min) in the furnace.

e- Cleaning the slag from the surface of the molten metal.

f- Carefully removing the crucible from the furnace.

g- Pouring into the steel mold from the graphite crucible.

h- Solidification of the molten metal by quenching in water tank.

TABLE VII- The castings inoculated with master alloys at different temperatures and holding times, grain size and Brinell hardness test results.

Sample Number	Concentration		Casting Temperature (^{o}C)	Holding Time (min)	Average Grain Size (μm)	Hardness BHN (Kg/mm^2)
	Wt % Ti	Wt % B				
1	0.016	0.001	700	1	450	24.4
2	0.014	0.001	700	5	403	24.6
3	0.015	0.001	700	10	319	24.6
4	0.015	0.001	700	30	333	24.4
5	0.015	0.000	700	60	510	23.2
6	0.015	0.000	700	120	478	26.9
7	0.014	0.001	740	1	348	23.6
8	0.015	0.002	740	5	294	24.2
9	0.016	0.001	740	10	333	25.0
10	0.015	0.001	740	30	283	23.4
11	0.014	0.000	740	60	306	26.4
12	0.015	0.001	740	120	510	26.1
13	0.013	0.001	780	1	547	24.6
14	0.017	0.002	780	5	364	23.0
15	0.022	0.003	780	10	247	23.6
15A	0.092	0.008	780	10	174	24.2
15B	0.015	0.001	780	10	273	26.4
16	0.0017	0.001	780	30	450	22.2
17	0.017	0.001	780	60	510	22.6
18	0.015	0.000	780	120	850	25.0
19	0.014	0.001	720	10	333	23.8
20	0.014	0.001	750	10	547	23.0

	Sample Number	Concentration		Casting Temperature (^{o}C)	Holding Time (Min)	Average Grain (μm)	Hardness BHN (Kg/mm^2)
		Wt % Ti	Wt % B				
	21	0.018	0.000	800	10	-	23.4
	22	0.017	0.002	720	1	364	24.2
	23	0.013	0.000	720	5	403	23.6
	24	0.016	0.001	720	30	425	25.1
	25	0.015	0.000	720	60	510	24.8
	26	0.016	0.000	720	120	450	23.4
ETIAL 5	27[X]	0.019	0.004	720	1	478	27.4
	28[X]	0.015	0.003	720	5	638	28.2
	29[X]	0.016	0.003	720	10	333	28.4
	30[X]	0.013	0.002	720	30	294	28.9
	31[X]	0.013	0.002	720	60	383	26.4
	32[X]	0.014	0.002	720	120	403	27.4
ETIAL 60	33[XX]	0.015	0.002	720	1	237	41.5
	34[XX]	0.018	0.00	720	5	172	39.8
	35[XX]	0.021	0.003	720	10	140	42.4
	36[XX]	0.014	0.002	720	30	160	37.7
	37[XX]	0.016	0.002	720	60	200	39.3
	38[XX]	0.017	0.004	720	120	223	38.5
	39	0.023	0.002	720	10	273	25.9
	40	0.027	0.003	720	10	333	24.2
	41	0.039	0.004	720	10	225	24.6
	42	0.069	0.006	720	10	178	24.6
	42A	0.010	0.000	720	10	306	25.2
ETIAL 5	43[X]	0.019	0.003	720	10	283	27.9
	44[X]	0.023	0.003	720	10	383	27.4
	45[X]	0.030	0.004	720	10	225	27.1
	46[X]	0.074	0.010	720	10	239	28.5
	46A[X]	0.012	0.002	720	10	364	26.9
	46B[X]	0.033	0.005	720	10	201	26.1
ETIAL 60	47[XX]	0.019	0.002	720	10	201	39.3
	48[XX]	0.026	0.003	720	10	191	38.9
	49[XX]	0.056	0.007	720	10	159	38.1
	49A[XX]	0.028	0.002	720	10	207	37.3
	50[XX]	0.042	0.004	720	10	191	41.5
	50A[XX]	0.011	0.001	720	10	264	37.6

Sample Number	Concentration		Casting Temperature (^{o}C)	Holding Time (Min)	Average Grain Size (μm)	Hardness BHN (Kg/mm^2)
	Wt % Ti	Wt % B				
51	0.012	0.001	700	1	696	24.6
52	0.012	0.001	700	5	450	24.6
53	0.012	0.002	700	10	364	24.8
54	0.013	0.001	700	30	425	25.0
55	0.011	0.001	700	60	294	24.2
56	0.014	0.001	700	120	294	25.7
57	0.014	0.002	740	1	510	23.8
58	0.011	0.001	740	5	294	22.6
59	0.012	0.001	740	10	348	23.8
60	0.011	0.000	740	30	403	22.2
61	0.011	0.001	740	60	332	22.6
62	0.010	0.002	740	120	403	21.3
63	0.013	0.000	780	1	450	23.2
64	0.012	0.001	780	5	383	23.0
65	0.012	0.001	780	10	425	23.0
66	0.011	0.001	780	30	273	24.2
67	0.014	0.002	780	60	283	23.8
68	0.010	0.001	780	120	383	21.4
69	0.012	0.001	720	10	510	22.6
70	0.010	0.001	750	10	450	22.2
71	0.011	0.002	800	10	383	23.4
ETİAL-7 72	0.006	0.000	720	-	-	24.2
ETİAL-5 73[X]	0.007	0.001	720	-	-	25.8
ETİAL-60 74[XX]	0.006	0.001	720	-	-	40.6

ETIAL-7 aluminum is used in samples (1-26,39-42A,51-71)

x ETIAL-5 aluminum is used in samples (27-32,43-46B)

xx ETIAL-60 aluminum is used in samples (33-38, 47-50A)

The samples (1-50A) are inoculated with master alloy (17) which has block-like aluminides (Al_3Ti), and the samples (51-71) are inoculated with master alloy (18) containing flake-like aluminides (Al_3Ti).

The samples (72-74) are cast without the addition of master alloy.

All of the samples are quenched in steel mold inserted in water.

5.3 Metallographic Examination

5.3.1. Metallography Of The Master Alloys

The chilled test samples were cut longitudinally from half part. On mechanical polishing, emery papers of increasing fineness were used and this was followed by polishing with alumina paste, washing in water, and finally drying in a steam of air. The diluted hydroflouric acid (0.5 % HF) was used as the etching reagent. Finally, the microstructures of the master alloys were investigated in detail under an optical microscope, and the microphotographs were taken by using a camera (See Figure 23).

5.3.2 Metallography Of Castings Inoculated With Tibor

The chilled castings (~500 g. samples) were cut horizontally from the half part and carefully ground and polished. After careful polishing process, macro etching was carried out with the mixture of various diluted acids with following compositions:

Hydrochloric acid (HCL) = 60 %

Nitric acid (HNO_3) = 30 %

Hydroflouric acid = 5 %

Water (H_2O) = 5 %

Finally, the macrostructures of the castings were investigated in detail under on optical microscope, and the photographs of the grain structures were taken in natural size scala (Figure 41-43).

After the macro etching of the castings, micro etching was carried out for microscopic examination of the grain structure. Small parts were cut from the horizontal half part of the chilled castings (See Figure 30). All of the specimens were subjected to wet grinding on Knuth-Rotor instrument up to grain 1200. Specimen surfaces of 1 cm^2 were polished electrolytically for subsequent anodic etching. This is the method stated by L.J. Barker [15] for revelation of the structure: By anodic oxidation in an aqueous solution of boron fluoride acid, an optically anisotropic oxide layer is formed on the surface of the specimen.

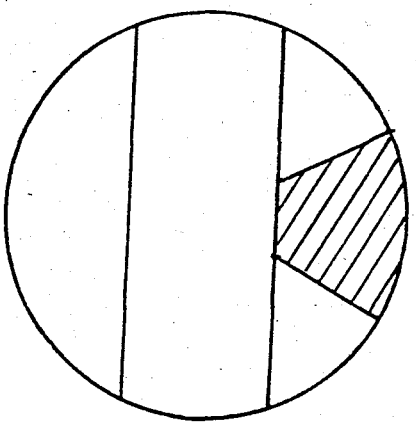

Figure30- Specimen for microetching (Shaded area).

The combination of an electrolytic polishing process and electrolytic etching described below significantly reduces the time required for the preparation of a specimen.

After the wet grinding of the specimens, electropolishing was performed. Typical conditions for electropolishing are

as follows|15|.

Electrolyte : 62 ml perchloric acid (70 %) 700 ml ethanol, 100ml 2-butoxyethanol (also known as butly cellosolve and ethylene glycol monobutly ether) 137 ml distilled water.

Current density : 3.85 amp. per square centimeter (about 40 V dc), (Specimen is anode)

Time : 20 sec

Remarks : Rinse in warm water, dry in warm air. To prevent or minimize overheating of the specimen, polish in 10sec. intervals, allowing it to cool during "off" periods.

After the electropolishing of the specimens,electroetching was performed with exchanging of electrolyte. The electrolyte used for etching and anodizing respectivelly consists of boron fluoride acide (HBF_4) and distilled water mixed in the portion 1:20. Approximate working temperatures of the electrolytes are 18-20^{o}C. By continuous operation heat is generated, but this may be avoided by connecting the cooling hoses incorporated in the polishing table to a suitable cooling liquid supply (water was used). Typical electroetching conditions are as follows :

Electrolyte : Boron fluoride acide (HBF_4) and distilled water mixed in the proportion 1:20.

Voltage(V) : 10-15 V dc.

Time : 90 sec |For 99.7 % Al|

120 sec |for 99.5 % Al and Etial 60 Al|

Flow sething : 6

Polishing Grade : 4

Remarks : After etching, the specimen is rinsed in running water and then dried. The specimen surface should not be dried by wiping as this may damage the oxide layer formed by etching.

After the electropolishing and electroetching processes, microscopic examination was performed by using polarised light, and mirophotographs of the grain structure of the specimens were taken.

After taking the microphotographs of the specimens, average grain sizes were measured by using "Lineal Intercept (or Heyn) method"|16|. In this method, estimation of the grain size is performed by counting the number of grains intercepted by one or more straight Lines sufficiently long to yield at least 50 intercepts. It is often desirable to select a combination of test line length and magnification such that a single test will yield approximately 50 intercepts. One such test will nominally allow estimation of grain size to the nearest whole ASTM size number, at the location tested. Additional lines, in a predetermined array, should be counted to obtain the precision required. This method explained above is called "Lineal Intercept (or Heyn) Method".

An "Intercept" is a segment of test line overlaying one grain. An "intersection" is a point where a test line is cut by a grain boundary. When counting intercepts, at the end of a test line which penetrates into a grain are scored as

half intercepts. When counting intersections, the end points of a test line are not intersections and are not counted except when the end appears to exactly touch a grain boundary, when 1/2 intersection should be scored. A tangential intersection with a grain boundary should be scored as 1 intersection. An intersection apparently coinciding with the junction of 3 grains should be scored as 1 1/2. With irregular grain shapes, the test line may generate two intersections with different parts of the same grain, together with a third intersection with the intruding grain. The two additional intersections are to be counted.

Average grain sizes of the castings obtained by using Heyn Method are given in Table VII.

5.4 Tension Tests

The test bars, which were removed from the mid slices provided by lateral sectioning of ingots, were machined down to the tension test specimens and subsequently polished to prevent the probable surface defects produced during machining (see Figure 31.(a) and 31.(b)). Tension tests were performed at room temperature and tensile testing machine was used during tension tests. The dimensions of the test specimen are given in Figure 32 |17|.

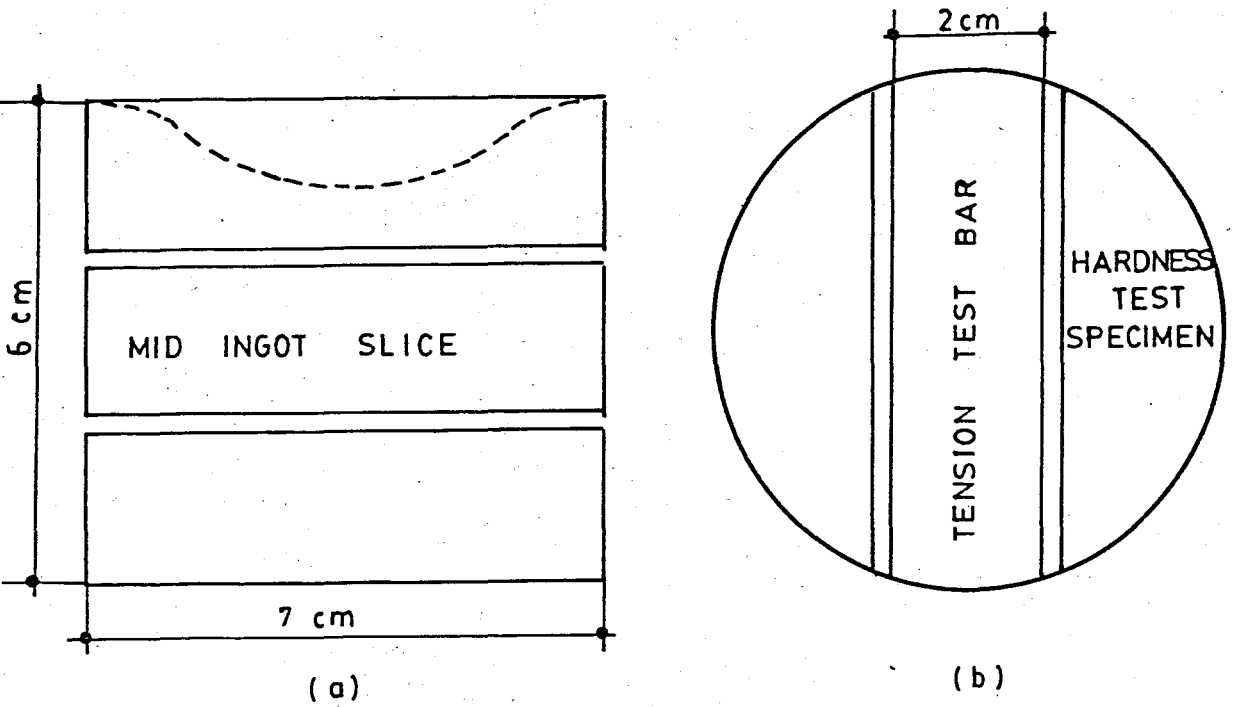

Figure 31- Test specimens obtained from ingot castings.
(a) Vertically cut (b) Horizontally cut

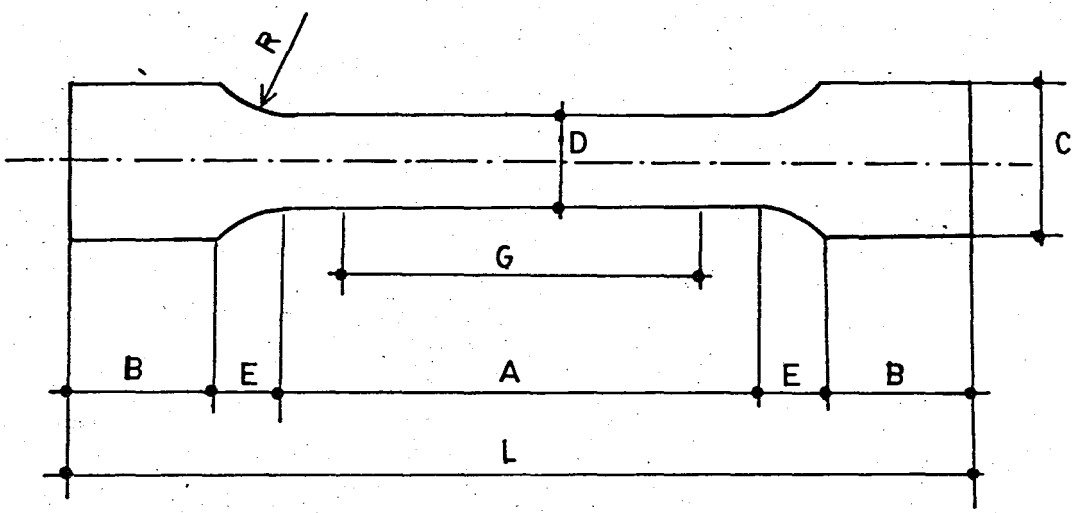

Figure 32- Dimensions of the circular section test specimen |17|.

	mm
G-Gage length	: 25.0 ± 0.10
D-Diameter	: 6.25 ± 0.12
R-Radius of fillet	: 5
A-Length of reduction section	: 32
B-Length of end section	: 12
C-Diameter of end section	: 11.25
E-Length of fillet section	: 4.33
L-Over-all Length	: 64.66

5.5 Hardness Tests

Vickers-Brinell hardness tester (Figure 22) was used during tests. Brinell hardness numbers of the specimens were measured at 31.5 kg load with 2.5 mm ball diameter (Table VII). Vickers hardness numbers of the specimens (33-38,74) were measured at 10 kg load (Table IX).

Specimens for hardness tests were obtained from the mid slices of the laterally sectioned ingots (Figure 31 b). The specimen surfaces were machined to provide parallel surface for correct testing.

The Brinell hardness number (BHN) is expressed as the load P divided by the surface area of the indentation. This is expressed by the formula,

$$BHN = P/\ (\pi D_1/2)(D_1 - \sqrt{D_1^2 - d^2}\ )$$

where P = applied load, kg

D_1 = diameter of ball, mm

d = diameter of indentation, mm

It will be noticed that the units of the BHN are kilograms per square milimeter.

The Vickers hardness test uses a square base diamond pyramid as indenter and Vickers Hardness Number (VHN) is defined as the load divided by the surface area of the

indentation which is calculated from microscopic measurements of the lengths of the diagonals of the impression.

$VHN = 1.854\ P/L^2$ where P = employed load, kg

$L = (d_1 + d_2)/2$

d_1 = diagonal Length

d_2 = second diagonal length

5.6 Experimental Results

5.6.1 Results of Metallographic Examination

a- Microstructures of the master alloys

Figure 33 shows the microstructure of master alloy 18 that is prepared by the simultaneous addition of the salts (K_2TiF_6 and KBF_4) into the molten aluminum (ETIAL-7) at 900°C and is stirred with a graphite rod for 10 minutes. The master alloy 18 is then carefully removed from the furnace, placed in a hole (just adequate for the mold) in an asbestos and allowed to cool. In this way a reproducible cooling rate of ~0.60 Ks^{-1} is obtained. Master alloy 18 obtained under these conditions shows the long needle-like aluminide (Al_3Ti) particles interior of the grain, and boride particles (AlB_2, TiB_2) located at the grain boundaries.

Figure 33- Microstructure of master alloy 18, magnification 165 X,10 minutes stirring time, 900^{o}C casting temperature, ~0.60 Ks^{-1} cooling rate.

Figure 34 shows the microstructure of master alloy 3 that is prepared by the simultaneous addition of the salts (K_2TiF_6 and KBF_4) into the molten aluminum (ETIAL 7) at 900^{o}C and is stirred with a graphite rod for 10 minutes. The master alloy 3 is then carefully removed from the furnace, placed in a hole (just adequate for the mold) in a firebrick and allowed to cool. In this way a reproducible cooling rate of 0.65$^{0}Ks^{-1}$ is obtained. Master alloy 3 obtained under these conditions shows flake-like aluminide crytals interior of the grain, and boride particles (AlB_2, TiB_2) located at the cell boundaries. Flake-like aluminide crytals of the master alloy 3 is shorter than the flake-like aluminide crytals of the master alloy 18.

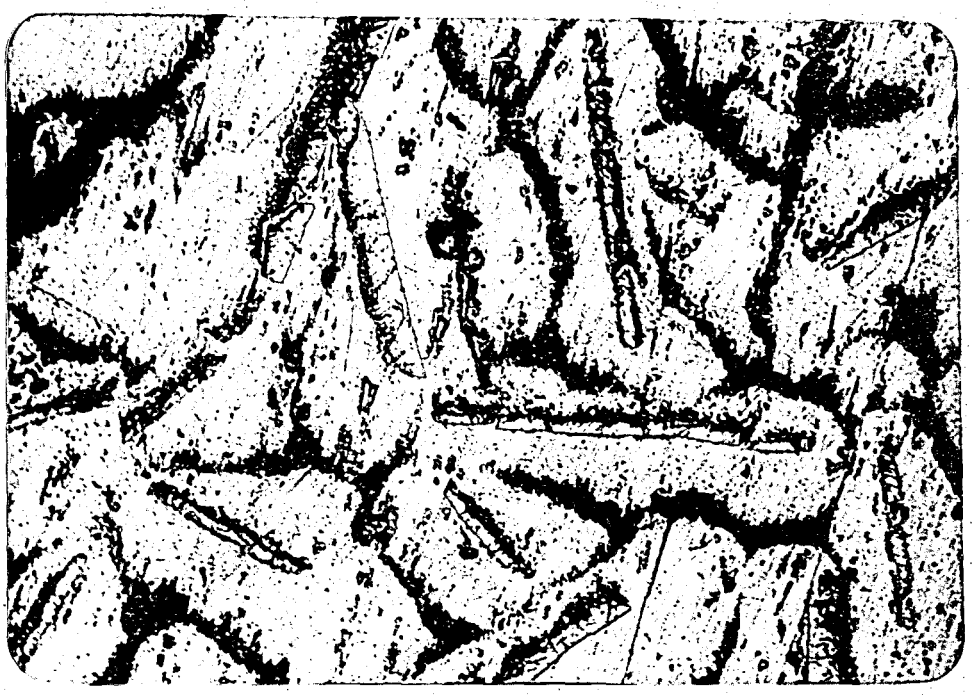

Figure 34- Microstructure of the master alloy 3, magnification 165 X, 10 minutes stirring time, 900°C casting temperature, ~0.65 Ks^{-1} cooling rate.

Figure 35 shows the microstructure of master alloy 4 which is prepared by the simultaneous addition of the salts into the molten aluminum (Etial-7) at 900°C and is stirred with a graphite rod for 10 minutes. The master alloy 4 is then carefully removed from the furnace, poured into a steel mold and allowed to cool. In this way high cooling rate is obtained. Master alloy 4 obtained under these conditions contains small well-dispersed boride particles and short, thin aluminide particles distributed throughout an aluminum matrix.

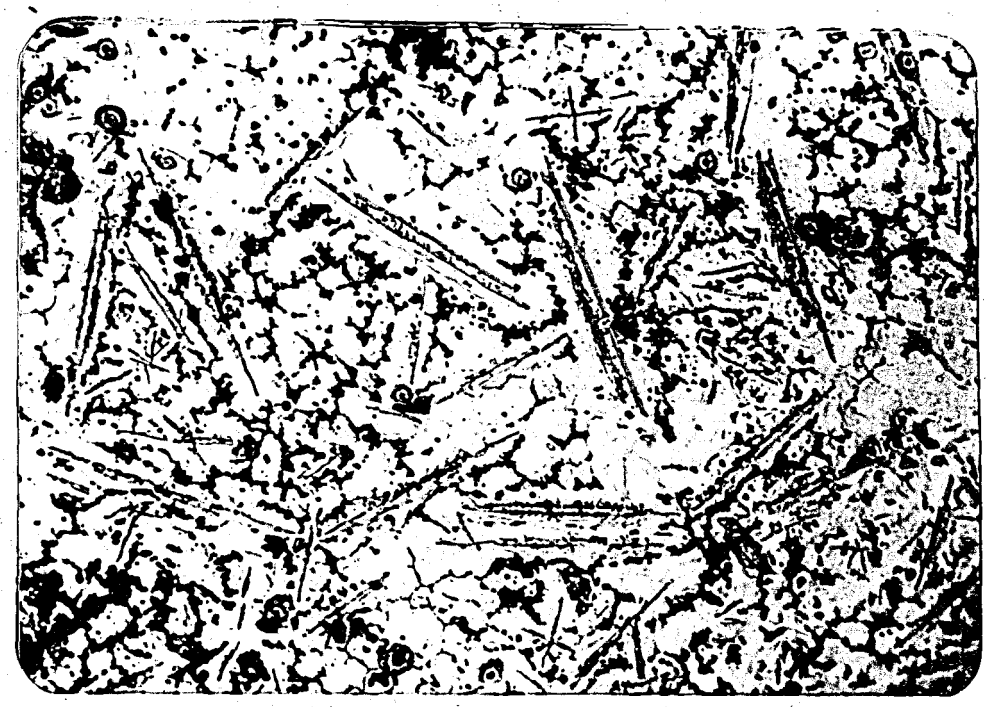

Figure 35- Microstructure of master alloy 4, magnification 165X 10 minutes stirring time, 900°C casting temperature, solidification in steel mold.

Figure 36 shows the microstructure of master alloy 6 which is prepared by the simultaneous addition of the salts into the molten aluminum (Etial-7) at 900°C and is stirred with a graphite rod for 4 minutes. The master alloy 6 is then carefully removed from then furnace, placed in a hole (just adequate for the mold) in a firebrick and allowed to cool with the cooling rate of 0.65 $^{0}Ks^{-1}$. Aluminide particles have a needle like appearance, but are really plates, as can be seen in the lower right-hand corner of the Figure 36.

Figure 36- Microstructure of master alloy 6, magnification 165x, 4 minutes stirring time, 900°C casting temperature, ~0.65 $^{0}Ks^{-1}$ cooling rate.

Figure 37- A typical microstructure in master alloy where salts are added at high temperature (900°C). (Etching is performed electrolytically)

A typical microstructure in master alloy containing flake like aluminide particles is shown in Figure 37. The other microstructure photographs of the Flake-like master alloys obtained in the present study are given in appendix.

The microstructure of master alloy 17 is shown in Figure 38. It is prepared by the simultaneous addition of the salts into the molten aluminum (ETIAL-7) at low temperature of 800°C and is stirred with graphite rod for 9 minutes. It is then carefully removed from the furnace, placed in a hole (just adequate for the mold) in an asbestos and allowed to cool with the cooling rate of $0.60\ ^{\circ}Ks^{-1}$. Master alloy 17 obtained under these conditions shows the block-like aluminide (Al_3Ti)

particles and the small boride particles located mainly at the cell boundaries. Block-like aliminide particles are smaller and more compact than the flake-like ones.

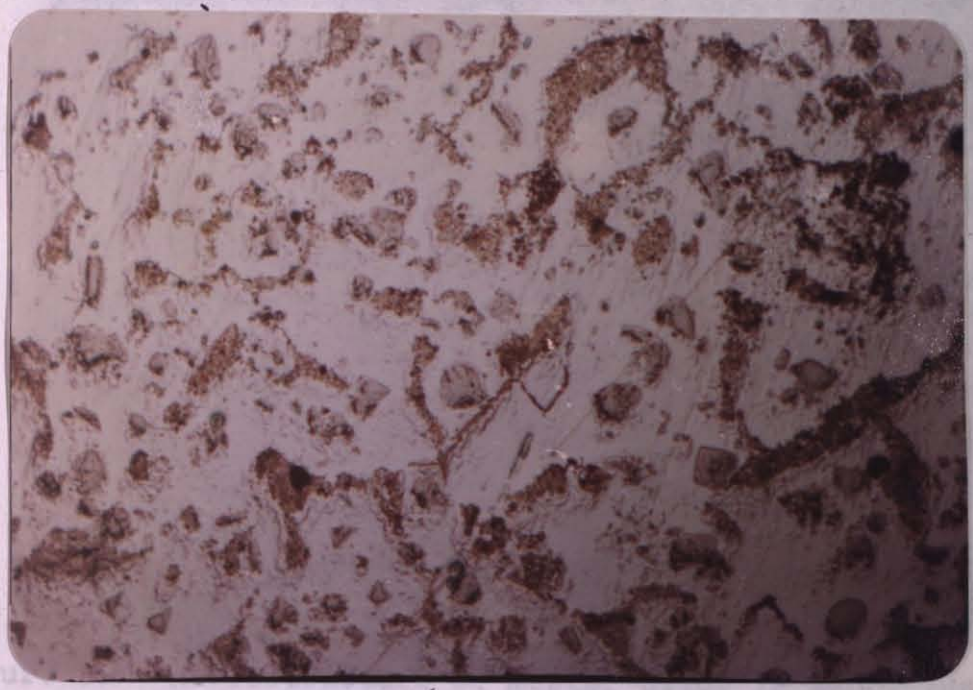

Figure 38- Microstructure of master alloy 17, magnification 165x, 9 minutes stirring time, 800°C casting temperature, $0.60^{\circ}Ks^{-1}$ cooling rate.

Figure 39 shows the microstructure of master alloy 12 which is prepared by the simultaneous addition of the salts into the molten aluminum (Etial-7) at 800°C and is stirred with a graphite rod for 9 minutes. It is then carefully removed from the furnace, placed in a hole (just adequate for the mold) in a firebrick and allowed to cool with the cooling rate of $0.65^{\circ}Ks^{-1}$. Master alloy 12 obtained under these conditions shows the block-like aluminide particles and the small boride particles located mainly at the cell boundaries.

Block-like aluminide particles of the master alloy 12 are smaller than the aluminide particles of the master alloy 17.

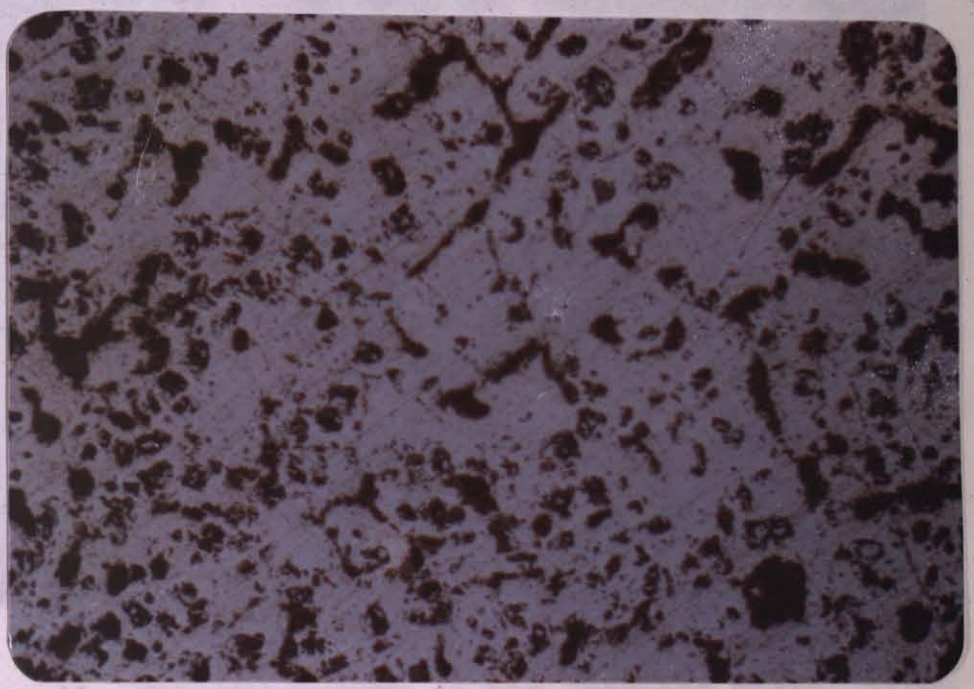

Figure 39- Microstructure of master alloy 12 magnification 165 x, 9 minutes stirring time, 800°C casting temperature 0.65°Ks^{-1} cooling rate.

The other microstructure photographs of the block-like master alloys obtained in the present study are given in appendix. Figure 40 shows the microstructure of the master alloy which is imported from the Kawecki Billiton Company. This master alloy contains small well-dispersed TiB_2 particles and larger $TiAl_3$ particles distrubuted throughout an aluminum matrix.

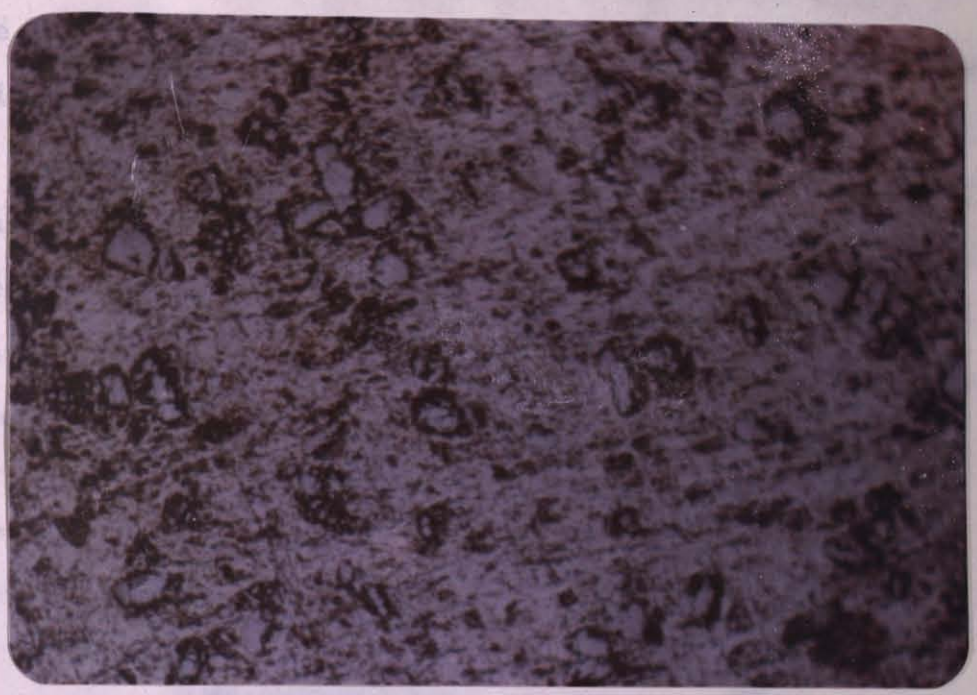

Figure 40- Microstructure of the imported master alloy containing block-like aluminide particles, Magnification 165 X .

b- Macrostructures of The Castings Inoculated With Master Alloys

Figure 41(a) shows the macrostructure of the sample 72 which is cast without the addition of master alloy into the Etial-7 aluminum at 720°C. There are columnar grains near the mold wall and are coarse equiaxed grains at the center of the ingot.

Figure 41-(b) shows the macrostructure of the sample 9 which is cast with the addition of the master alloy 17 into the Etial-7 aluminum at 740°C temperature for 10 minutes holding time. The effect of inoculation with master alloy 17 is observed in this Figure 41-(b) There are completely fine equiaxed grains throughout the ingot. As the holding time increases the size of the equiaxed grains increases and near the mold wall small columnar grains form as shown in Figure 41(c) for 120 minutes holding time at 740°C.

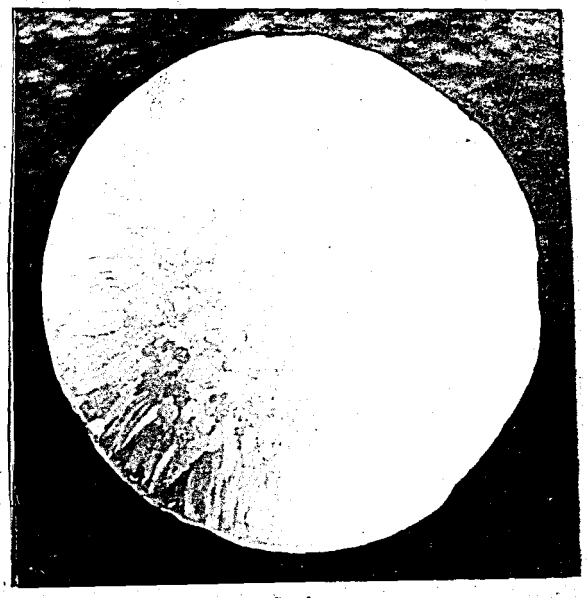

(a)

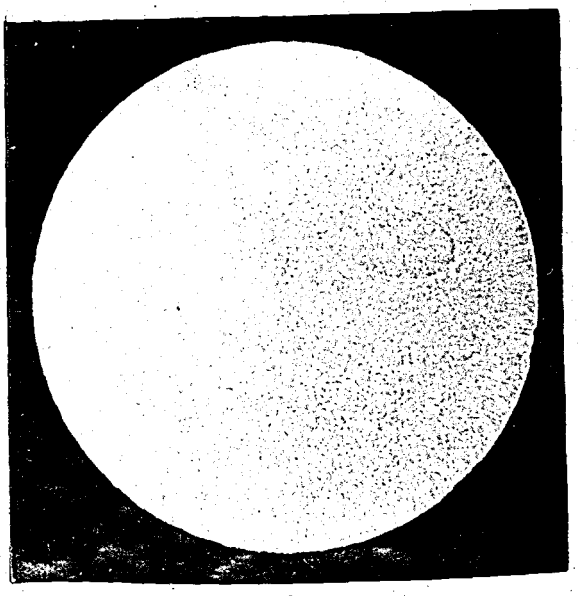

(b)

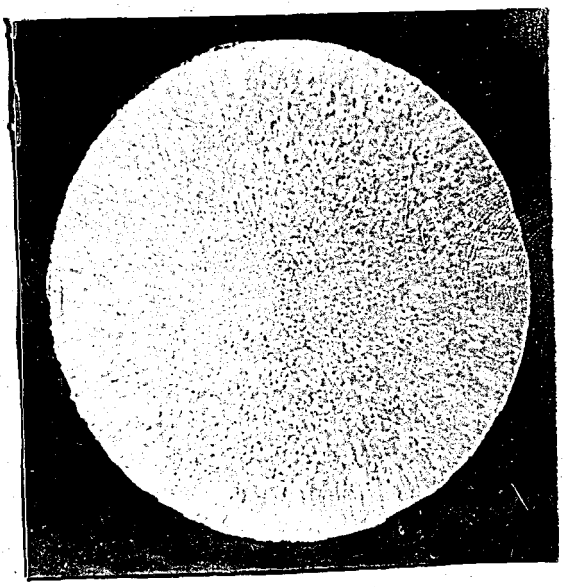

(c)

Figure 41- Macrostructures of the Etial-7 castings, magnification 0.9 X,

(a) Sample 72 is cast without master alloy addition;

(b) Sample 9 is cast with the addition of master alloy 17 at 740°C, 10 minutes holding time ;

(c) Sample 12 is cast with the addition of master alloy 17 at 740°C, 120 min. holding time.

The macrostructures of the Etial-5 castings are shown in Figure 42. Figure 42-(a) shows the sample 73 which is cast without the addition of master alloy into the Etial-5 aluminum at 720°C. There are columnar grains near the mold wall and are mainly coarse equiaxed grains at the center of ingot.

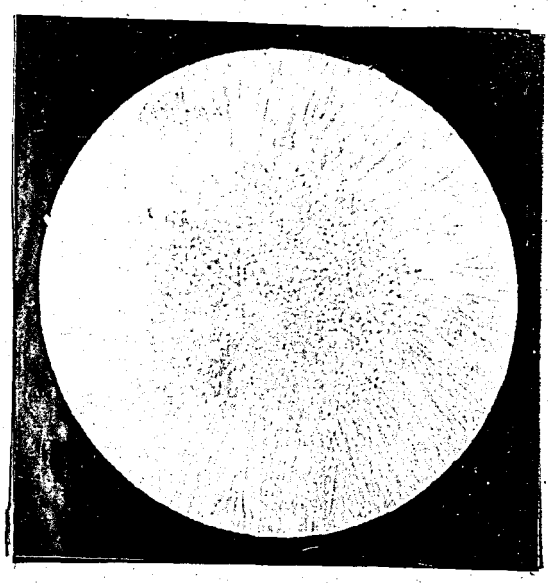

(a)

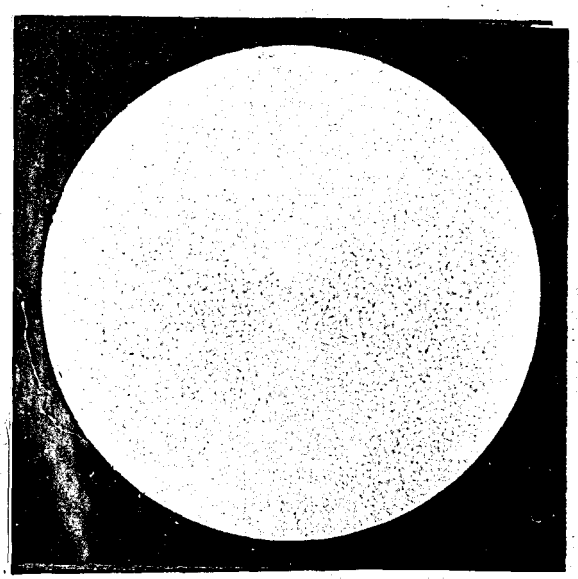

(b)

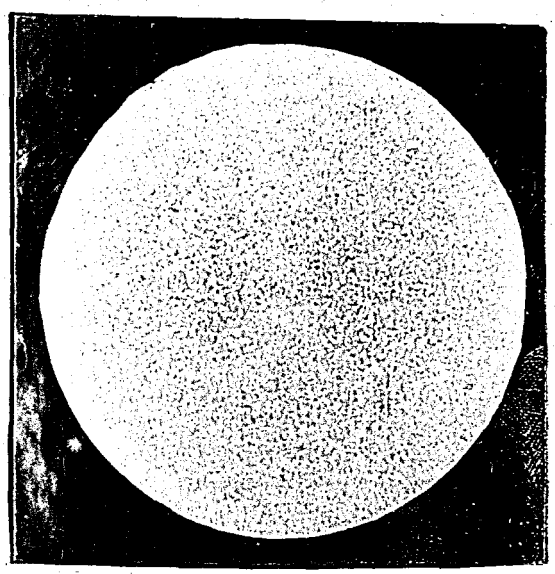

(c)

Figure 42- Macrostructures of the Etial-5 castings, magnification 0.9X,(a) Sample 73 is cast without master alloy addition ;(b) Sample 29 is cast with the addition of master alloy 17 at 720°C, 10 minutes holding time ;(c) Sample 32 is cast with the addition of master alloy 17 at 720°C, 120 min holding time.

Figure 42(b) shows the macrostructure of the sample 29 which is cast with the addition of the master alloy 17 into the Etial-5 aluminum at 720°C temperature for 10 minutes holding time. There are completely fine equiaxed grains throughout the ingot. The macrostructure of sample 32 cast with the addition of the master alloy 17 into the Etial-5 aluminum at 720°C temperature for 120 minutes holding time is shown in Figure 42 (c). The sample 32 has larger equiaxed grains than the sample 29 due to increasing holding time.

The macrostructures of the Etial-60 castings are shown in Figure 43. Figure 43 (a) shows the sample 74 which is cast without the addition of master alloy at 720°C. There are partially columnar grains, the lengths of which are smaller than the lengths of the Etial-5 aluminum, and are course equiaxed grains at the center of the ingot. Figure 43 (b) shows the sample 35 cast with the addition of the master alloy 17 into Etial-60 aluminum at 720°C temperature for 10 minutes holding time. From the Figure 43(b) completely very fine equiaxed grains are seen throughout the ingot. The size of the equiaxed grains in Etial-60 castings is smaller than the others (Etial-5 and Etial-7). The finest equiaxed grains are obtained by inoculating the Etial-60 aluminum at 720°C temperature with 10 minutes holding time. The size of the equiaxed grain increases with increasing holding time, Figure 43(c) shows the macrostructure of the sample 38 cast by the inoculation of master alloy 17 at 720°C temperature for120 minutes holding time. There are greater equiaxed grains than the sample 35 throughout the ingot.

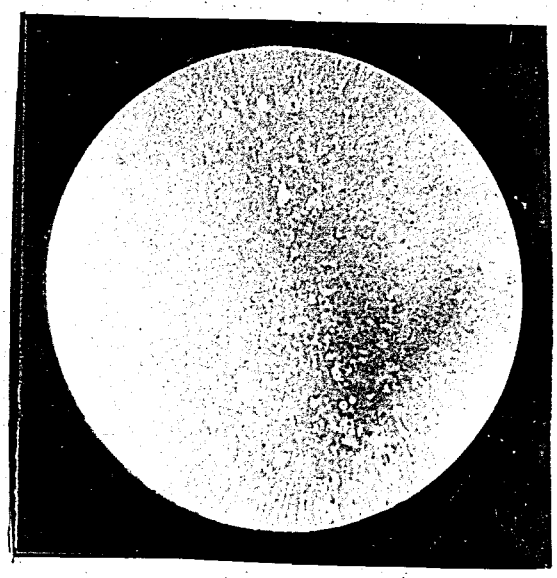

(a)

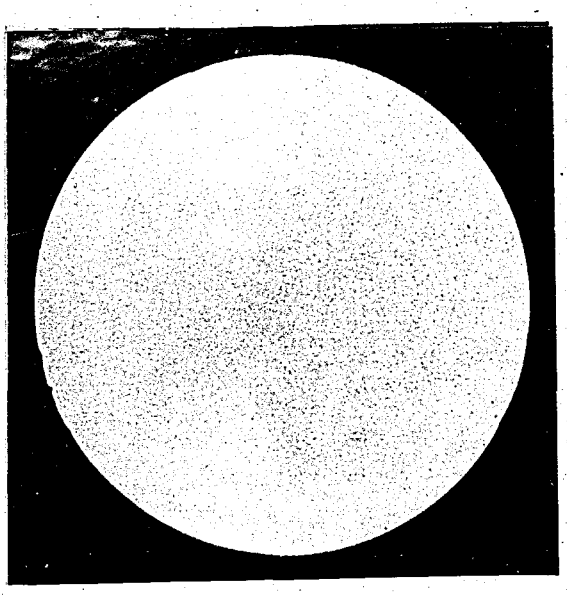

(b)

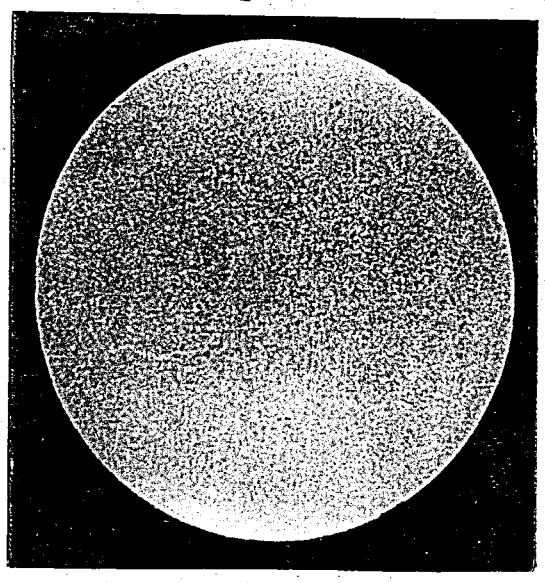

(c)

Figure 43- Macrostructures of the Etial-60 castings, magnification 0.9X ,(a) Sample 74 is cast without master alloy addition ;(b) Sample 35 is cast with the addition of master alloy 17 at 720°C, 10 minutes holding time ;
(c) Sample 38 is cast with the addition of master alloy 17 at 720°C, 120 minutes holding time:

c- Microstructures Of The Castings Inoculated With Master Alloys

Figure 44(a) shows the microstructure of an alloy Etial-7 ingot cast without addition of a master alloy ; this ingot has a fine dentrite spacing and narrow columnar grains. By contrast, in Figure44(b) which shows a section from an alloy Etial-7 ingot cast with the addition of master alloy 17 at 720 C for 10 minutes holding time, the dentrite structure is somewhat coarser but the grains are much smaller and are equiaxed.

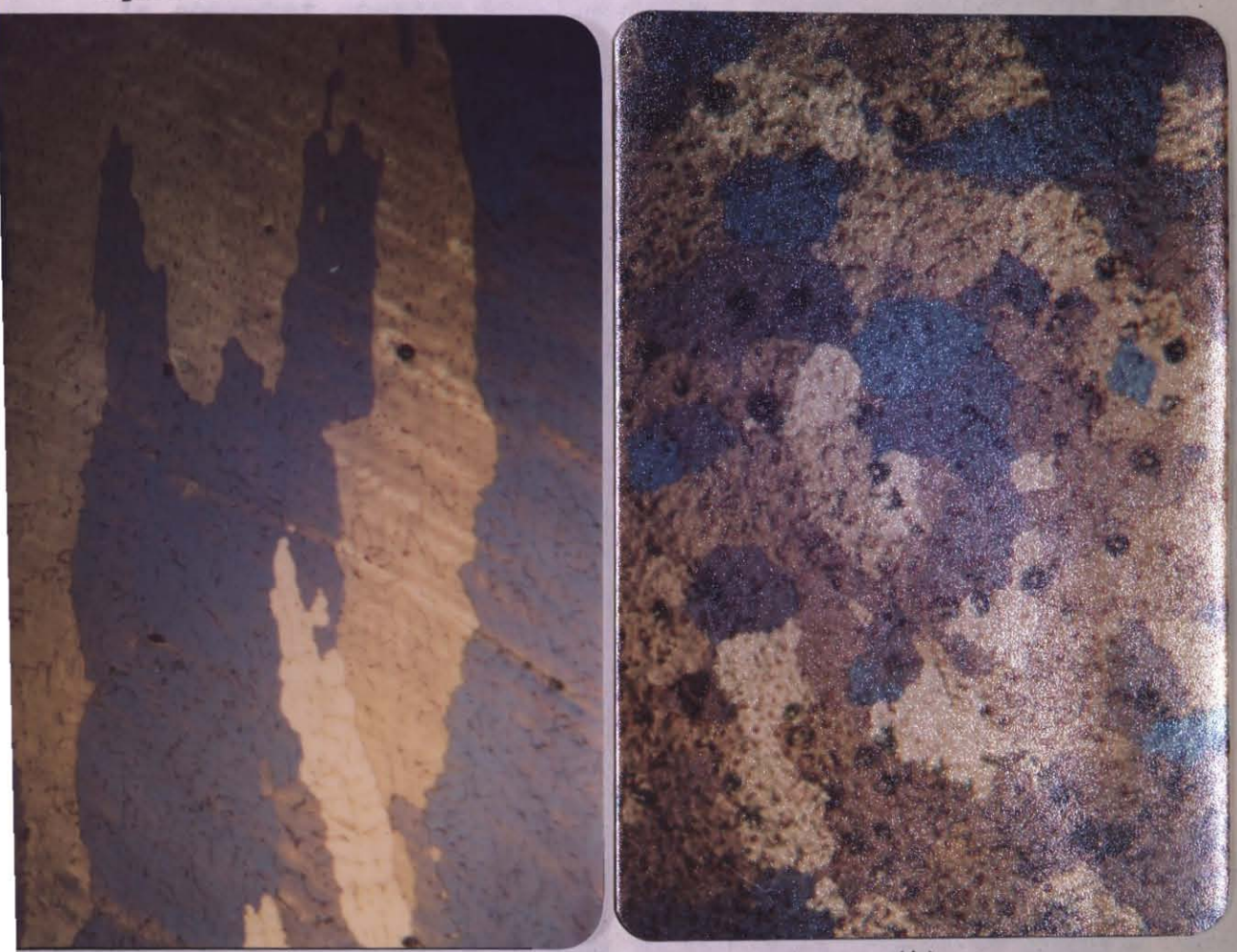

(a) (b)

Figure 44- Microstructures of the Etial-7 Castings, magnifica-

tion 40.5X (a) Sample 72 is cast without addition of master master alloy;(b) Sample 19 is cast with the addition of master alloy 17 at 720°C, 10 minutes holding time.

Figure 45(a) shows the microstructure of an alloy Etial-5 ingot cast without addition of a master alloy ; this ingot has a fine dentrite spacing and narrow, long columnar grains. By contrast, in Figure45(b) which shows a section from an alloy Etial-5 ingot cast with the addition of master alloy 17 at 720 C for 10 minutes holding time, the dentrite structure is somewhat coarser but the grains are much smaller and are equiaxed.

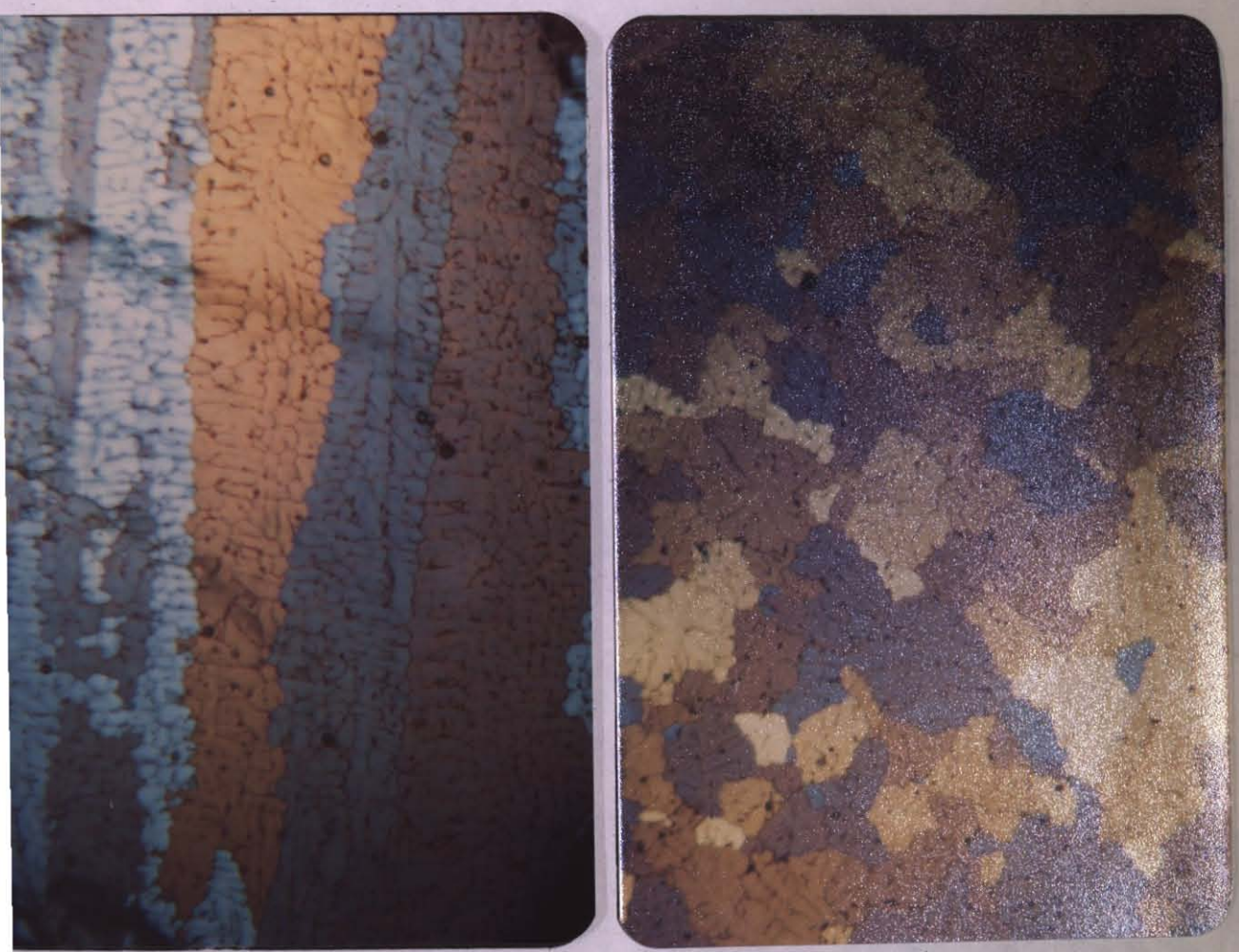

(a) (b)

Figure 45- Microstructures of the Etial-5 Castings, magnification 40.5X (a) Sample 73 is cast without addition of master alloy;(b) Sample 29 is cast with the addition of master alloy 17 at 720°C, 10 minutes holding time.

Figure 46-(a) shows the microstructure of an alloy Etial-60 ingot cast without addition of a master alloy ; this ingot has a fine dendrite spacing but wide columnar grains. By contrast, in Figure46(b) which shows a section from an alloy Etial-60 ingot cast with the addition of master alloy 17 at 720°C temperature for 10 minutes holding time, the dentrite structure is somewhat coarser but the grains are much smaller and are equiaxed.

(a)

(b)

Figure 46- Microstructures of the Etial-60 castings, magnification 40.5x (a) Sample 74 is cast without addition of master alloy (b) Sample 35 is cast with the addition of master alloy 17 at 720°C, 10 minutes holding time.

After the estimation of the average grain sizes by using Heyn method, grain refining curves are plotted. The grain sizes which are given in Table VII are plotted against holding time. The effects of various parameters of grain refining efficiency, such as temperature, other alloying elements and type of master alloys are investigated in detail.

Figure 47 shows the effect of holding time on grain refining performance of the master alloy 17, containing block-like aluminide particles, added into Etial-7 aluminum castings with the addition rate of approximately 0.01 % Ti. From the grain refining curves of the inoculated castings, these are observed ; after addition of the grain refiner, the grain size initially decreases with holding time, reaching a minimum (the ultimate grain size), after this,further holding increases grain-size. Maximum improvement in grain size is obtained approximately at 10 min holding time. In the Figure 47-(b) and (c), the grain refining curves show humps. These humps may lay out due to experimental or measurement errors.

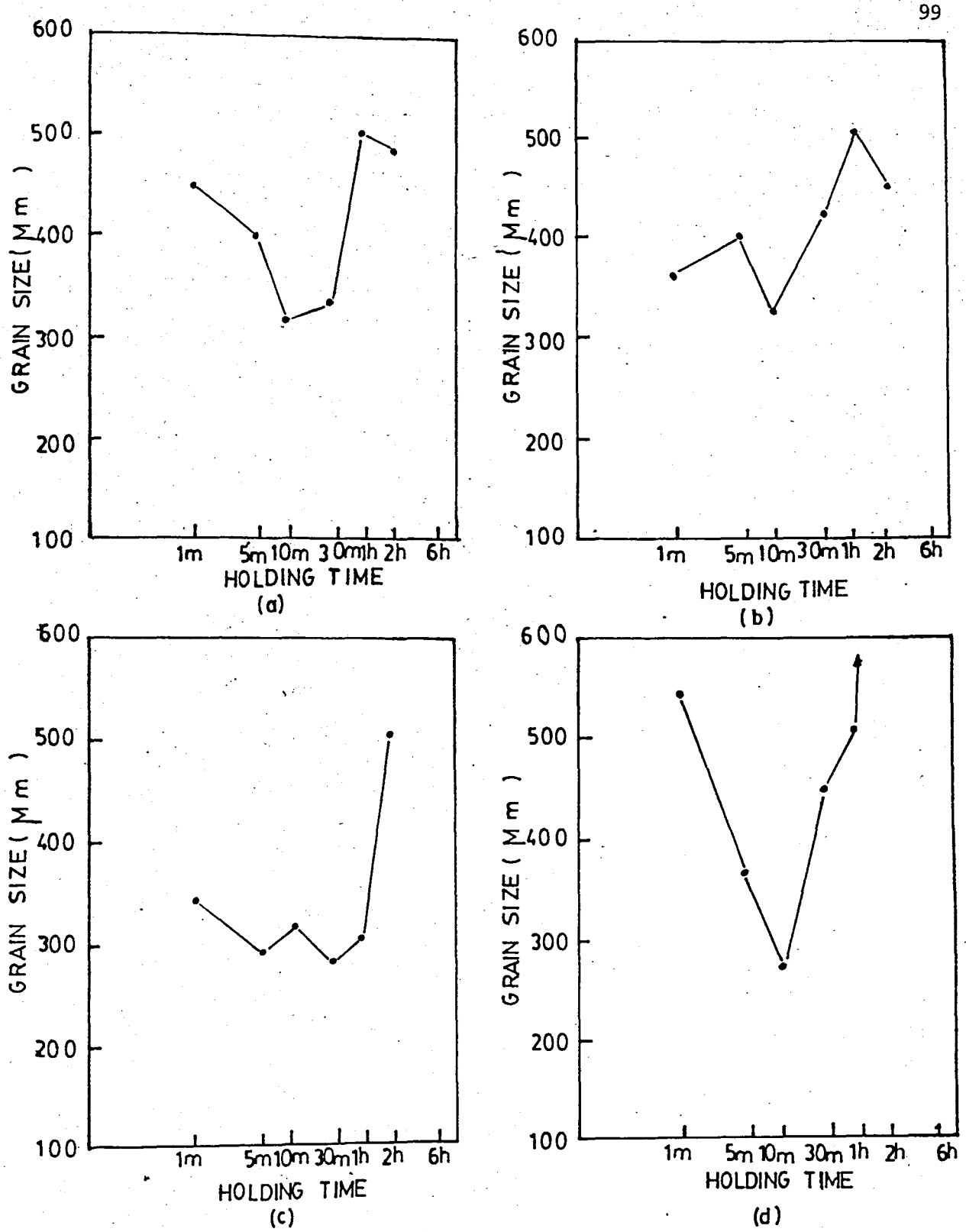

Figure 47- Effect of holding time on grain refining performance of the master alloy 17, containing block-like aluminide particles, added into Etial-7 aluminum castings with the addition rate of approximately 0.01 % Ti.
(a) at 700°C ; (b) at 720°C ; (c) at 740°C ; (d) at 780°C

Figure 48 shows the effect of holding time on grain refining performance of the master alloy 17, containing block-like aluminide particles, added into Etial-5 and Etial-60 aluminum castings at 720 C with the addition rate of appoximatelly 0.01 % Ti. The grain refining curve belonging to Etial-5 aluminum castings is shown in Figure 48(a). From this figure, after the addition of master alloy 17, the grain size initially decreases with holding time, reaching a minimum at 30 minutes, after this, grain-size increases rapidly with increasing holding time. The grain refining curve of Etial-60 aluminum castings is shown in Figure48(b). From this figure, after the addition of the grain refiner, the grain-size initially decreases with holding time, a minimum at 10 minutes, after this holding gives increasing grain-size.

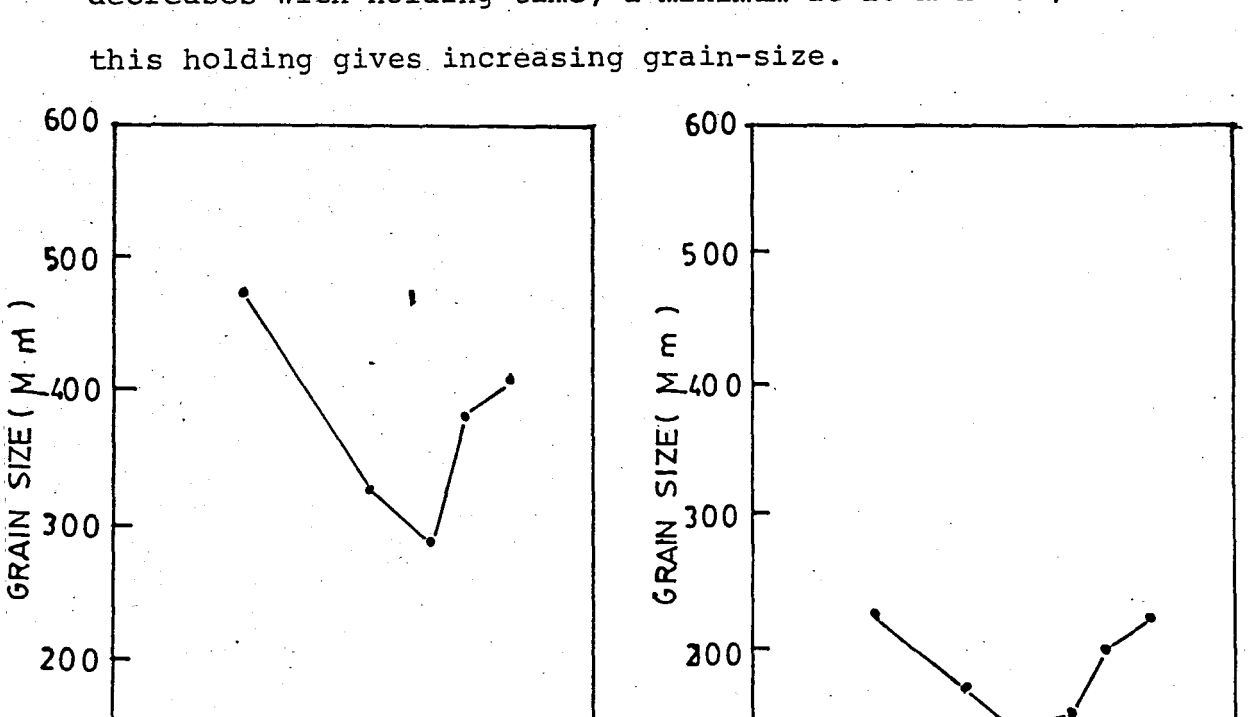

Figure 48- Effect of holding time on grain refining performance of the master alloy 17, containing block-like aluminide particles,added into molten aluminum at 720°C with the addition rate of approximatelly0.01
(a) Etial-5 castings ;(b) Etial-60 castings

Figure 49 shows the effect of holding time on grain refining performance of the master alloy 18, containing flake-like aluminide particles, added into Etial-7 aluminum castings with the addition rate of approximately 0.01 % Ti. Figure 49(a) shows the grain refining curve of Etial-7 castings inoculated with master alloy 18 at 700 C. From this Figure, after the addition of master alloy, the grain size decreases continuously with holding time, and shows a hump at 30 minutes, after this, further holding gives decreasing grain-size. Figure49(b) shows the grain refining curve of Etial-7 castings inoculated with master alloy 18 at 740 C. After the addition of master alloy, the grain size decreases rapidly with holding time, it begins to increase after 5 minutes to 30 minutes and then grain size decreases with holding time and after 60 minutes holding time, the grain size again increases with inreasing holding time. Finally, figure49(c) shows the grain refining curve of Etial-7 castings inoculated with master alloy 18 at 780 C. From this figure, after addition of the master alloy, the grain size decreases continuously with holding time, and shows a hump at 10 minutes holding time, after this, grain size decreases rapidly with holding time, reaching a minimum (the ultimate grain size) at 30 min holding time. After 30 min holding time, further holding increases grain-size. From the grain refining curves of the Etial-7 castings inoculated by master alloy 18 containing flake-like aluminide particles show maximum improvements in grain size with increasing holding time.

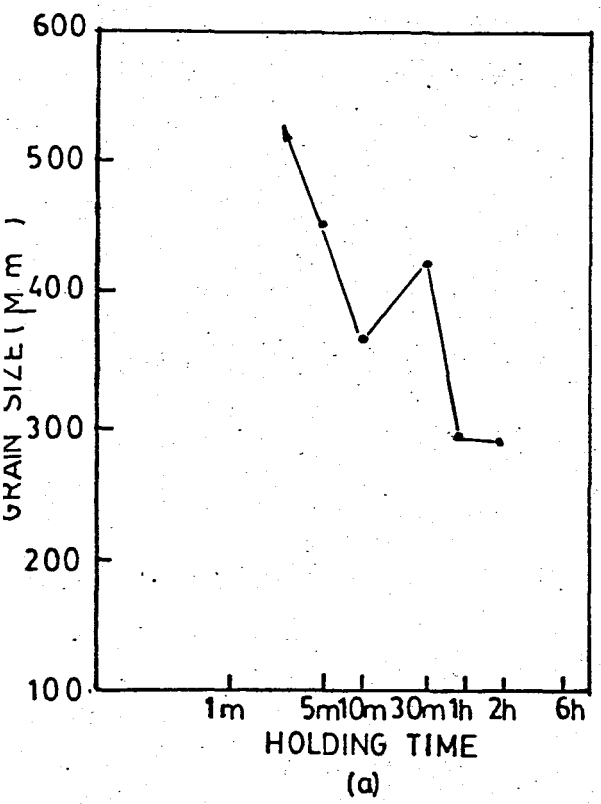

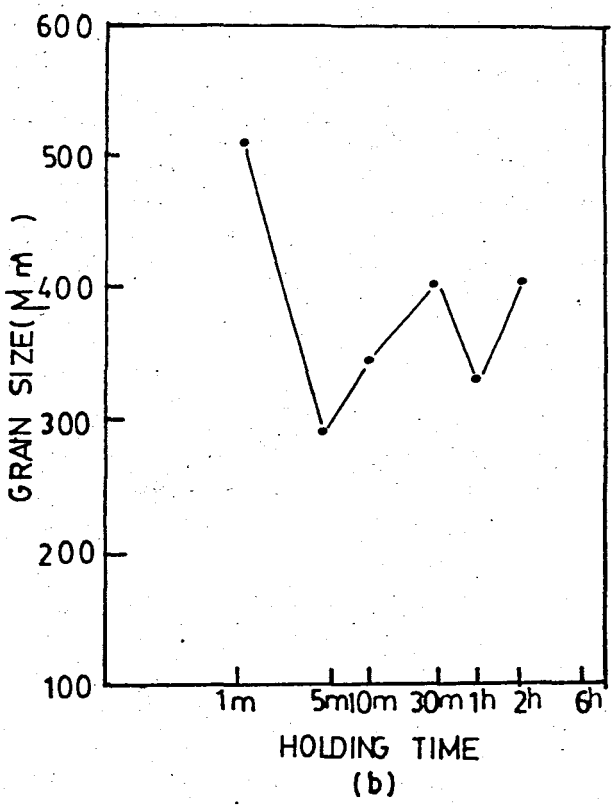

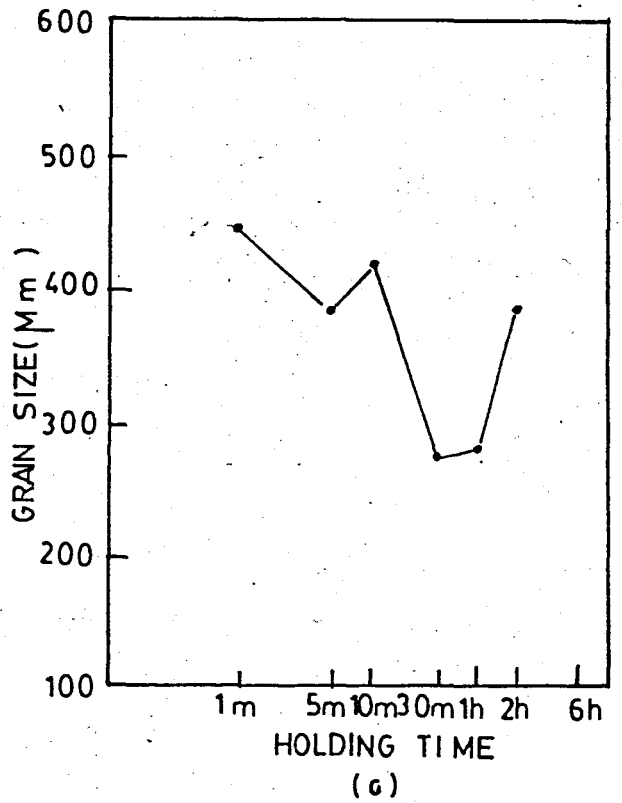

Figure 49- Effect of holding time on grain refining performance of the master alloy 18, containing flake-like aluminid particles, added into Etial-7 aluminum castings with the addition rate of approximately 0.01 % Ti.
(a) at 700°C ;(b)at 740°C ; (c) at 780°C

Figure 50 shows the effect of alloy composition on grain refining performance of the master alloy 17, containing block-like aluminide particles, added into ingots with the addition rate of approximately 0.01 % Ti at 720 C. Maximum grain refinement is obtained by using Etial-60 aluminum alloy the composition of which is given in Table V. The grain refinement of Etial-5 aluminum castings is more successful than Etial-7 aluminum castings.

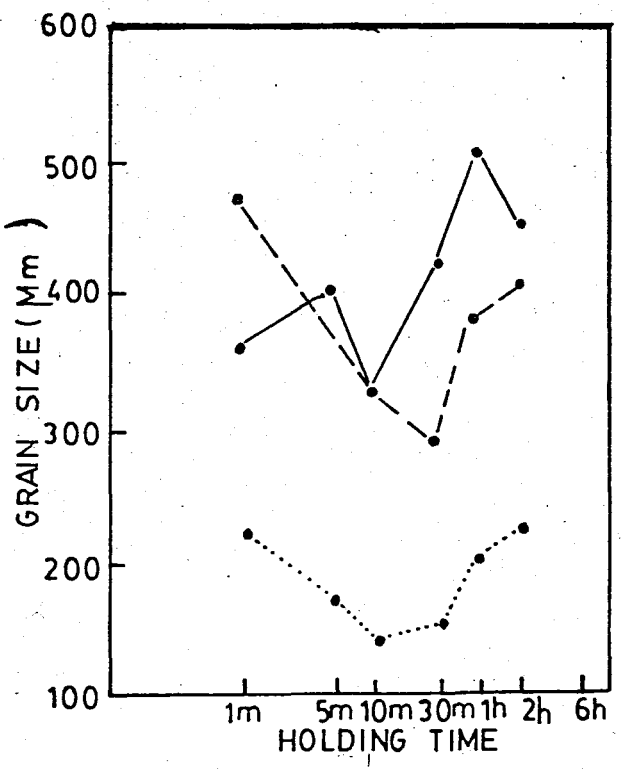

Figure 50- Effect of alloy composition on grain refining performance of the master alloy 17, containing block-like aluminide particles, added into ingots with the addition rate of approximately 0.01 % Ti at 720 °C.

———————— Etial-7 aluminum alloy

---------- Etial-5 aluminum alloy

..... Etial-60 aluminum alloy

Figure 51 shows the effect of temperature on grain refining performance of the master alloy 17, containing block-like aluminide particles, added in Etial-7 aluminum ingots with the addition rate of approximately 0.01 % Ti at different temperatures. After addition of the grain refiner, the grain size initially decreases with holding time, reaching a minimum at approximately 10 min. , at different temperatures (700°C, 720°C, 740°C and 780°C),after this, grain size increases rapidly with increasing holding time, especially at 780°C.

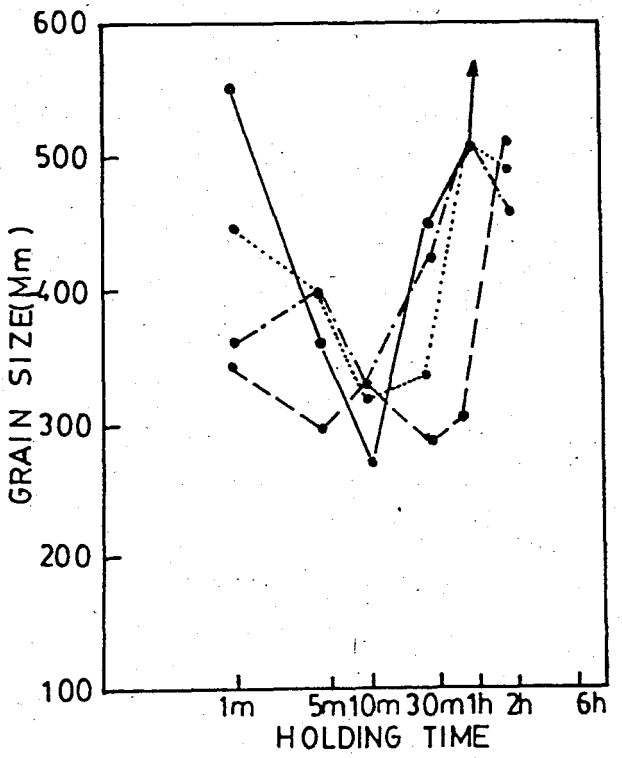

Figure 51- Effect of temperature on grain refining performance of the master alloy 17, containing block-like aluminide particles, added into Etial-7 aluminum ingots with the additon rate of approximately 0.01 % Ti.

.....700°C -------740°C

—·—·—·—720 °C ———— 780 °C

Figure 52 shows the effect of temperature on grain refining performance of the master alloy 18, containing flake-like aluminide particles, added into Etial-7 aluminum ingots with the additon rate of approximately 0.01 % Ti at different temperatures. After addition of the grain refiner, the grain size continously decreases with holding time at 700°C. For the temperature of 740°C and 780°C, the grain size initially decreases with holding time, reaching a minimum at one hour (for 740°C) and at 30 min. (for 780°C), after this, grain size increases rapidly with increasing holding time.

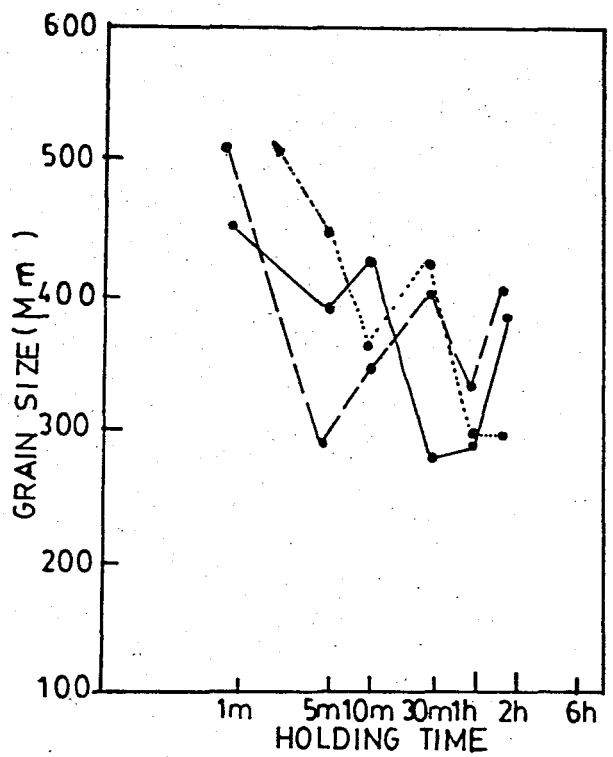

Figure 52- Effect of temperature on grain refining performance of the master alloy 18, containing flake-like aluminide particles, added into Etial-7 aluminum ingots with the addition rate of approximately 0.01%T

..... 700°C ; -------- 740°C ; _____ 780°C

Figure 53 shows the effect of alloy composition on grain refining performance of 5/1 TİBAL master alloy produced by London and Scandinavian Metallurgical Co Limited in England. This master alloy is added into min 99.7 % Al corresponding to Etial-7 aluminum alloy and alloy 6063 corresponding to Etial-60 aluminum alloy at 720°C with the addition rate of 0.01 % Ti. After addition of the grain refiner, grain-size initially decreases with holding time, reaching a minimum at approximately 10 min holding time, after this, grain size increases with increasing holding time for both of the alloys (6063 and 99.7 % Al). From the figure, the grain refinement of alloy 6063 is more succesful than min 99.7 % Al alloy.

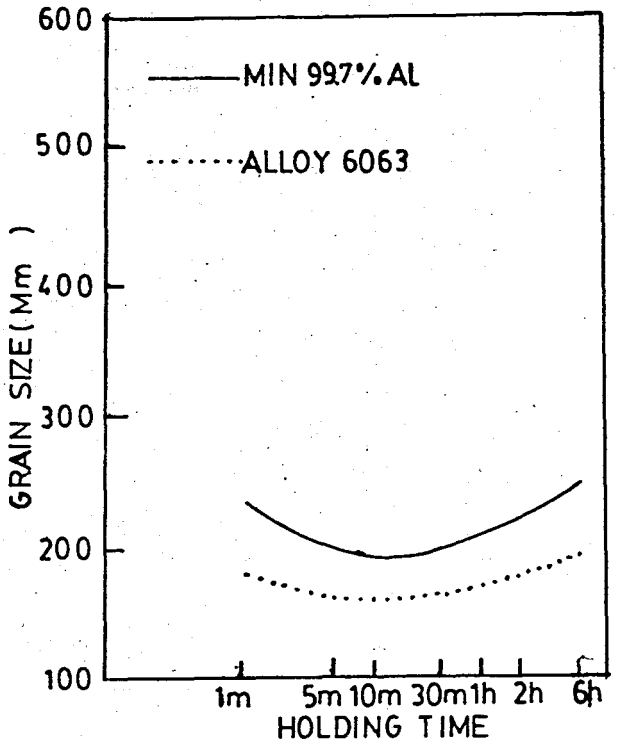

Figure 53- Effect of alloy composition on grain refining performance of 5/1 TİBAL master alloy, containing block-like aluminide particles, added into alloy 6063 and min 99.7 % Al ingots with the addition rate of 0.01 % Ti at 720°C.

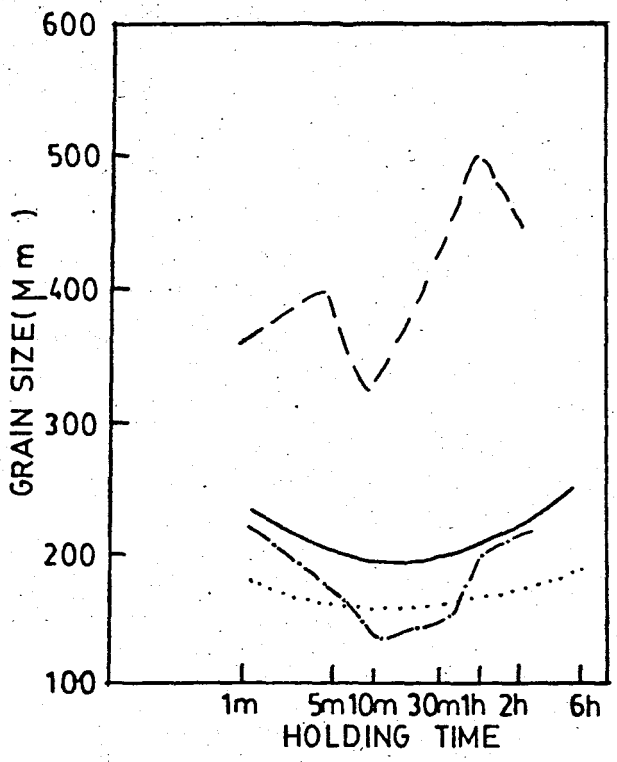

Figure 54- Comparison of the grain refining performance of the master alloys.

------ Etial-7 alloy
------ Etial-60 alloy
_____ MIN. 99.7 % Al
..... Alloy 6063

Results obtained in this Study

Results obtained by LSM (London & Scandinavian Metallurgical co limite

The comparison of grain refining performance between master alloy obtained in this study and master alloy obtained by the previous workers is shown in Figure 54. The grain refinement improvement of the 99.7 % aluminum castings by using the master alloy 17 produced in this study is less than the master alloy produced by the previous workers. The element contents included in 0.3 pct of the 99.7 % aluminum used by previous workers for testing the grain refining performance of master alloy are not published. The difference between chemical compositions

of the commercially pure aluminum may be the reason for difference in grain sizes between the present study and previous studies.

This unknown portion of aluminum used by the other workers may increase the nucleation rate causing grain refinement. The differences may also be due to the experimental or measurement techiques. In the present study, grain size measurements are performed near the mold wall due to preparation of tensile test specimen from the center region of the ingot. Grain size generally begins to increase near the mold wall for 99.7 % aluminum ingots. this may be the cause for the greater grain size in the present study than the previous studies.

5.6.2 Results Of The Tension Tests

For the Etial-60 aluminum alloy inoculated with the master alloy 17 containing block-like aluminide particles and without inoculation, seven tension tests were performed by loading the specimen monotonically until failure. During loading the load vs. displacement was recorded graphically. The results obtained from tension tests are given in Table VIII.

TABLE VIII- ULTIMATE TENSILE STRENGTH, YIELD STRENGTH AND % ELONGATION DATA FOR ETIAL-60 CASTINGS

Sample Number	Casting Temperature (^{o}C)	Holding Time (Min)	UTS (MPa)	YS (MPa)	% Elongation	Average Grain Size (μm)
74	720	-	130.4	17.1	14.4	-
33	720	1	150.9	39.2	32	237
34	720	5	157.9	36.7	28	172
35	720	10	163.8	61.8	24	140
36	720	30	155.9	53.9	25.6	160
37	720	60	154.9	45.1	28.4	200
38	720	120	154	31.4	29.6	223

Figure 55- shows the load-elongation and stress-strain curve of the sample 74 which is cast without the addition of master alloy at 720^{o}C.

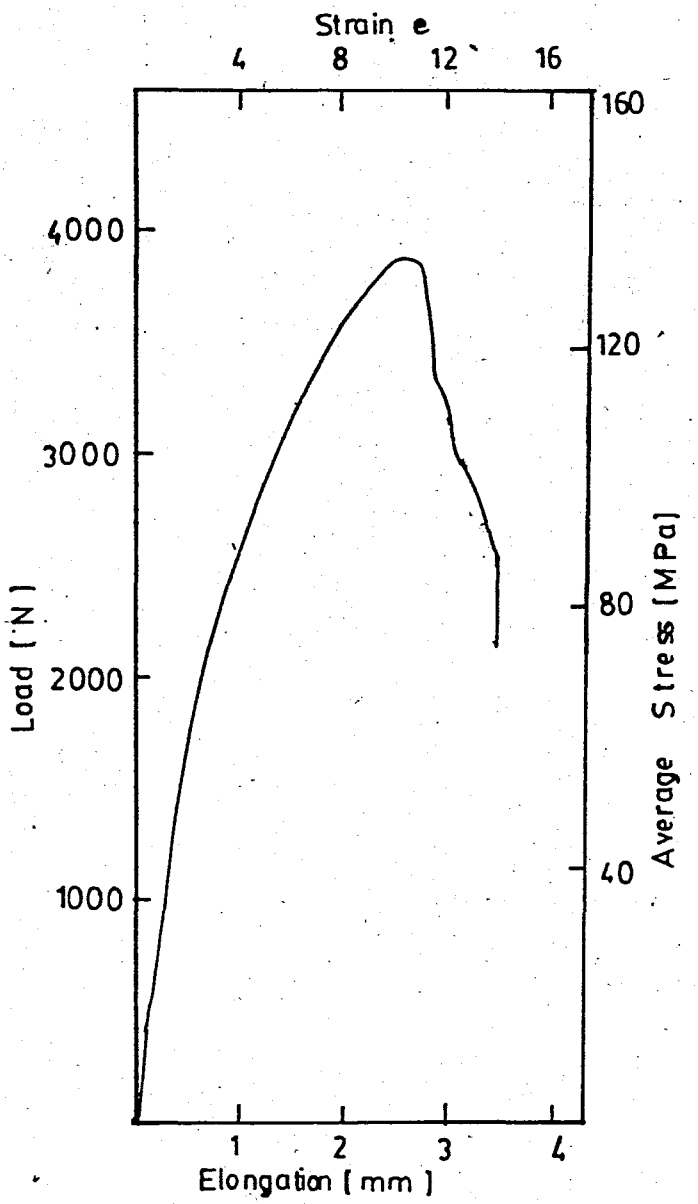

Figure 55- Load-elongation and Stress-strain curve of the sample 74.

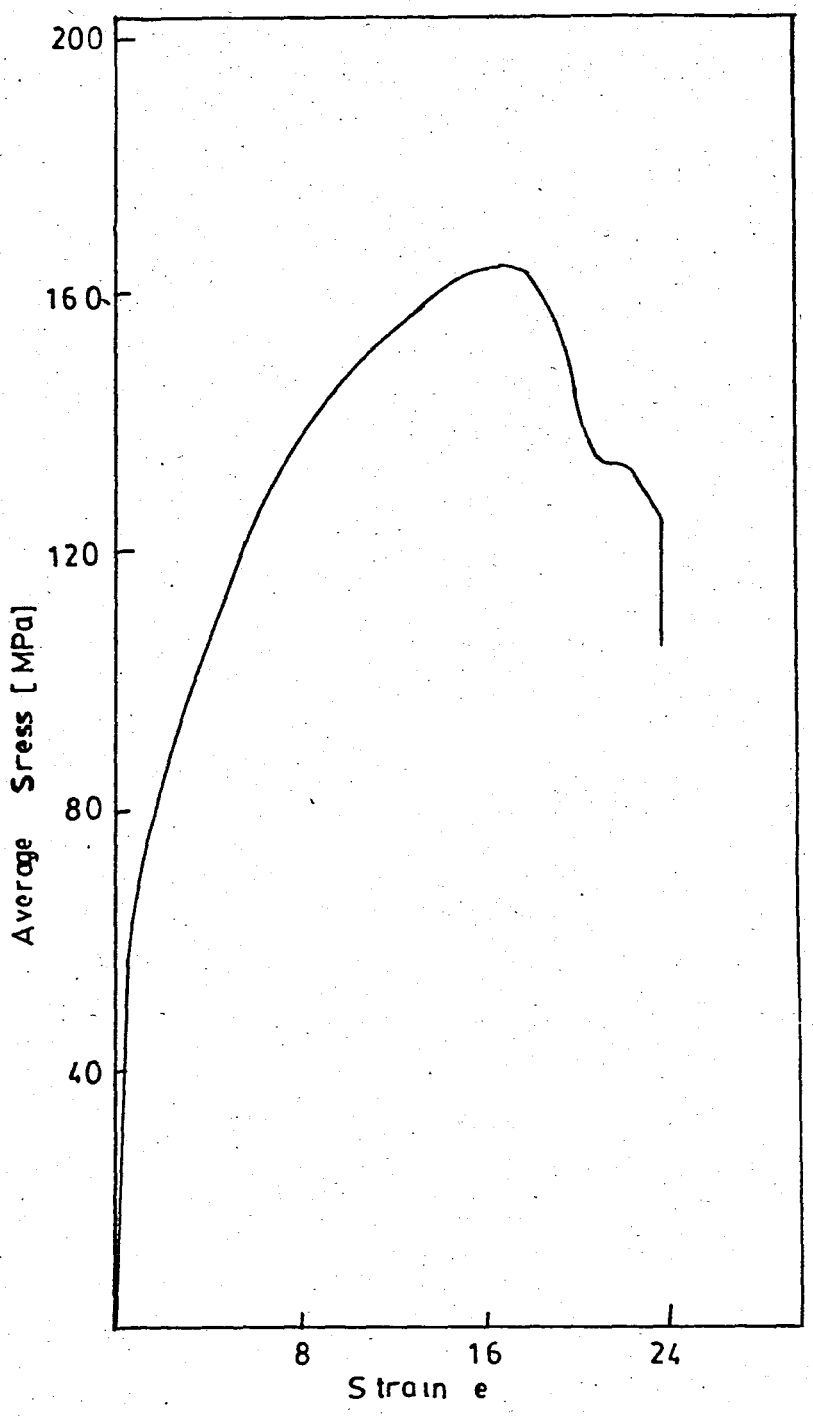

Figure 56- Stress-Strain curve of the sample 35 .

stress-strain curve of the sample 35 which is cast with the addition of master alloy 17, containing block-like aluminide particles, at 720°C for 10 min holding time is shown in Figure 56. The improvements in the strength properties indicate the effects of master alloy addition on the Etial-60 aluminum alloy ingots. Stress-strain Curves of the other samples are given in appendix. Yield and ultimate tensile stress of Etial-60 aluminum castings as a function of the grain size are shown in Figure 57.

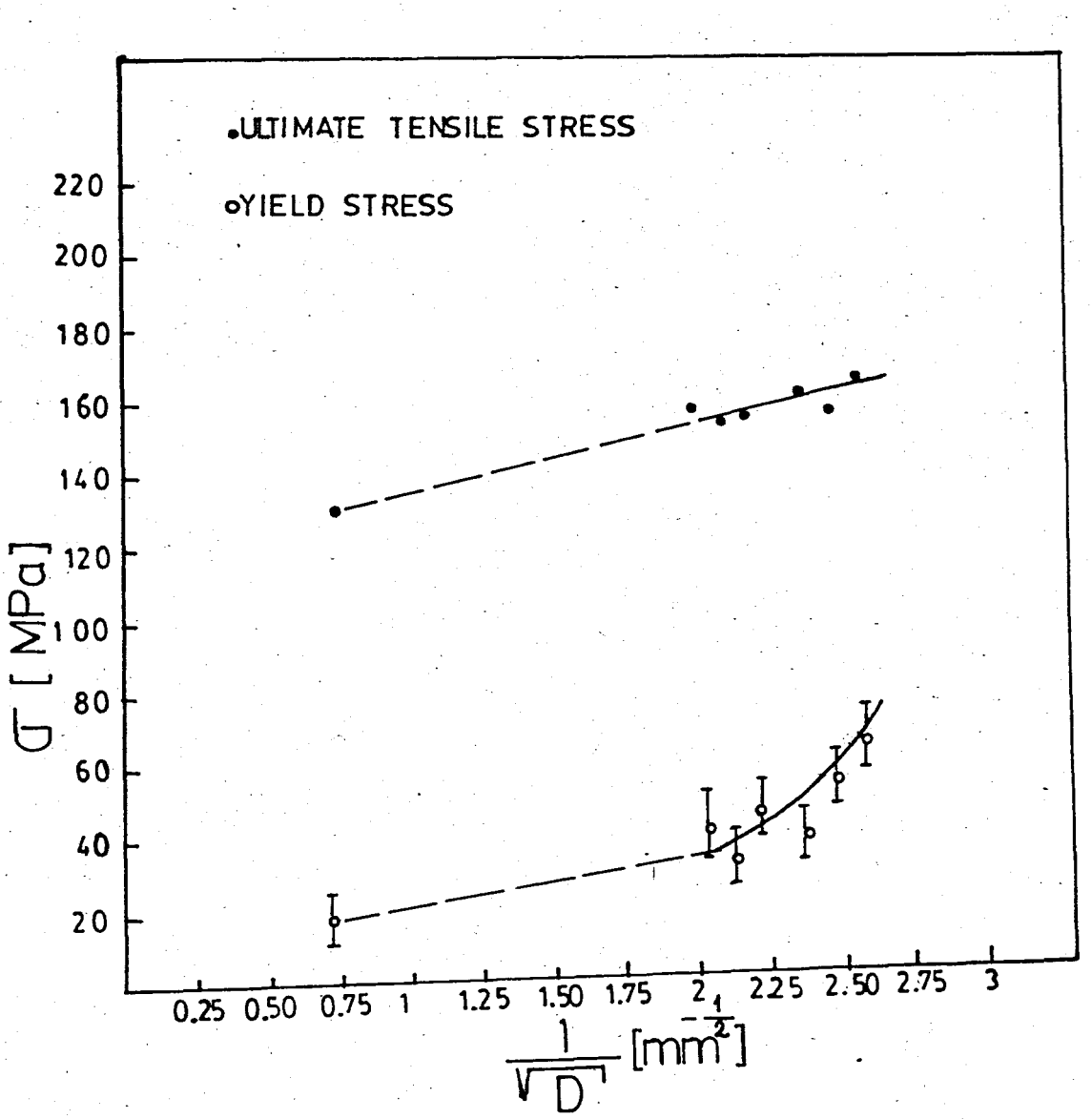

Figure 57- Yield and Ultimate Tensile stress of Etial-60 aluminum castings as a function of the grain size.

From the Figure 57,ultimate Tensile Stress and Yield Stress of the Etial-60 aluminum castings show increasing tendency with decreasing grain size. The determination of the yield strength of the specimens is quite tedious, and dependent on the sensitivity of the tension test instrument. Because of this reason the yield strength data obtained in the study does not indicate a high accuracy.

5.6.3 Results of The Hardness Tests

Seventy-eight hardness tests were performed for each group of alloys inoculated with master alloys containing block-like and flake-like aluminides, and three hardness tests were made for each group of alloys (ETIAL-7, ETIAL-5,ETIAL-60) which were not inoculated with master alloy. The results of the BHN tests are given in Table VII.

Secondly, seven hardness tests were carried out for the Etial-60 aluminum castings inoculated by the master alloy 17 containing block-like aluminide particles. The results of the VHN tests of the seven specimens are given in Table IX

TABLE IX- Vickers Hardness Test Results at 10 kg. Load

Sample Number	Concentration		Casting Temp. (^{o}C)	Holding Time (Min)	Hardness VHN (Kg/mm^2)
	Wt % Ti	Wt % B			
74	0.006	0.001	720	-	39.7
33	0.015	0.002	720	1	43.6
34	0.018	0.003	720	5	43.9
35	0.021	0.003	720	10	43.1
36	0.014	0.002	720	30	41.4
37	0.016	0.002	720	60	41.0
38	0.017	0.004	720	120	40.5

VI. DISCUSSION

6.1 On the Master Alloys and Castings

Metallographic examination of the master alloys showed that the boride (TiB_2,ALB_2) particles were located mainly at the cell boundaries. The size distribution and the morphology of the particles were independent of the formation temperature (800°, 850° or 900°C). Boride particles of the master alloy 18 into which the salts of K_2TiF_6 and KBF_4 were added at high temperature (900°C) were located completely at the cell boundaries (Figure 33). Although the master alloy 17 were prepared by adding the salts at low temperature (800°C), again the boride particles were located mainly at the cell boundaries (Figure 38). While the size and morphology of the boride particles seem to vary very little, Aluminide (Al_3Ti) particles can exhibit different morphologies and show a marked variation in size.

Aluminide particles, in the master alloys where the salts of K_2TiF_6 and KBF_4 were added at high temperature (900°C), have a needle-like appearance (Figures 33-37). Aluminide particles formed at a high temperature, low supersaturation and moderate cooling rates (0.60 $^{o}Ks^{-1}$ or 0.65$^{o}Ks^{-1}$) have a needle-like appearance, but are really plates as shown in the lower rihgt-

hand corner of the Figure 36. These particles having a needle-like appearance are called "Flake-like" crystals. At these conditions, the growth is controlled by long-range diffusion and is dentritic |5|. The dentrite arms grow in <110> directions. Growth is restricted inthe [001] direction, so the crystals are almost two dimensional, but a new layer occasionally can nucleate on the (001) plane. This second layer has the same growth behaviour as the first one. The flake-like Al_3Ti particles forming in the master alloys produced at the present study are typically sized about 50-200 microns in length.

Aluminide particles, in the master alloys where the salts of K_2TiF_6 and KBF_4 are added at low temperature (800°C), have a block-like appearance and are more compact than the flake-like particles and are also smaller as shown in Figures 38 and 39. At the conditions of low temperature (800°C), high supersaturation and moderate cooling rates ($0.60\,^{o}Ks^{-1}$ or $0.65\,^{o}Ks^{-1}$), frequent nucleation of new layers of the aluminides on the {001} planes can occur. When a layer nucleates, it begins to spread by lateral advance of the step bounding the layer. Nucleated layers can not grow continuously due to the decreasing temperature. Because of these reasons, block-like particles show well developed {001} and {011} surfaces and are smaller and are more compact than the flake-like ones. The size of the block-like particles increases with decreasing cooling rate. This is shown in Figures 38 and 39. Master alloy 17 shown in Figure 38 is chilled with the cooling rate of $0.60\ ^{o}Ks^{-1}$ and master alloy 12 shown in Figure 39 is chilled with the cooling

rate of 0.65 $^{o}Ks^{-1}$. Master alloy 17 has greater block-like particles than the master alloy 12 since the particles of master alloy 17 are hold a long time by means of the low cooling rate for growth. The block-like particles in the master alloys produced in the present study are typically sized about 6-60 microns in length.

The addition of the master alloy 17 containing blocky Al_3Ti crystals gives a better grain refinement after a short contact time than the addition of the master alloy 18 containing the flake-like Al_3Ti crystals. The grain refinement decreases with increasing contact time when AL-Ti-B master alloy 17 containing blocky aluminide particles is used (Figure 47). The grain refinement improves with increasing contact time when ternary AL-Ti-B master alloy 18 containing flake-like aluminide particles is used as shown in Figure 49.

Since block-like aluminide particles are more compact and smaller than the flake-like ones, the block-like aluminide particles dissolve more readily than the flake-like ones. If the ternary AL-Ti-B master alloy 17 containing blocky Al_3Ti crystals is held for a prolonged contact time, there would be a decreasing number of surviving Al_3Ti crystals, and consequently fewer nucleating sites. Because of decreasing nucleating sites, fading in grain refinement occurs with increasing holding time.

Ternary AL-Ti-B master alloy 18 containing flake-like Al_3T particles gives a better grain refinement with increasing contact time when diluted to hypoperitectic composition (the

addition rate of titanium is less than 0.15 wt %Ti). This improvement in grain refinement is due to the disintegration of agglomerates of boride particles (TiB_2 and AlB_2) and aluminide particles (Al_3Ti) during the contact time. Because of increasing nucleating sites, improvement in grain refinement occurs with increasing holding time for the master alloy 18.

The effect of addition temperatures of the master alloys added into the castings must also be considered in one context with the effect of holding time. If the addition temperature is very high, aluminide particles dissolve completely, and the master alloy used loses the grain refining effect on the castings. This is shown in Figure 51 and 52 that grain refinement effect of each master alloy decreases rapidly at high addition temperatures (740^{o} and 780^{o}C) and long holding times (60 min and 120 min).

6.2 On the Relationship Between The Grain-Size and Mechanical Properties

The variation of tensile strength, yield strength and elongation, due to the addition of the master alloy 17, depending on holding time and casting temperature is seen from the stress-strain curves of the ingots given in Figure 55 and Figure 56 and the experimental data given in Table VIII.

As the effects of the master alloy 17 addition in to the Etial-60 aluminum castings are considered, it is observed that the maximum improvements 25% in tensile strength and 261% in

yield strength are obtained at 10 min. holding time. The maximum improvement 122% in elongation is obtained at 1 min. holding time. Experimental results show that the strength of castings inoculated by the master alloy increases as their grain size is refined (Figure 57). This strengthening, which is generally presumed to be due to the direct influence of the grain-size refinement itself, is demonstrated by performing different mechanical property measurements such as UTS, YS, % elongation and hardness.

There is not any fully developed theory which is quantitative in every detail for the influence of grain size on the strength. The most advanced theory which has been proposed for the strength is one that attributes the influence of grain size to the stress concentrating character of individual slip bands being driven by the shear component of an applied stress [18].

This theory built on the notion that the grain boundaries of a polycrystal normally act as major barriers to the propagation of the dislocation slip and twinning processes which operate within the grain volumes. One of a number of models of the stress-concentrating character of a slip band gives a shear stress (ζ), dependence on slip band length or average grain diameter (D) of the form [18]

$$\zeta = \zeta_o + k_s D^{-1/2} \qquad (1)$$

where, ζ_o = the shear stress required to cause slip to occur in the absence of a grain boundary resistance

k_s = a measure of the stress concentration which is generated at the tip of a slip band.

The yield stress must be achieved within virtually all of the grains of the material and on sufficient deformation systems within each grain so that local continuity of plastic strain is maintained between grains, during bulk deformation of a polycrystal. This consideration involves the calculation of an average orientation factor, m, which is required to transform the operating shear systems within the grains onto the coordinate system of the bulk strain tensor. Because of this consideration, the value of ζ in equation (1) has been related to the externally applied stress (σ) to the following relation

$$\sigma = m \zeta \qquad (2)$$

by assuming that each grain within the polycrystal undergoes the same strain as the bulk material. Value of m has been computed for face-centered cubic (FCC) structures as m=3.1 |18|.

The foregoing description shows that two main ideas are required to understand even in a simple way the process of plastic yielding in a polycrystalline aggregate.

a) Internal shear stress concentrations are necessary for individual slip bands to break out of the confinement presented by the grains surrounding their own grain volume, as represented in equation (1),

b) and these shear stress must be related to the applied stress through consideration of maintaining continuity of strain within the material, as represented by equation(2). A combination of equation (1) and (2) gives the stress-grain size relationship [18].

$$\sigma = m \zeta_o + mk_s D^{-1/2} \qquad (3)$$

For yielding, ζ_o should be taken as the resolved shear stress for plastic flow in a single crystal undergoing deformation on multiple shear systems. This stress is usually slightly greater than the critical resolved shear stress for the onset of plastic flow on only one deformation system of a single crystal.

As a result of the tension tests of the aluminum castings inoculated by the master alloy (17), it is shown that the grain refinement of the castings significantly effects the ultimate tensile strength (UTS) and yield strength(YS) properties. Also, high improvements in ductility measurements (elongation) indicate the large extent to which the inoculated castings can be deformed without fracture in metalworking operations such as rolling and extrusion.

The variations of the hardness value of the inoculated and not inoculated alloy castings with increasing holding time, casting temperature, addition rate of the master alloy, type of master alloy and the kind of aluminum are shown in Table VII and IX.

From the examination of those illustrated data, it is predicted that some of the inoculated ingots of Etial-7 and Etial-60 aluminum with block-like master alloy 17 or flake-like master alloy 18, exhibit a small improvement in BHN. Conversely,the decreasing tendency in BHN were observed in some of the castings inoculated with master alloys especially including flake-like particles (Table VII, samples 51-71).The increasing tendency in BHN were observed in Etial-5 aluminum castings with the addition of master alloy (Table VII, samples 43-46B; 27-32).

The BHN of the cast alloys inoculated master alloys were not systematically effected by the increase in casting temperature, addition rate and holding time. The slightly increasing tendency in VHN with the addition of master alloy 17 was seen in Etial-60 aluminum castings (Table IX.samples 33-38).

As a result of the hardness tests performed in the present study, it can be claimed that, the grain refinement of aluminum castings by using master alloy,produced in this study, does not effect significantly the hardness of the material. This is a good result, since "in general, hardness usually implies a resistance to deformation, and for metals the property is a measure of their resistance to permanent or plastic deformation" |19| . The master alloys essentially are used in the production of ingots, extrusion billets and sheets for fabrication and these products are used in metalworking operations such as rolling and extrusion in order to obtain foil and various profile. The ability of the metal to flow plastically before fracture is an important factor in the operations of rolling

and extrusion.

Finally, there is no significant effect in hardness value of the castings inoculated with the master alloys produced in the present study and this implies that produced master alloys can be used in extrusion billets and rolling slabs.

VII. CONCLUSIONS

The effects of ternary Al-Ti-B master alloys (Tıbor) on microstructure and mechanical properties of aluminum castings were determined. The effect of inoculation with master alloy on solidifying castings has been explained by mainly two theories "a. Boride Theory, b. Peritectic reaction theory" previously. The boride theory can not explain the experimental results obtained in this study. The peritectic reaction theory will not give a general explanation of the grain refinement results if some mechanism by which the number of aluminide particles can increase with contact time is not considered in the case when master alloy with flaky crystals is used.

The morphology of Al_3Ti has a marked influence on the grain refinement-contact time characteristic of a master alloy. Block-like aluminide (Al3Ti) particles show good grain refinement after a short contact time, but the grain refining ability fades rather quickly as the contact time is increased. Master alloy containing flake-like aluminide crystals shows an increase in the grain refining ability with increasing contact time.

Block-like aluminide (Al3Ti) crsytals in the master alloy are obtained at low temperature ($\sim 800^{\circ}C$) and moderate cooling

rate ($\sim$0.6 K^{o}/s). Flake-like aluminide (Al_3Ti) crystals in the master alloy are obtained at high temperature ($900^{o}C$) and moderate cooling rate ($\sim 0.6^{o}K/s$).

The grain refinement of aluminum castings inoculated by tibor effects significantly the ultimate tensile strength (UTS), the yield strength (YS) and elongation (e) properties of the aluminum castings.

REFERENCES

1. G.S. Cole and G.F. Bolling, "Development of Ultrafine-Grain Metallic Structures by Solidification", Proceedings of the 16th Sagamore Army Materials Research Conference, Syracuse University, New York, pp.31-63, 1970.

2. G.S Cole, K.W. Casey and G.F Bolling, "The Solidification of Inoculated Aluminum Ingots", Metallurgical Transactions, Vol.1, pp.1413-1416, 1970.

3. B. Chalmers, "Principles of Solidification", J.Wiley and Sons, New York, 1964.

4. L. Backerud, "On the Grain Refining Mechanism in Al-Ti-B Alloys", Jerkontorets Ann, Vol.155, pp. 422-424,1971.

5. L.Arnberg, L.Backerud, H.Klang, "Grain Refinement of Aluminum", Metals Technology, pp. 1-17, January 1982.

6. G.P.Jones and J.Pearson, "Factors Affecting the Grain-Refinement of Aluminum Using Titanium and Boron Additives", Metallurgical Transactions B, Vol. 7B, pp.223-234,1976.

7. J.A. Marcantonio and L.F. Mondolfo, "Grain Refinement in Aluminum Alloyed with Titanium and Boron", Metallurgical Transactions, Vol. 2, pp.465-471, 1971.

8. I. Maxwell and A Hellawel, "The Constitution and Solidificaiton of Peritectic Alloys in the System Al-Ti", Acta Metallurgica, Vol.23, pp. 895-909,1975.

9. D.A.Granger, "Solidification structures of Aluminum Alloy Ingots" Metals Handbook, "Metallography and Phase Diagrams", Vol.8, pp.163-168, 1973.

10. T.W. Clyne and M.H.Robert, "Stability of Intermetallic Aluminides in Liquid Aluminum and Implications for Grain Refinement", Metals Technology, pp.177-185, May 1980.

11. A. Cibula, "The Effect of Grain Size on the Tensile properties of High-Strength Cast Aluminum Alloy" Journal of the Institute of Metals, Vol. 76, pp.321, 1949-1950.

12. J. Moriceau "Discussion of the Mechanisms of Aluminum Grain Refining by Titanium and Boron" Revue De L. Aluminum, Vol. 12, pp. 977-988, 1972.

13. Donald T. Hawkings and Ralph Hultgen, "Constitution of Binary Alloys" Metals Handbook, "Metallography and Phase Diagrams", Vol. 8, pp. 264, 1973.

14. Geoffery K.Sigworth, "The Grain Refining of Aluminum and Phase Relationships in the Al-Ti-B system", Metallurgical Transactions A, Vol.15A, pp.277-282, 1984.

15. P.R Sperry and M.H. Bankard, "Metallographic Technique for Aluminum Alloys", Metals Handbook "Metallography and Phase Diagrams", Vol. 8, pp.120-129, 1973.

16. "Estimating the Average Grain size of metals", Annual Book of ASTM Standards, "Metallography:Nondestructive Tests", Vol.11, pp.212-213, 1976.

17. "Tension Testing of Metallic Materials", Annual Book of ASTM Standards, "Die-Cast Metals, Light Metals and Alloys", Vol. 7, pp. 656, 1976.

18. R.W. Armstrong, "Strength Properties of Ultrafine-Grain Metals", Proceedings of the 16 th Sagamore Army Materials Research Conference, Syracuse University, New York, pp. 1-23, 1970.

19. George E.Dieter, "Mechanical Metallurgy", Mc.Graw Hill, Tokyo, 1976.

APPENDIX

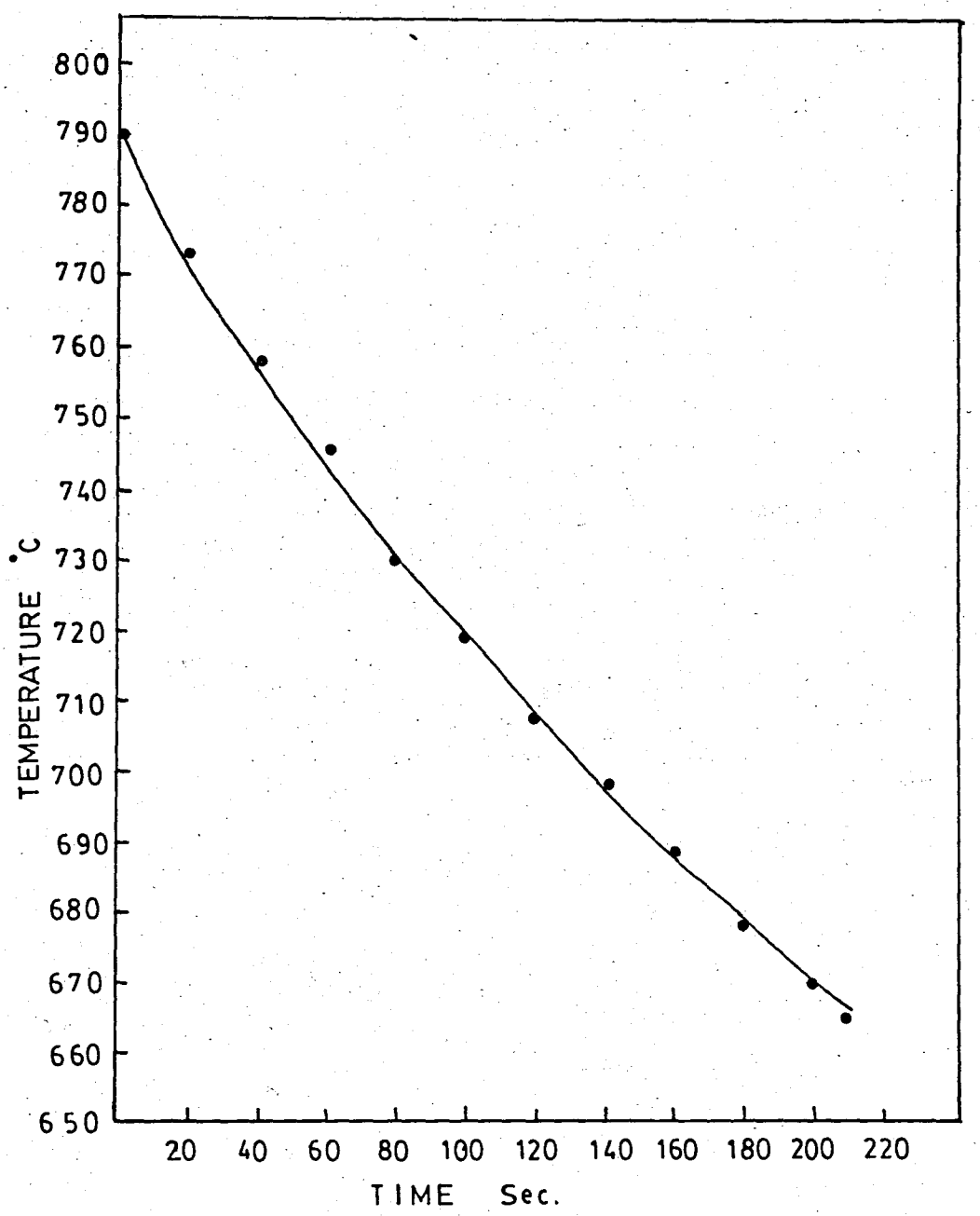

Cooling Curve of the master alloy 17 chilled in asbestos.

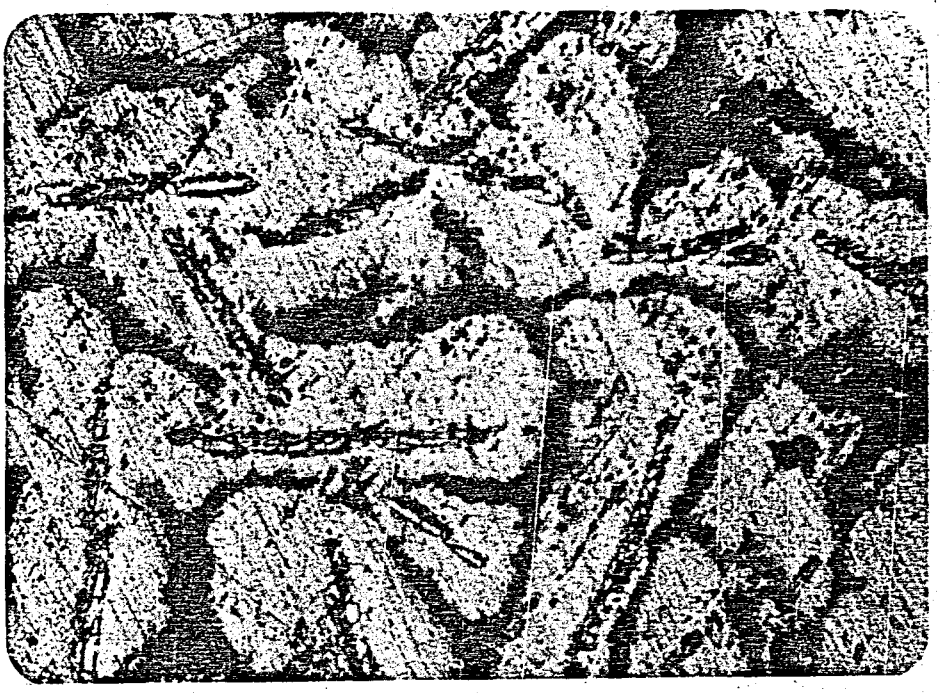

Microstructure of master alloy 1, magnification 165X, 7 minute stirring time, 900°C casting temperature.

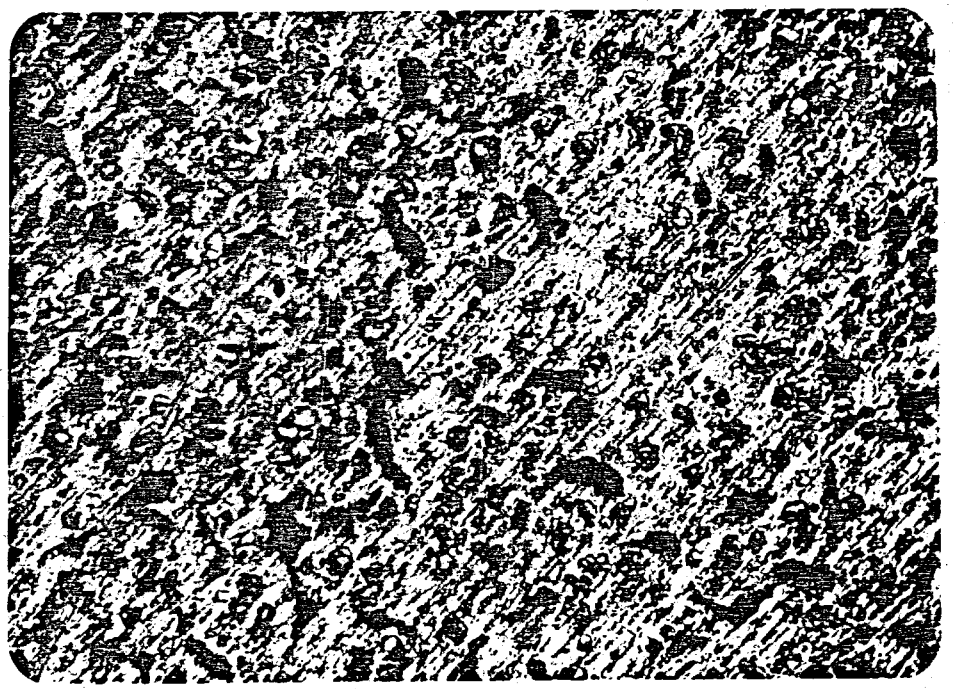

Microstructure of master alloy 2, magnification 165X, 5 min. stirring time, 900°C casting temperature.

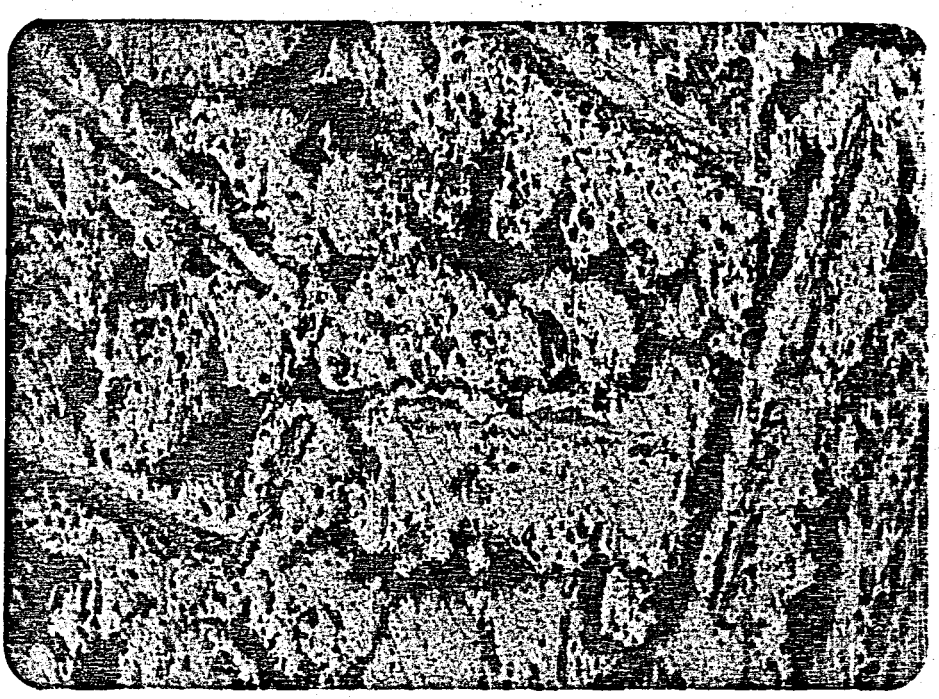

Microstructure of moster alloy 5, magnification 165X, 5 min stirring time, 900°C casting temperature, solidification in air.

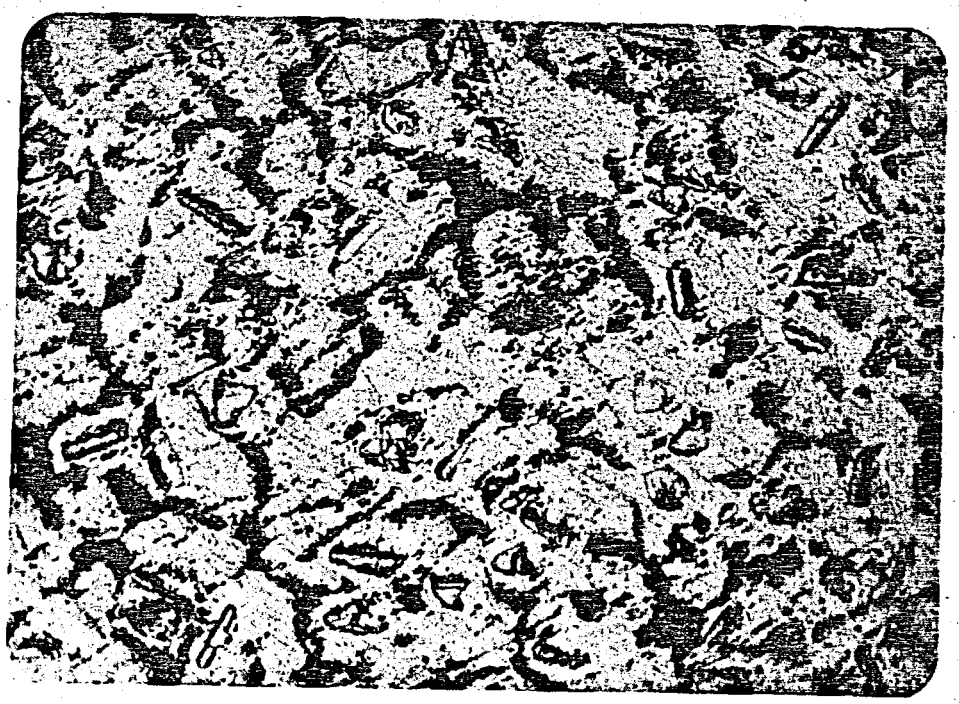

Microstructure of master alloy 7 magnification 165X, 5 min. stirring time, 900°C casting temperature, solidification in air.

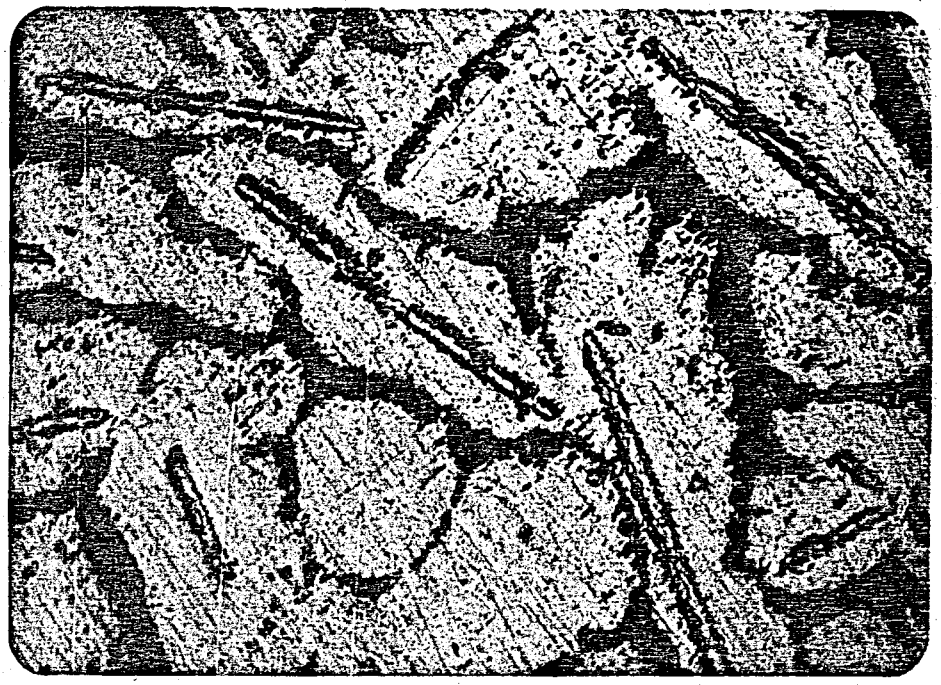

Microstructure of master alloy 8, magnification 165X, 5 min. stirring time, 900°C casting temp., solidification in firebrick.

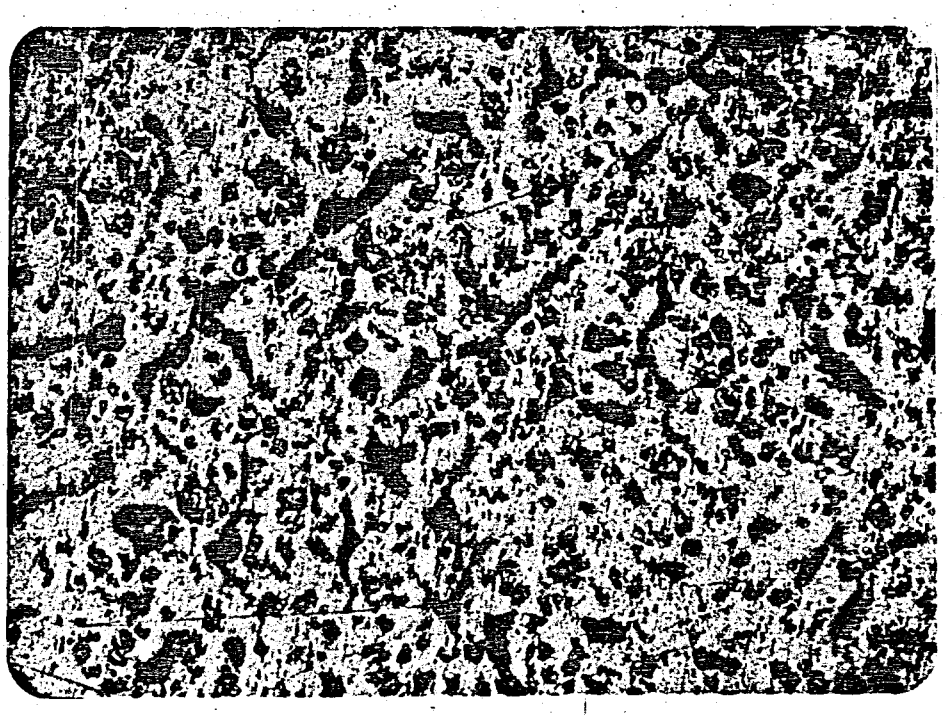

Microstructure of master alloy 9, magnification 165X, 5 min. Stirring time, 800°C casting tem., Solidification in fibebrick.

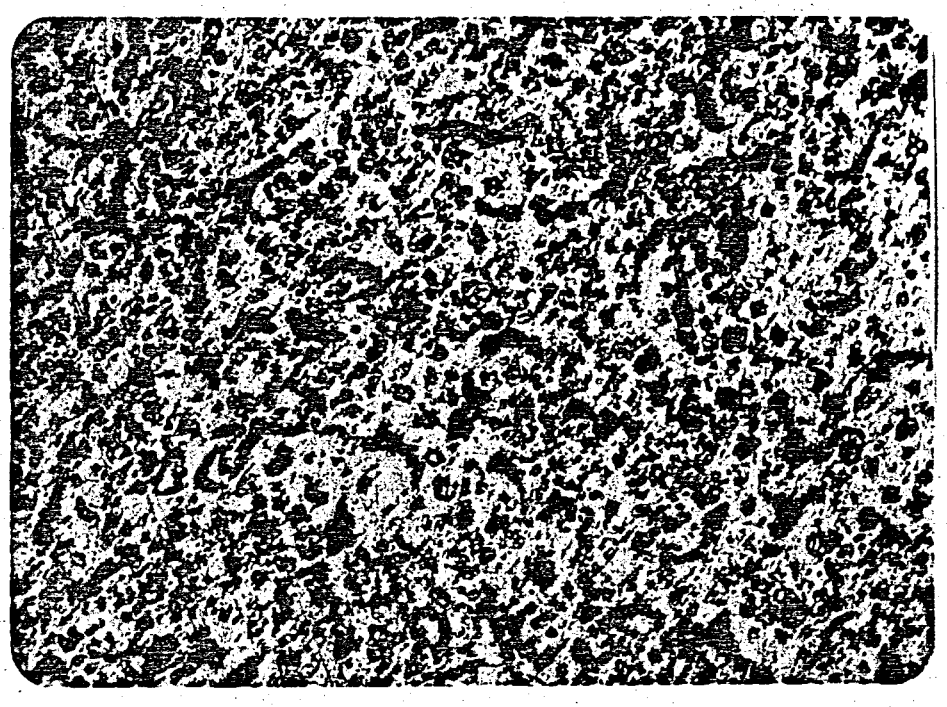

Microstructure of master alloy 10, magnification 165X, 7 min. stirring time, 800°C casting temp., solidification in firebrick.

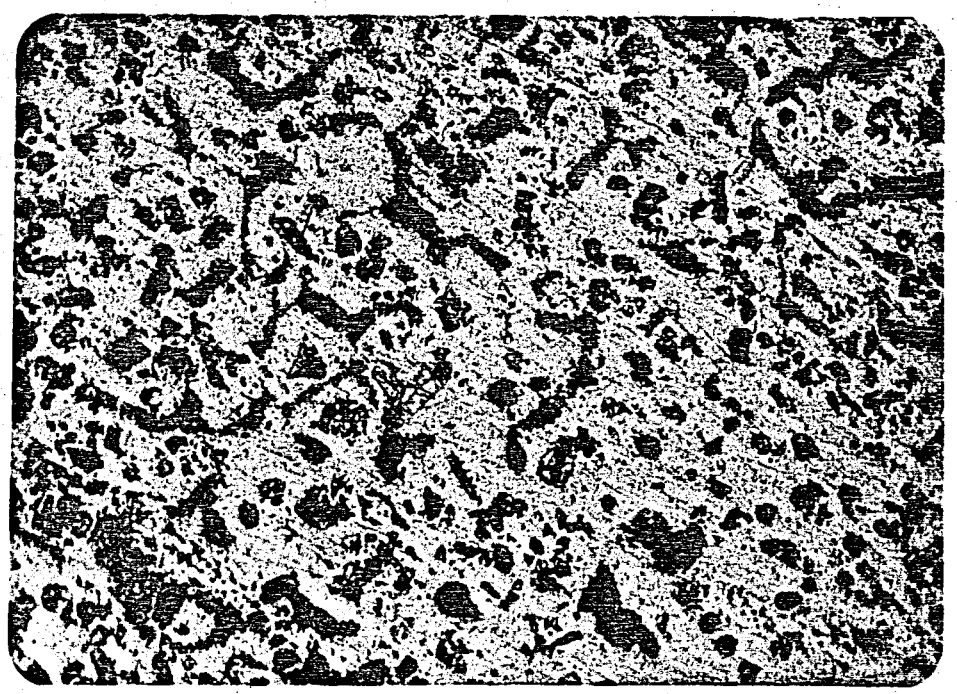

Microstructure of master alloy 11, magnification 165X, 10 min. stirring time, 800°C casting temp., solidification in firebrick.

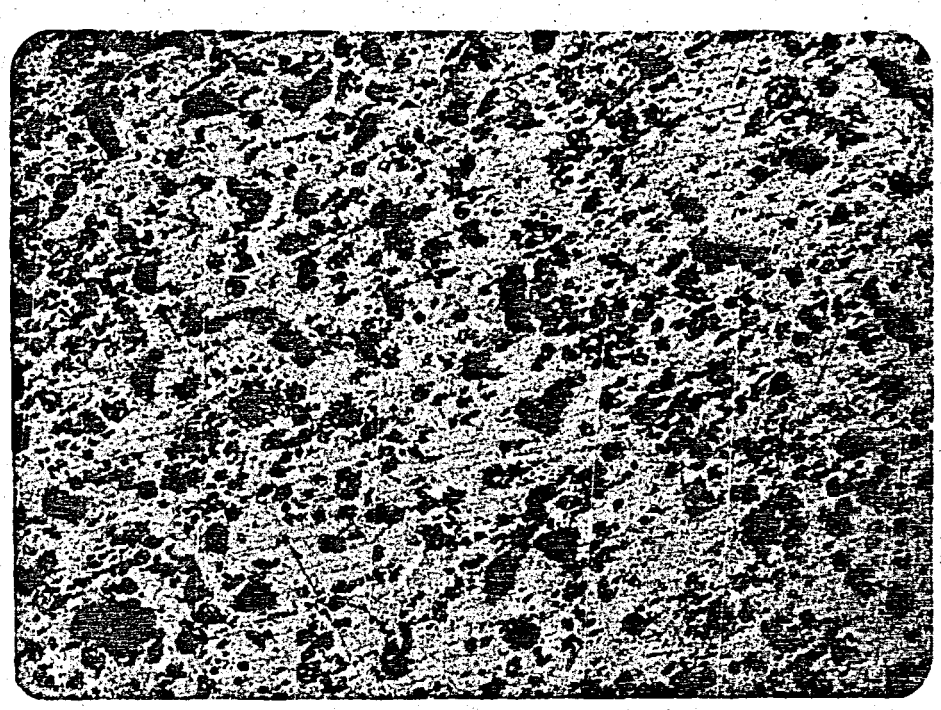

Microstructure of master alloy 13, magnification 165X, 4 min stirring time, 800°C casting temp., Solidification in firebrick.

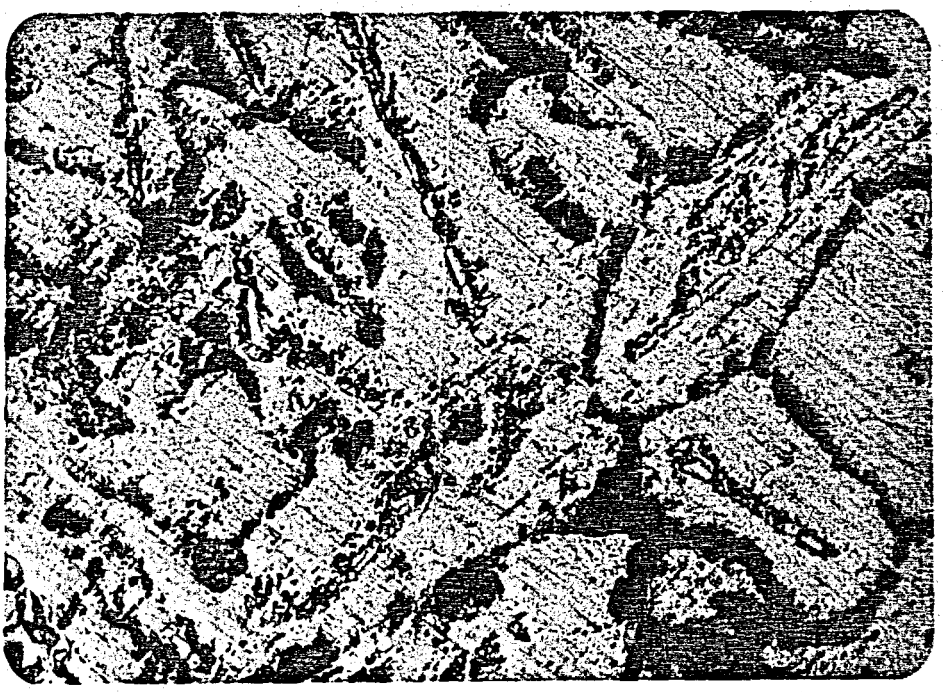

Microstructure of master alloy 14, magnification 165X, 5 min stirring time, 900°C casting temp., Solidification in firebrick.

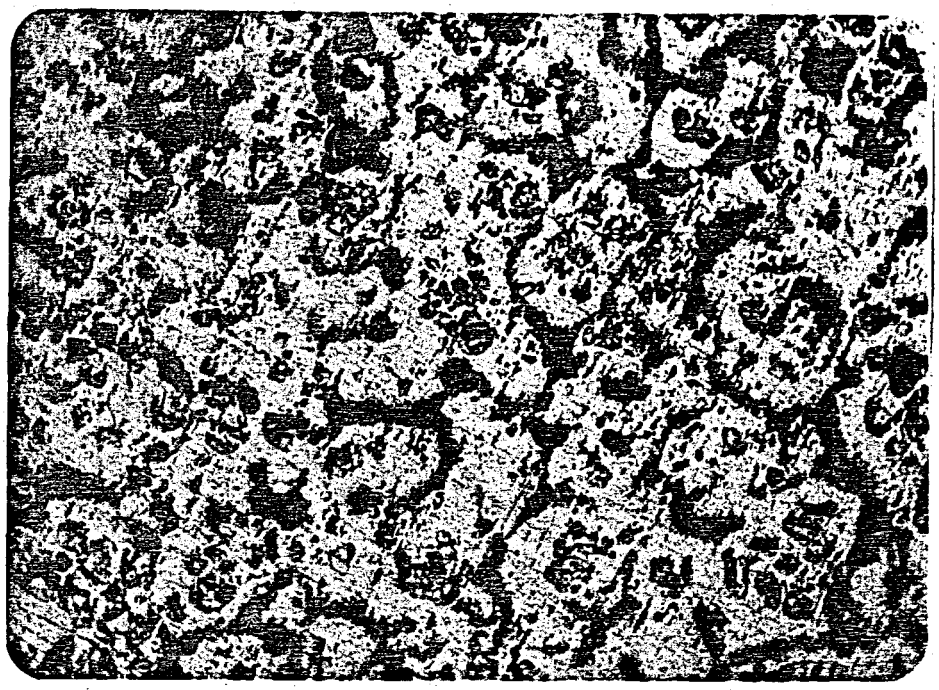

Microstructure of master alloy 15, magnification 165X, 7 min stirring time, 800°C casting temp., solidification in firebrick.

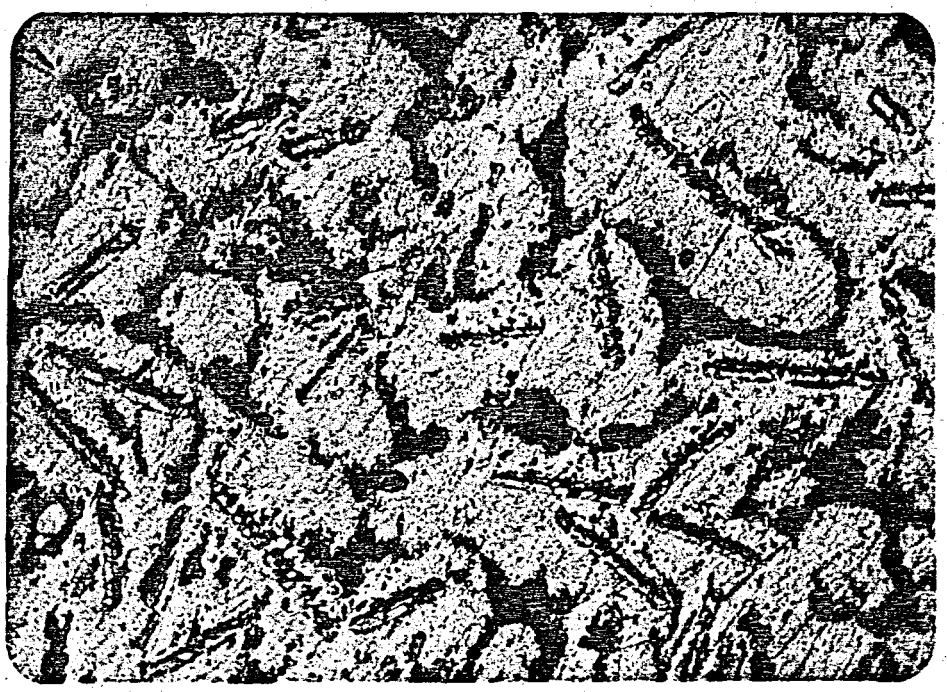

Microstructure of master alloy 16, magnification 165X, 5 min stirring time, 850°C casting temp., Solidification in firebrick.

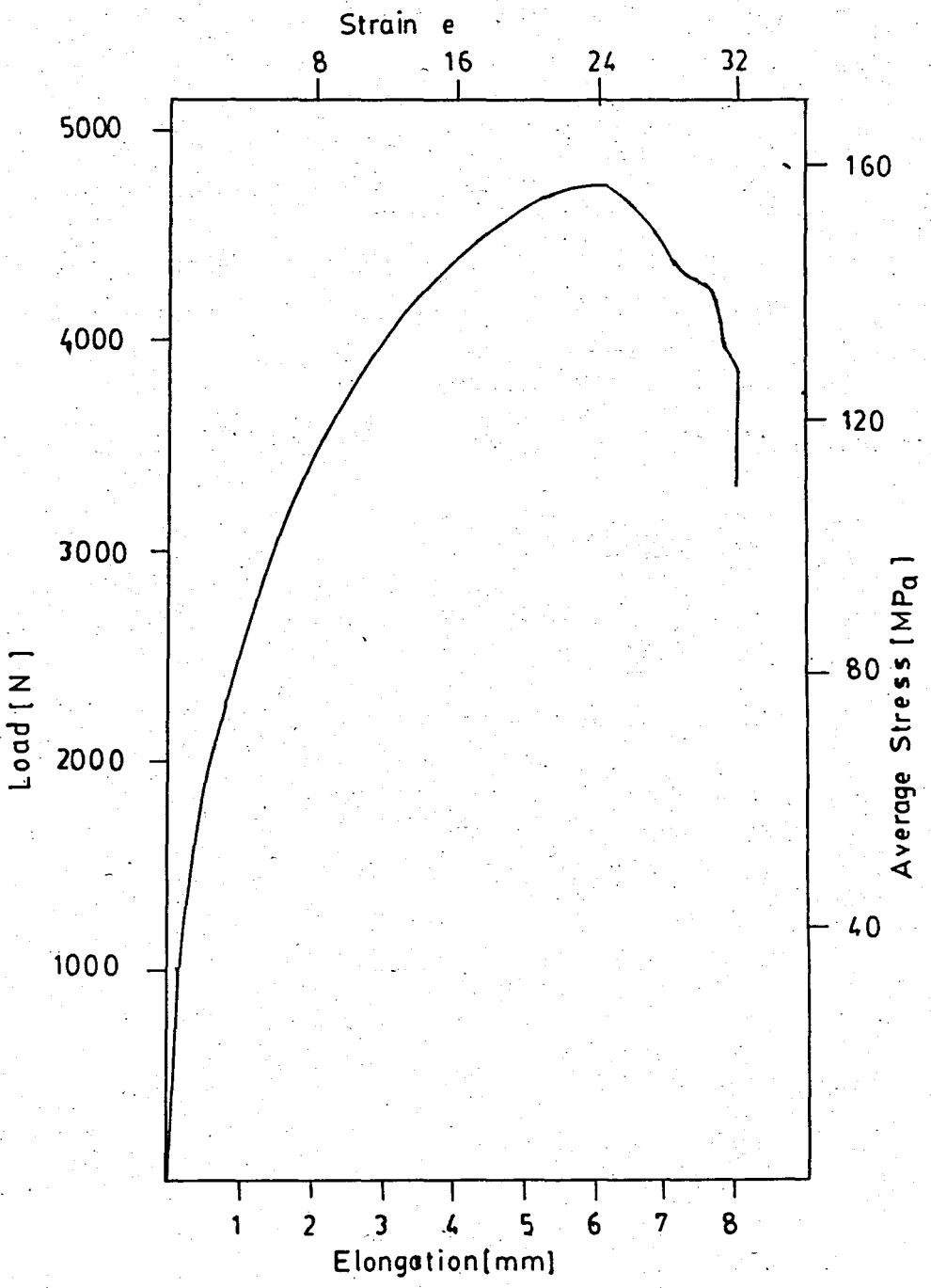

Load-Elongation and Stress-Strain curve of the sample 33.

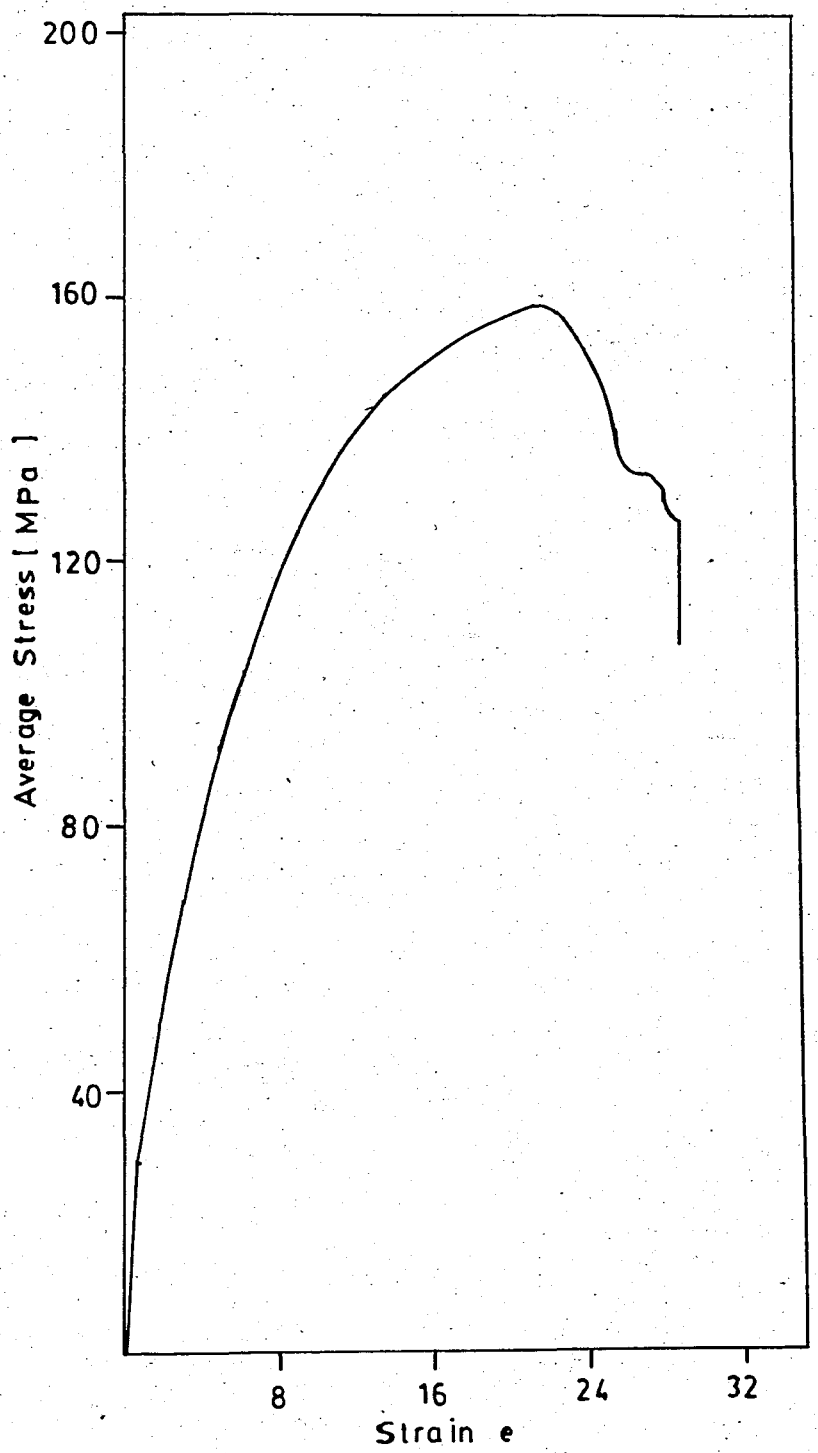

Stress-strain curve of the sample 34.

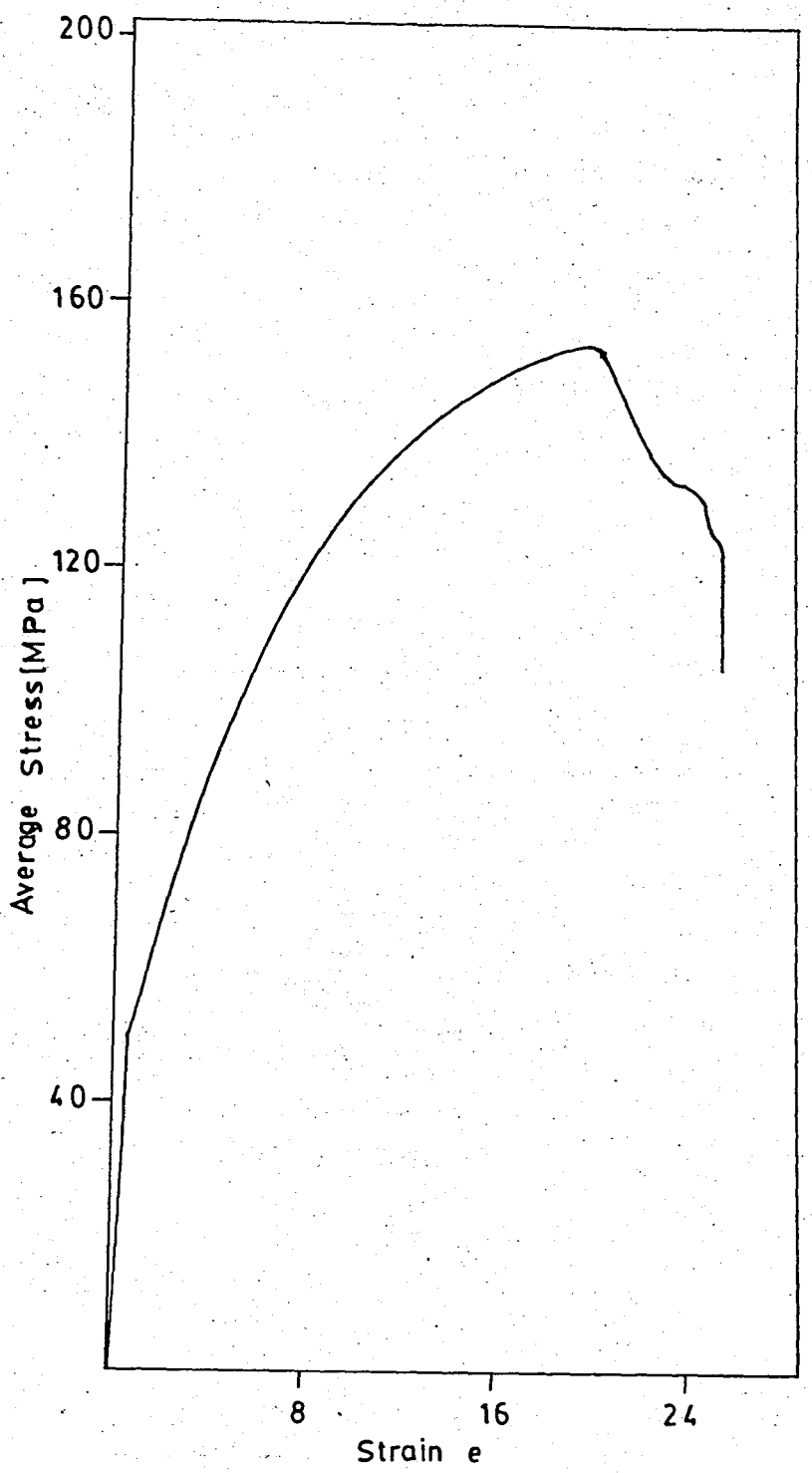

Stress-strain Curve of the sample 36.

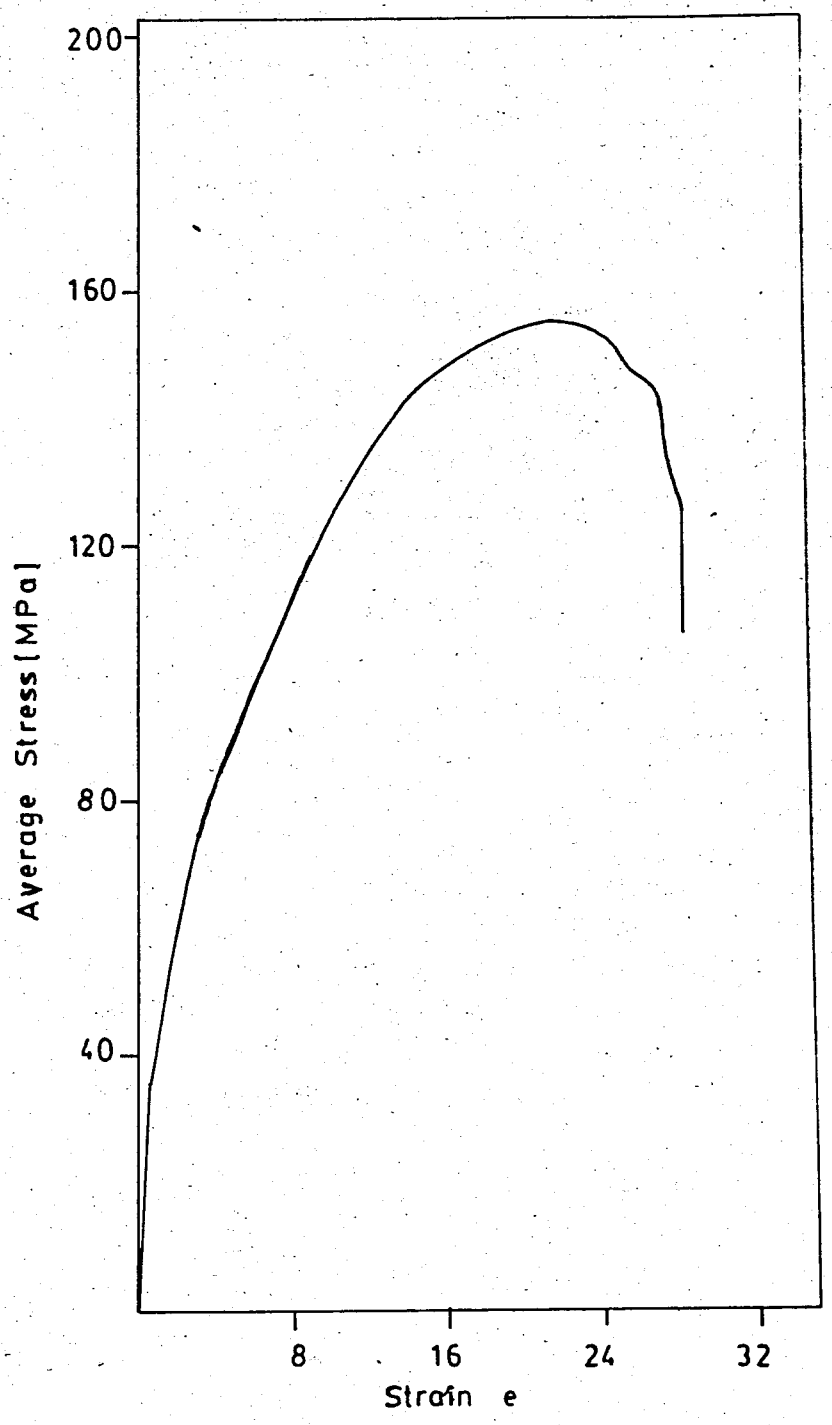

Stress-Strain Curve of the sampe 37.

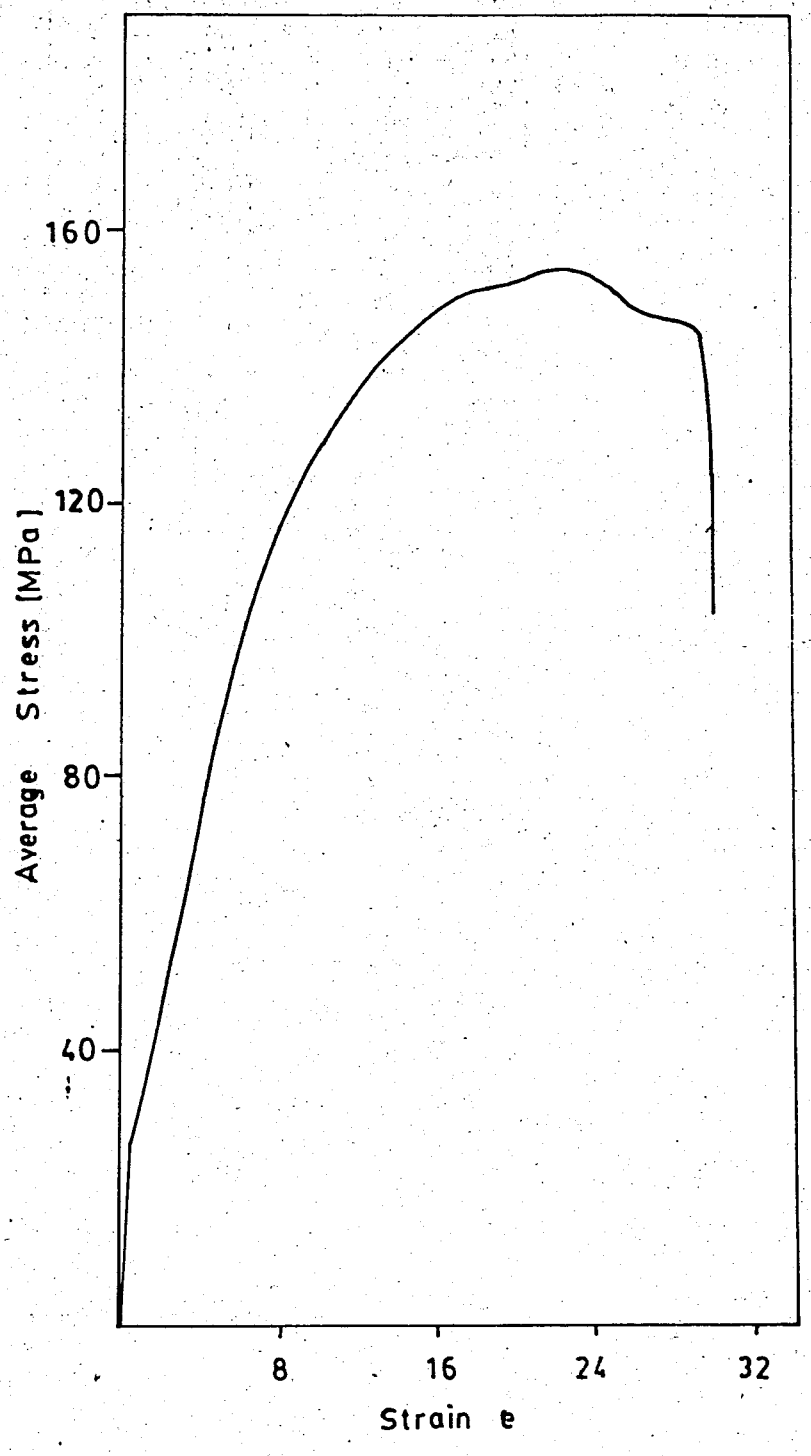

Stress-Strain Curve of the sample 38.